# Intraseasonal Variability in the Tropics

# Madden and Julian, 1972

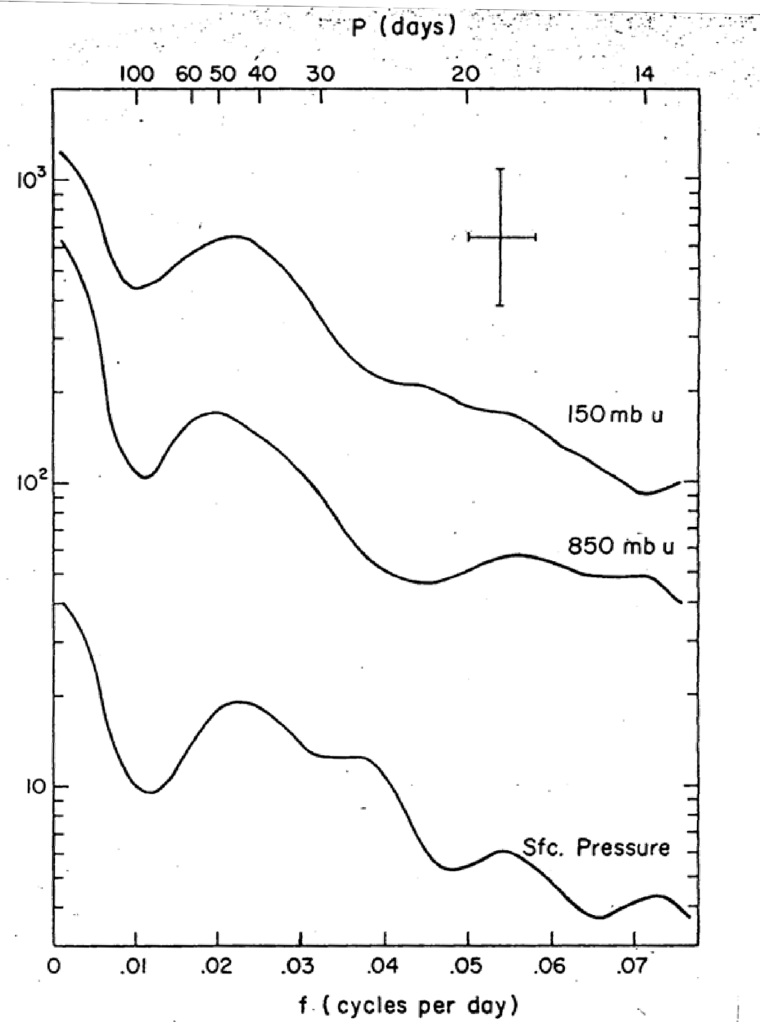


FIG. 2. Individual variance spectra for the 850- and 150-mb zonal wind component and station (sfc) pressure for the Canton Island record. The use of a logarithmic ordinate permits a constant scaling to be used for the chi-square degrees of freedom sampling analysis. This scaling [$\chi^2(0.1\%)/51$] and the bandwidth of the analysis, $\Delta f=0.0081$ day$^{-1}$, are shown by the cross. Spectral densities are normalized to unit bandwidth (m$^2$ sec$^{-2}$ day$^{-1}$).

# Madden and Julian, 1972

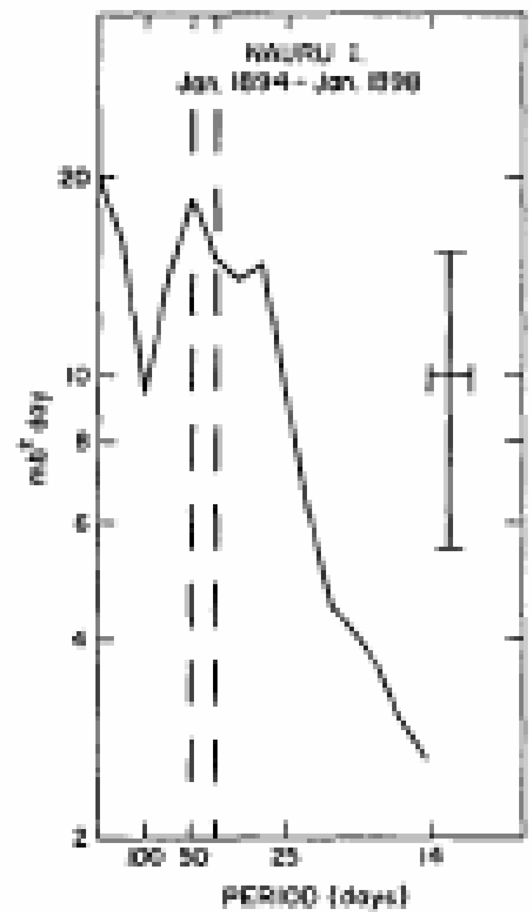


FIG. 2. Variance spectrum for station pressures at Nauru I. (0°24'S, 161°0'E). Ordinate is logarithmic and abscissa (frequency) is linear. The 40–50 day period range is indicated by the dashed vertical lines. Prior 95% confidence limits and the bandwidth of of the analysis (0.008 day⁻¹) are indicated by the cross.

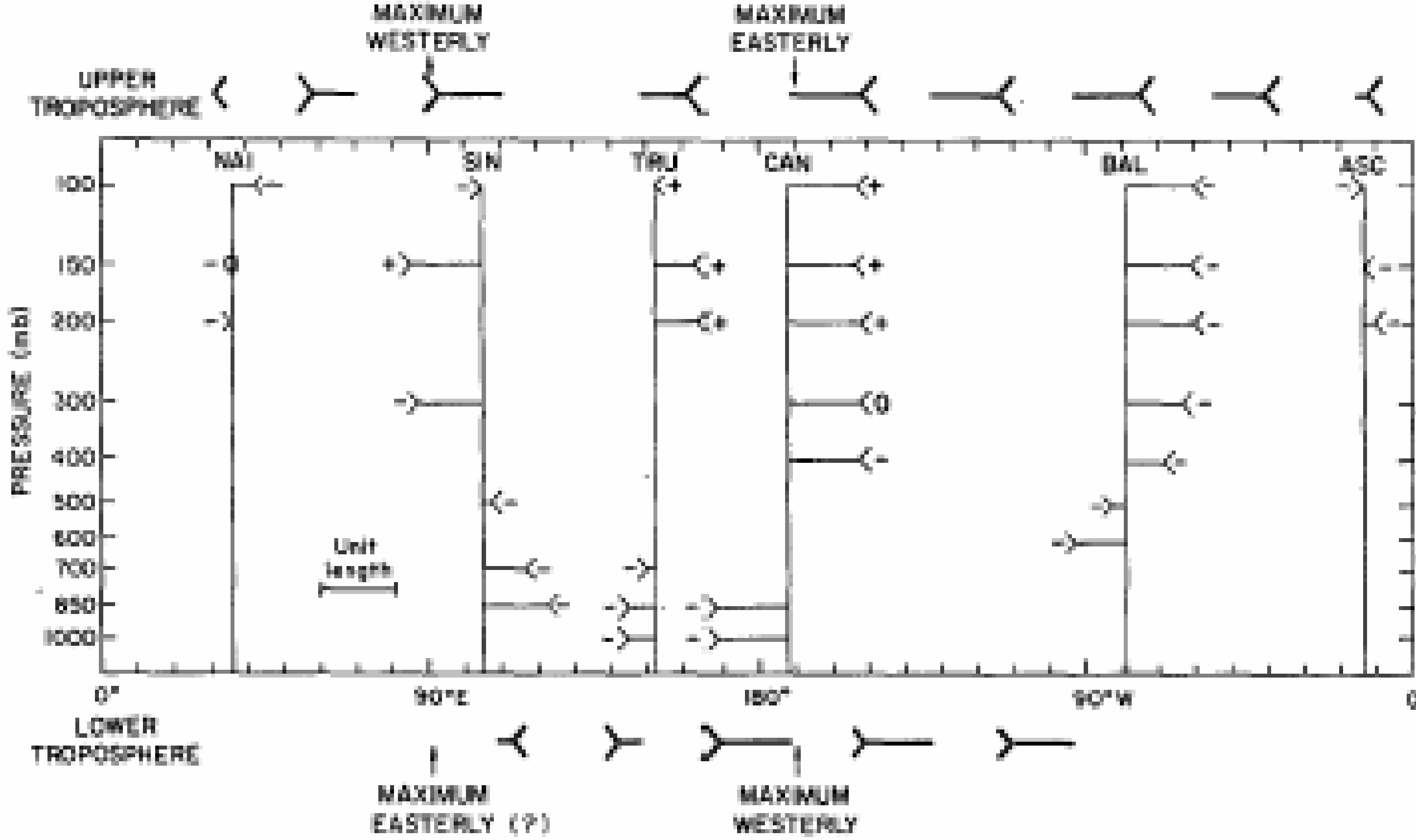


FIG. 6. Zonal wind oscillation in the equatorial plane at the time when the station pressure is a maximum at Canton based on the phase angles of Table 4. The unit length represents the maximum excursion at each location. The +, −, or 0 at the tail of each wind arrow represents the sign of the instantaneous local change of the zonal wind. Arrows are plotted only at levels whose coherence squares from Table 4 are above their background coherence square, and whose spectra, as tabulated in Table 3, indicate a peak. Heavy arrows at the top and bottom represent a schematic of the upper and lower tropospheric wind disturbance that is consistent with the plotted wind arrows and that will satisfy the local changes if it propagates eastward.

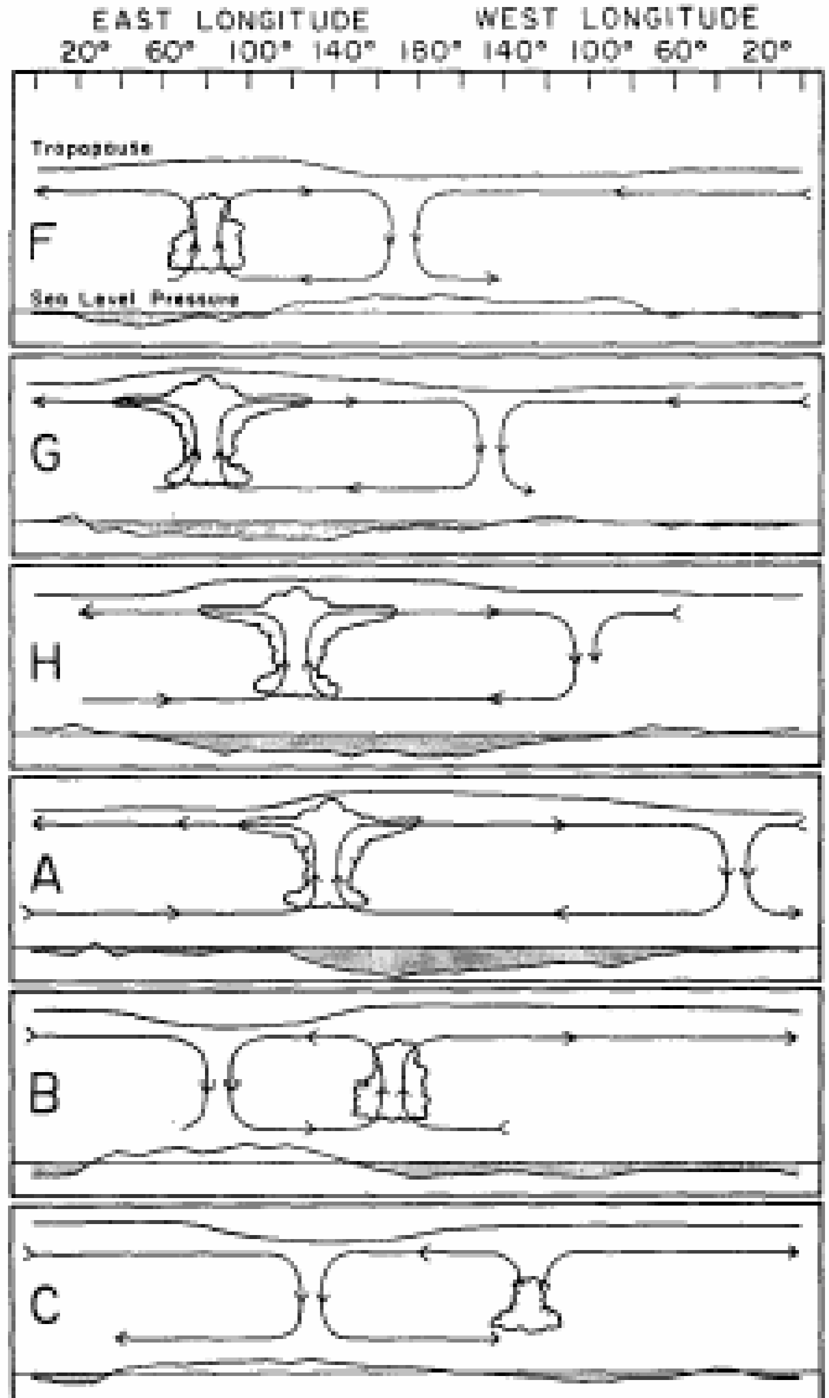
EAST LONGITUDE
WEST LONGITUDE
20° 60° 100° 140° 180° 140° 100° 60° 20°
Tropopause
Sea Level Pressure
F
G
H
A
B
C

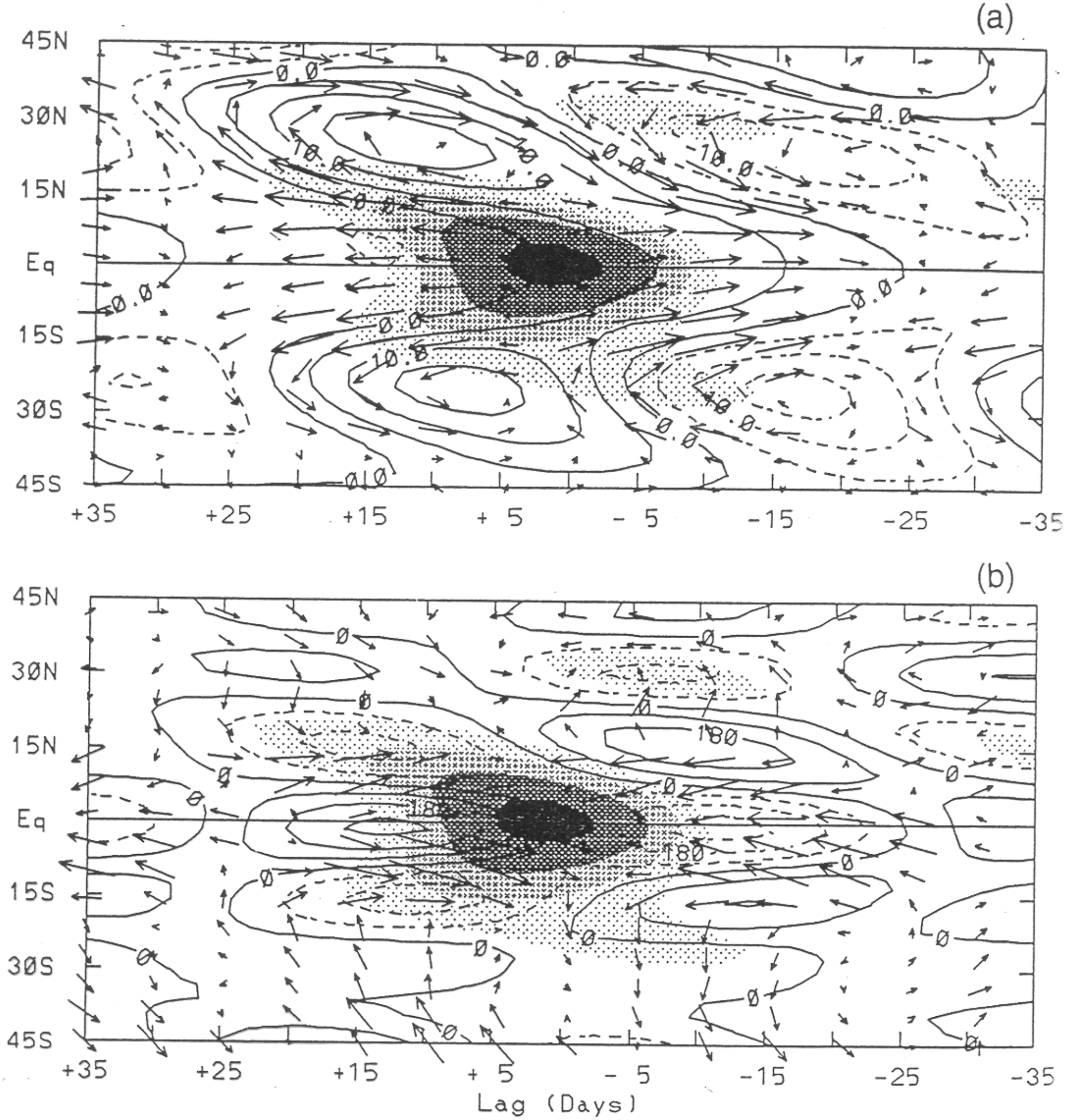


**Figure 2.** Latitude-lag map of (a) 200 mbar winds (vectors), MSUT (contours), and OLR (shaded) and (b) 1000 mbar winds (vectors) and divergence (contours) regressed onto OLR at 0°N, 125°E. All data are windowed according to significant activity at the equator (Figure 1b) and band-pass filtered to eastward wavenumbers 1–3 with 35 to 95-day periods. The regressed fields are shown for a one standard deviation fluctuation of the reference time series. Maximum vectors are 2.7 $ms^{-1}$ at 200 mbar and 0.7 $ms^{-1}$ at 1000 mbar. Contour interval for MSUT is $5.0 \times 10^{-2}$ K, and for 1000-mbar divergence it is $0.9 \times 10^{-7}\ s^{-1}$. Shading levels for OLR (positive means wet convection) start at 0.5 K, 1.75 K, 3.0 K, and 4.25 K.

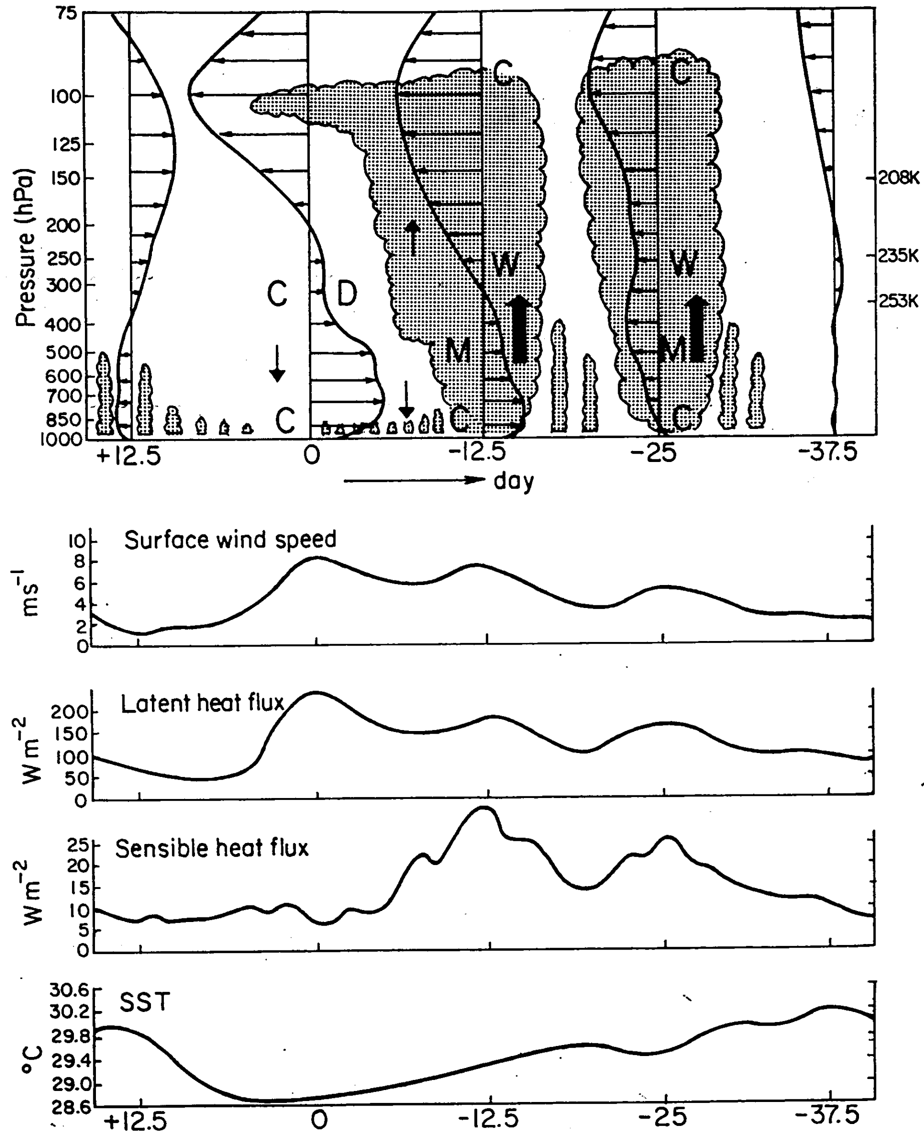


FIG. 16. A descriptive model of the kinematic, thermodynamic, and surface properties of the December to early January westerly wind burst as it passed the IFA. Day 0 is time of maximum low-level westerlies, with earlier times indicated by negative days (placed to the right so that the left portion of the diagram is to the west: see caution in text, however, about fully interpreting diagram as west–east section). Letters in figure refer to anomalies W: warm, C: cool, M: moist, and D: dry. Heavy arrows indicate strong vertical motion; light arrows weak vertical motion. Clouds are schematic, horizontal scales exaggerated. Temperatures corresponding to pressure levels are indicated on right.

Lin and Johnson, JAS, 1996

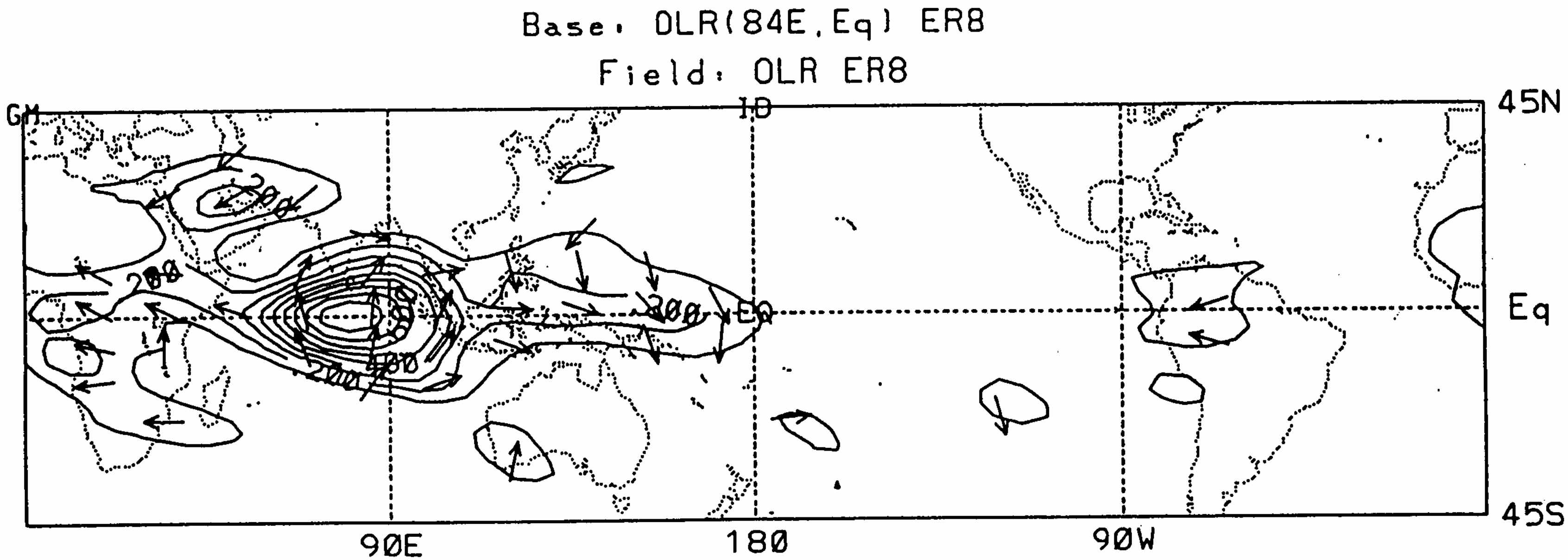


FIG. 4. Coherence squared (contoured) and phase (vectors) between OLR and itself at (0°,84°E) for ER8 truncation. $Coh^2 > 0.1$ significant at the 99% level; see text. Zero phase indicated by upward-directed vector. Clockwise rotation implies direction of phase propagation.

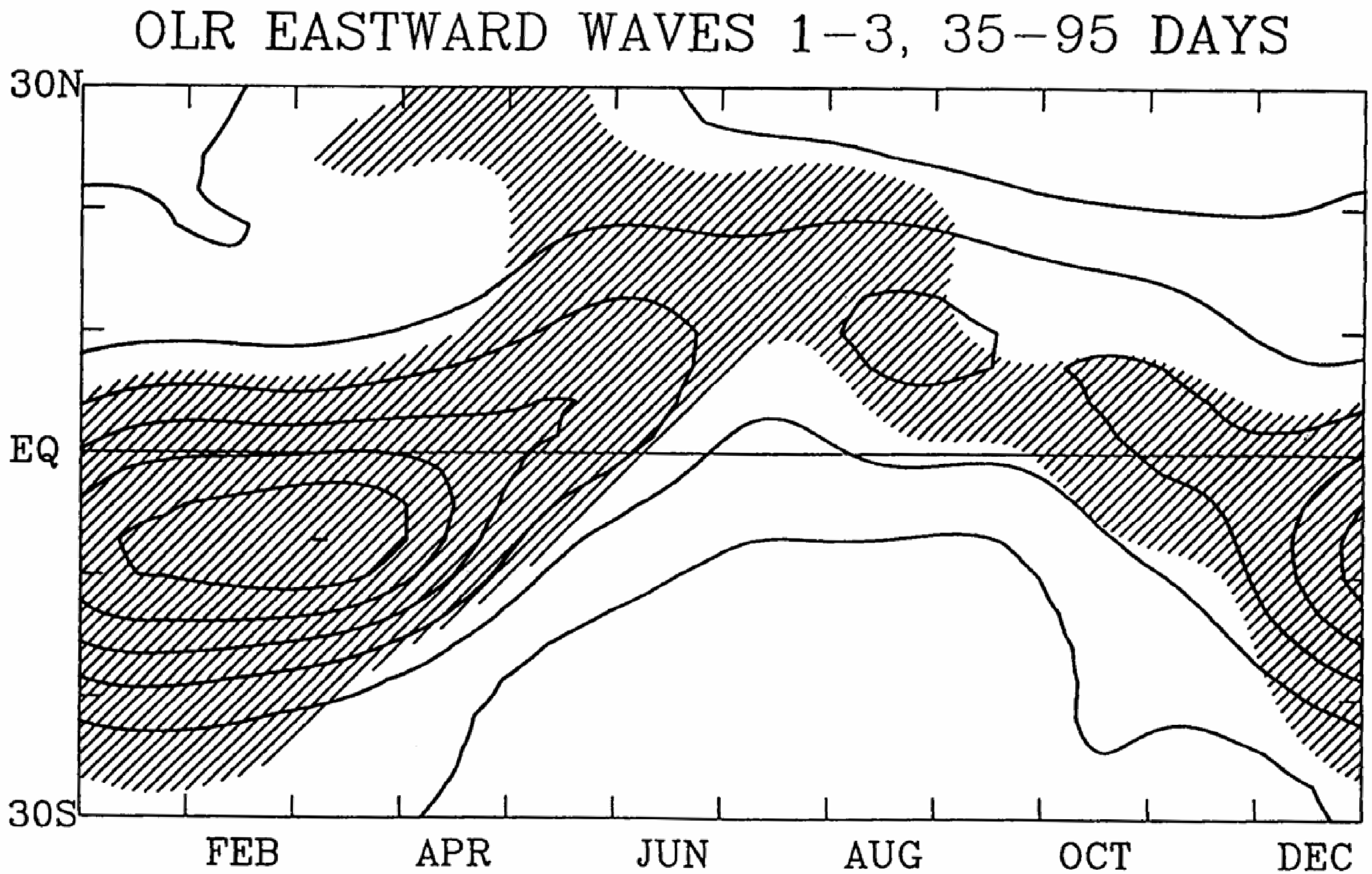


Fig. 1. Composite seasonal cycle of OLR variance for eastward wavenumbers 1-3 and 35-95 day periods. Time series at each latitude is smoothed with 100 day running mean before plotting. Units are arbitrary. Stripes represent times when signal is significant at 95% level relative to a composite background spectrum based on a Chi-square test. Adapted from Salby and Hendon (1994).

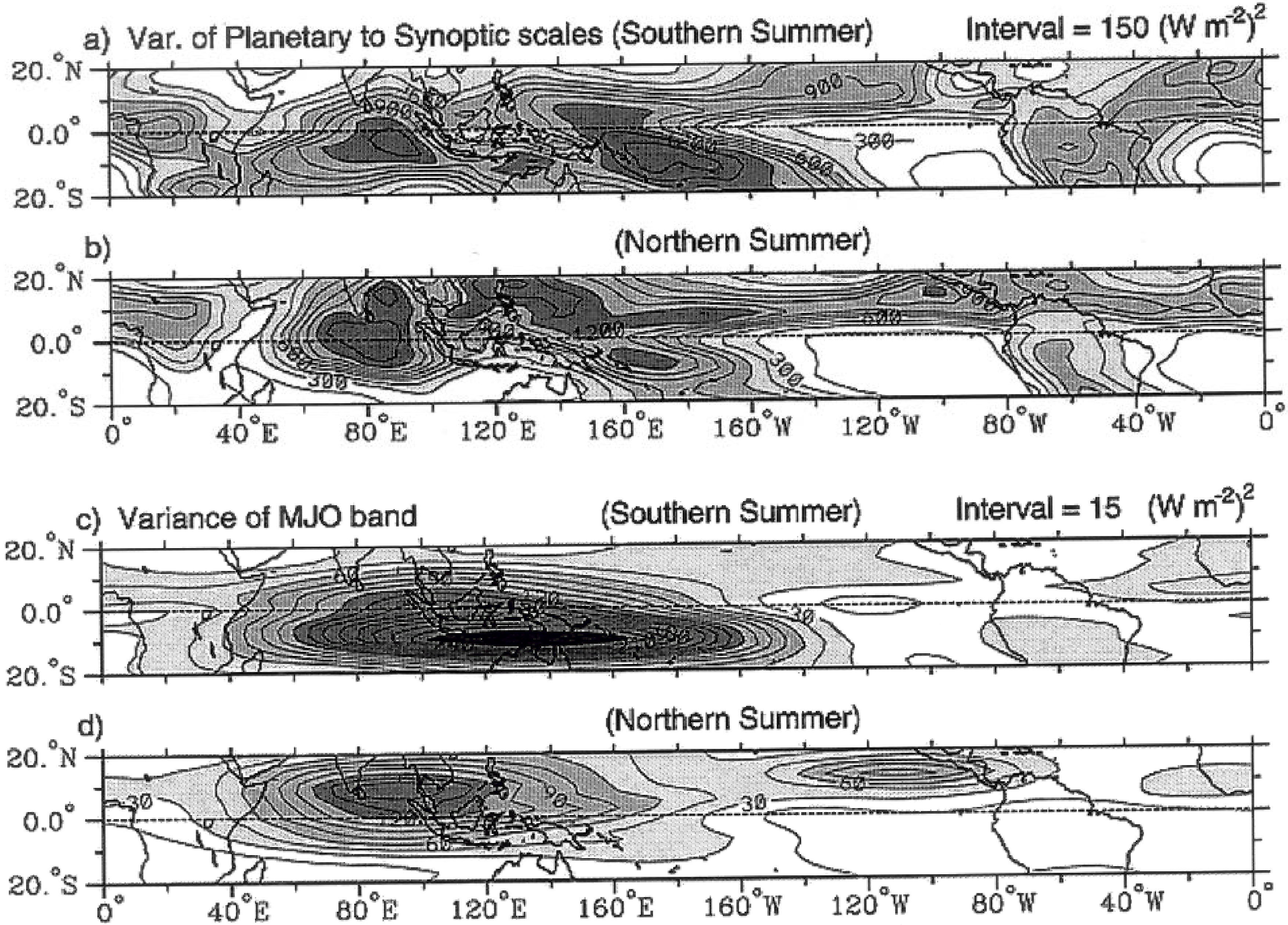
a) Var. of Planetary to Synoptic scales (Southern Summer)
Interval = 150 (W m-2)2
b) (Northern Summer)
c) Variance of MJO band
(Southern Summer)
Interval = 15 (W m-2)2
d) (Northern Summer)
20.°N
0.0°
20.°S
0°
40°E
80°E
120°E
160°E
160°W
120°W
80°W
40°W
0°
900
300
600
1200
30
60
90

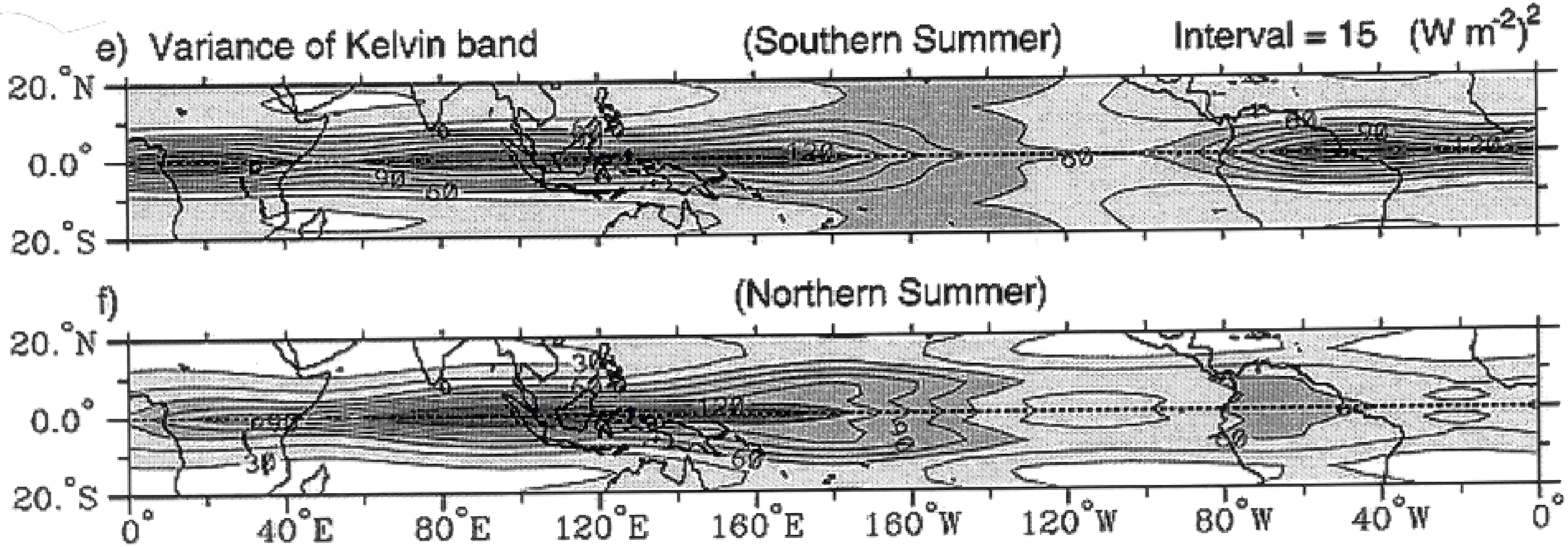
e) Variance of Kelvin band
(Southern Summer)
Interval = 15 (W m-2)2
f)
(Northern Summer)
20.°N
0.0°
20.°S
0°
40°E
80°E
120°E
160°E
160°W
120°W
80°W
40°W
0°

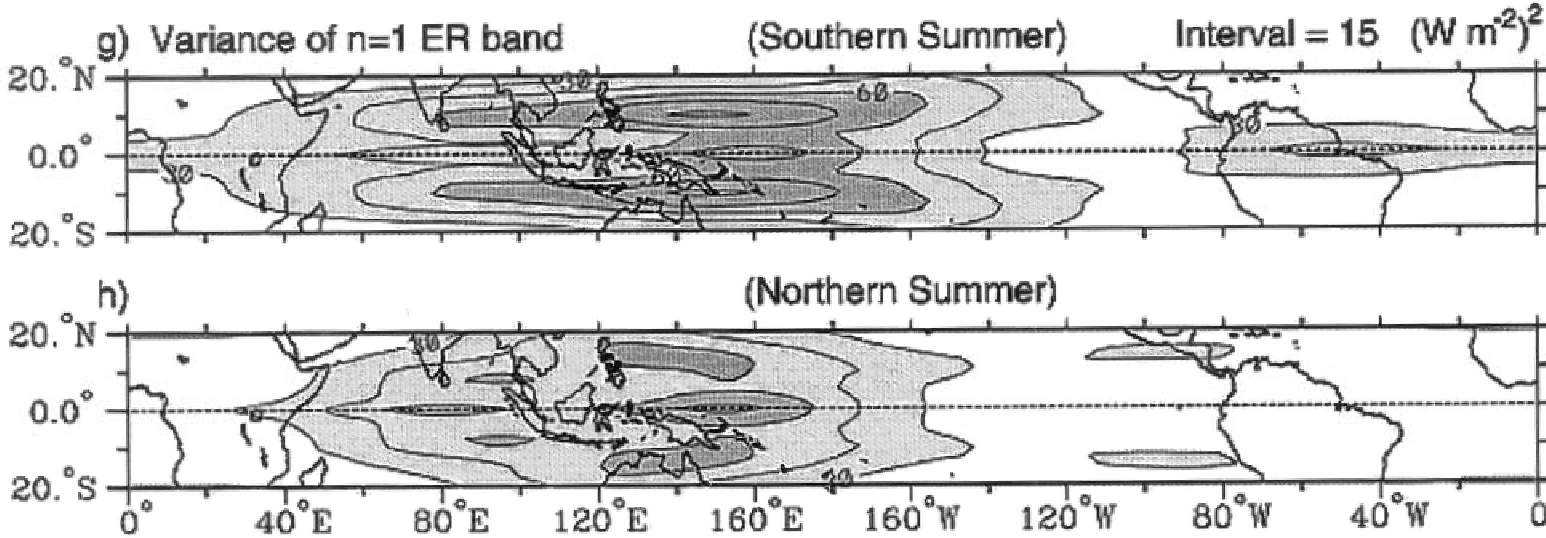
g) Variance of n=1 ER band
(Southern Summer)
Interval = 15 (W m-2)2
h)
(Northern Summer)
20.°N
0.0°
20.°S
0°
40°E
80°E
120°E
160°E
160°W
120°W
80°W
40°W
0°

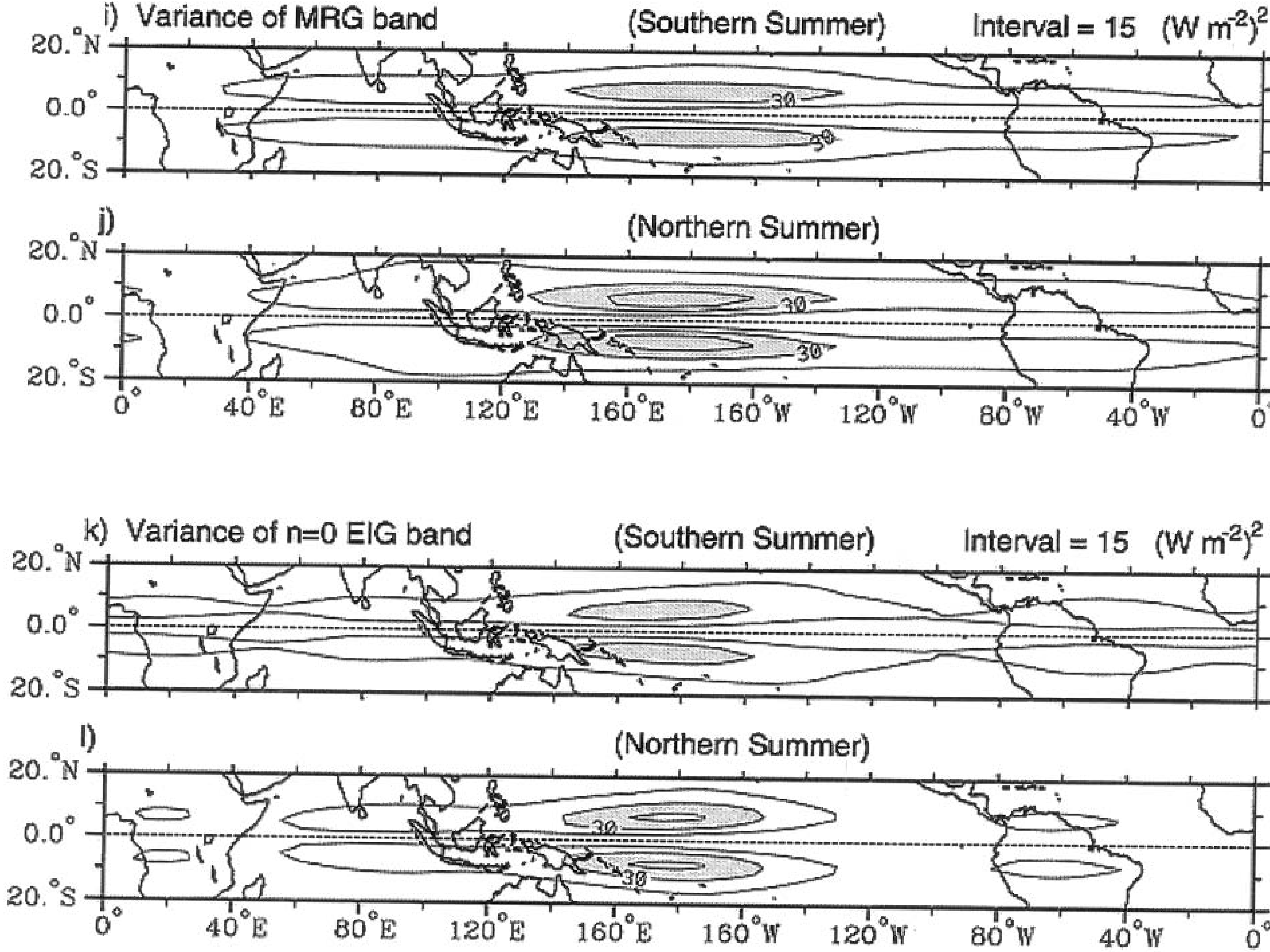
i) Variance of MRG band
(Southern Summer)
Interval = 15 (W m-2)2
j)
(Northern Summer)
k) Variance of n=0 EIG band
(Southern Summer)
Interval = 15 (W m-2)2
l)
(Northern Summer)
20.°N
0.0°
20.°S
30
0°
40°E
80°E
120°E
160°E
160°W
120°W
80°W
40°W
0°

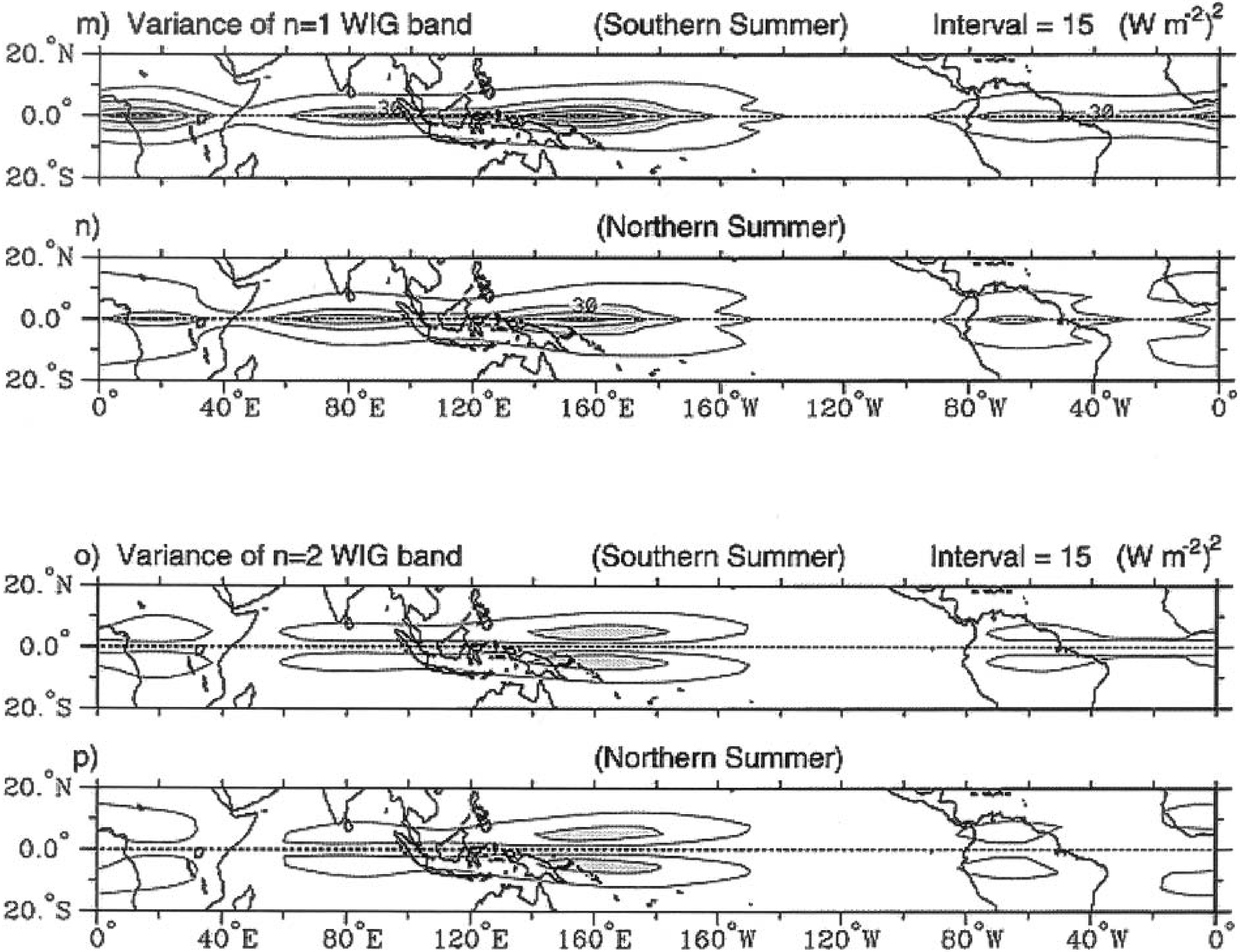
m) Variance of n=1 WIG band
(Southern Summer)
Interval = 15 (W m-2)2
30
n)
(Northern Summer)
30
o) Variance of n=2 WIG band
(Southern Summer)
Interval = 15 (W m-2)2
p)
(Northern Summer)
20.°N
0.0°
20.°S
0°
40°E
80°E
120°E
160°E
160°W
120°W
80°W
40°W
0°

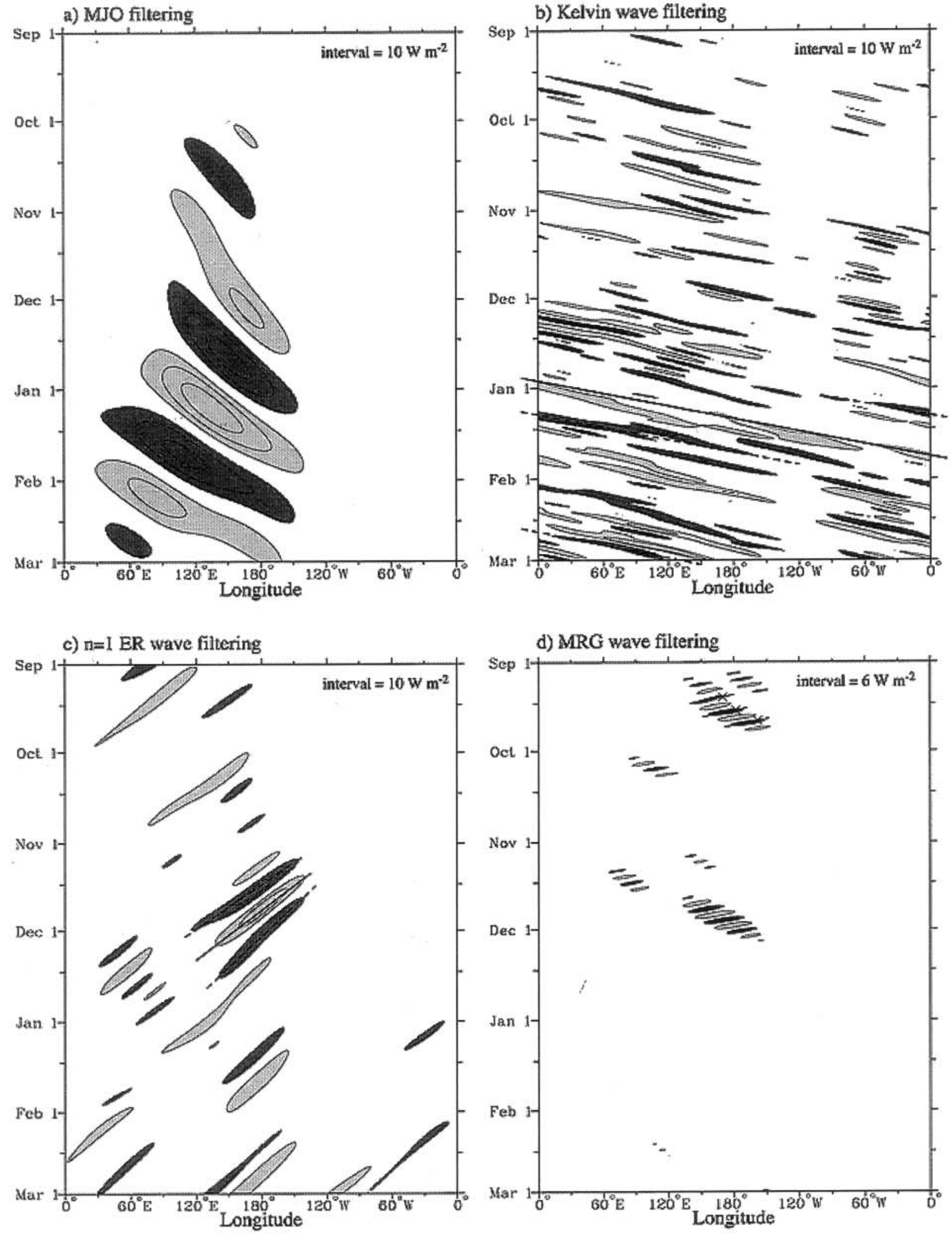


**Fig. 9. (a) Time-longitude section of the OLR anomalies for the MJO-filtered band for the same 6-month sample period as Fig. 8, averaged for the latitudes from 10°S to 2.5°N. The zero contour**

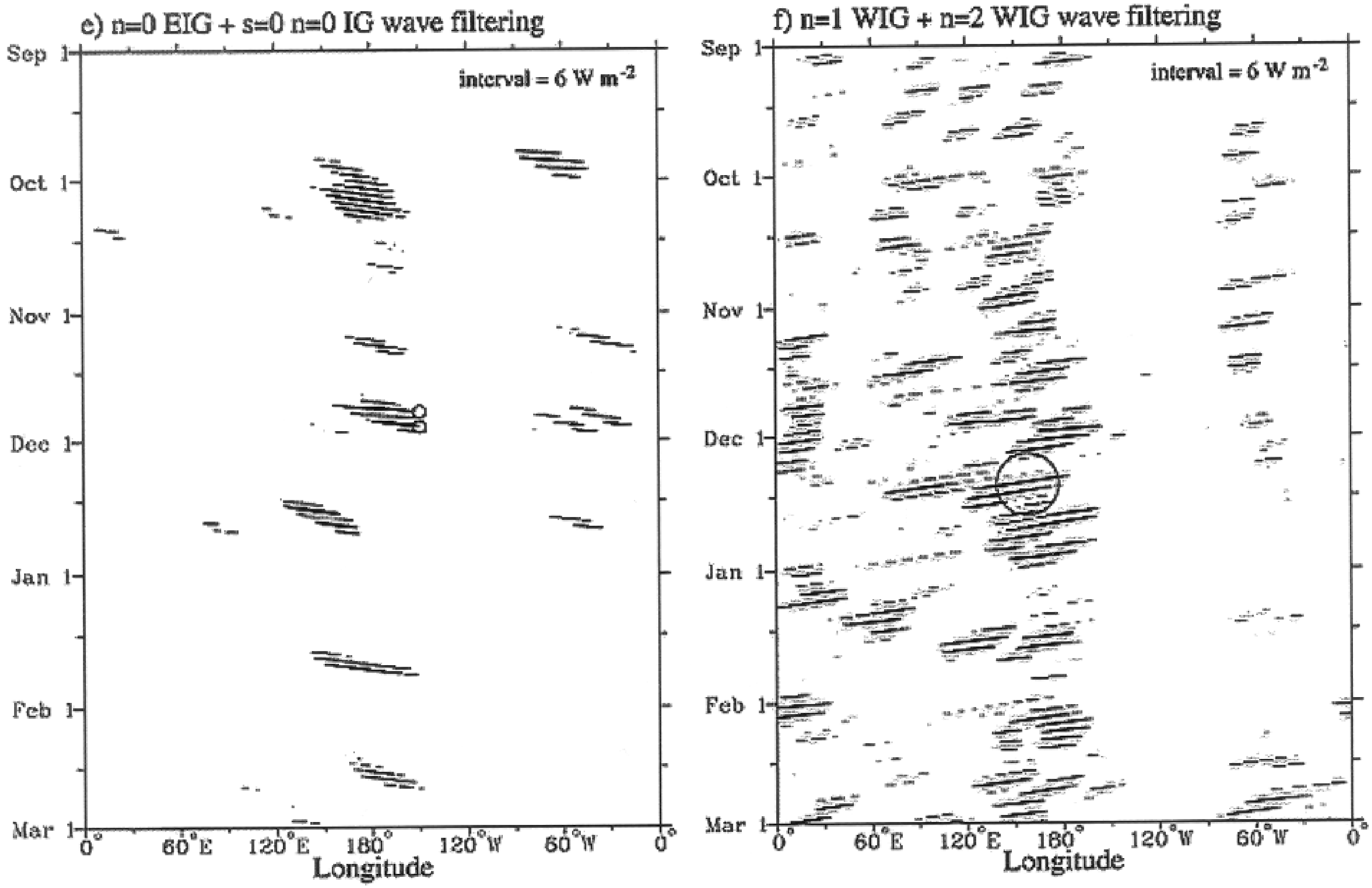


**Fig. 9 (*Continued*) (e) The $n = 0$ EIG wave-filtered plus the $s = 0$, $n = 0$ IG wave-filtered band. (f) The $n = 1$ WIG wave-filtered plus the $n = 2$ WIG wave-filtered bands.**

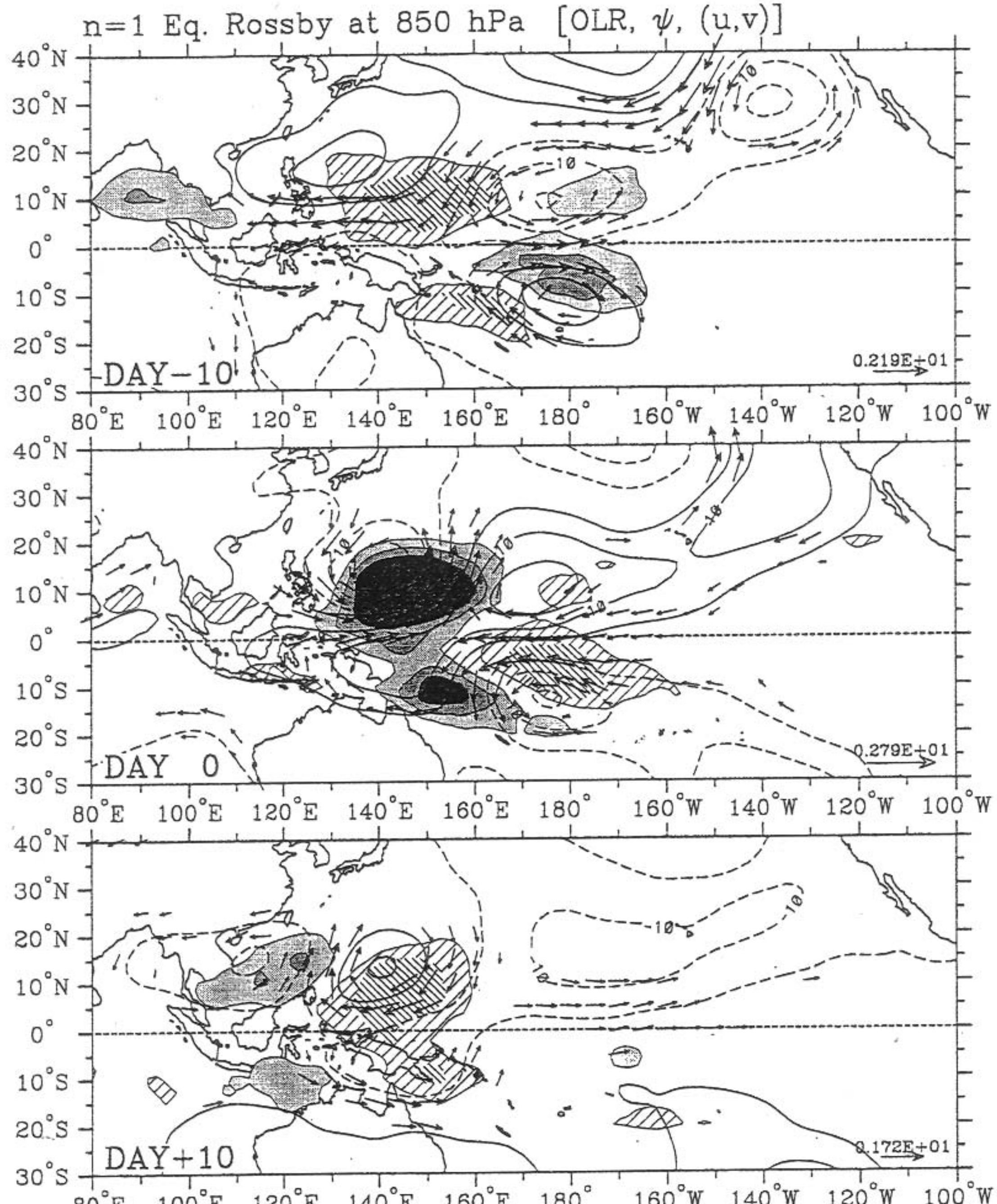

n=1 Eq. Rossby at 850 hPa [OLR, ψ, (u,v)]
DAY-10
0.219E+01
DAY 0
0.279E+01
DAY+10
0.172E+01
40°N
30°N
20°N
10°N
0°
10°S
20°S
30°S
80°E
100°E
120°E
140°E
160°E
180°
160°W
140°W
120°W
100°W

a) n=1 ER section at 150°E [T, (v,w)]

b) n=1 ER section at 140°E [u]

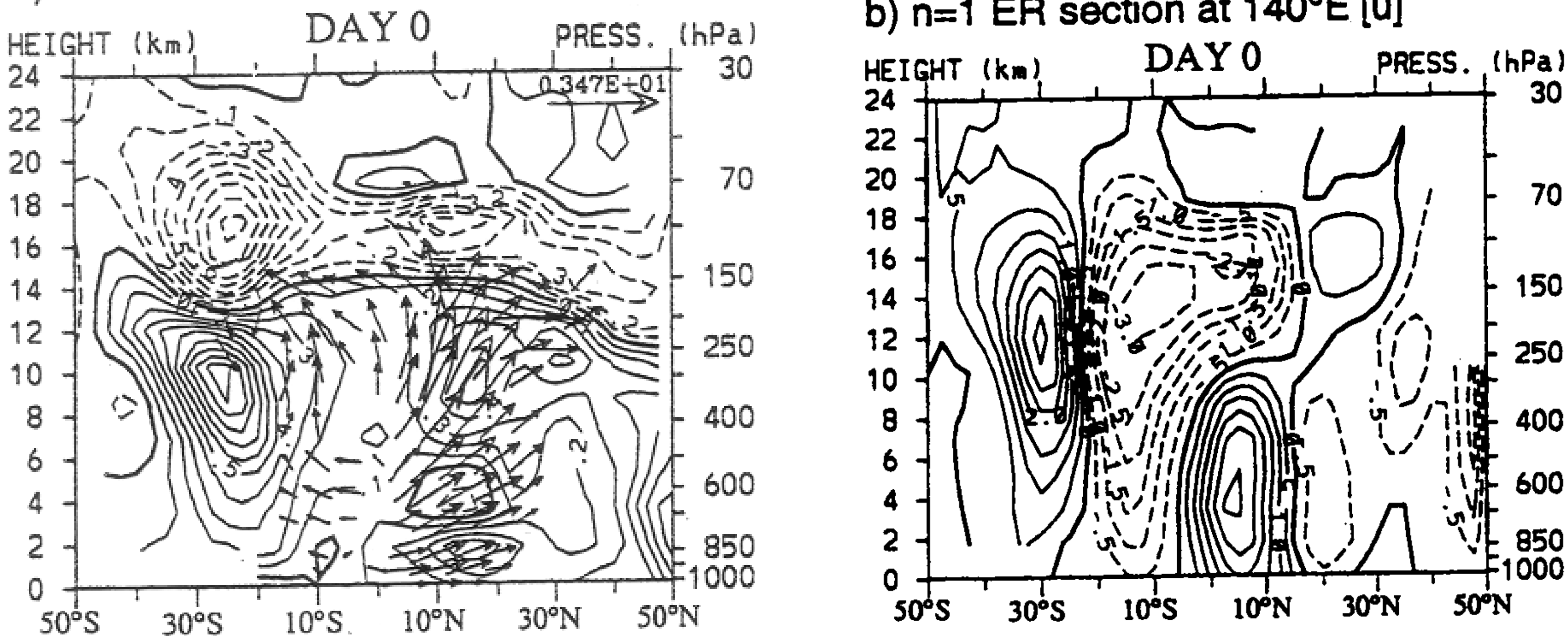

c) n=1 ER section along Eq. [u, (u,w)]

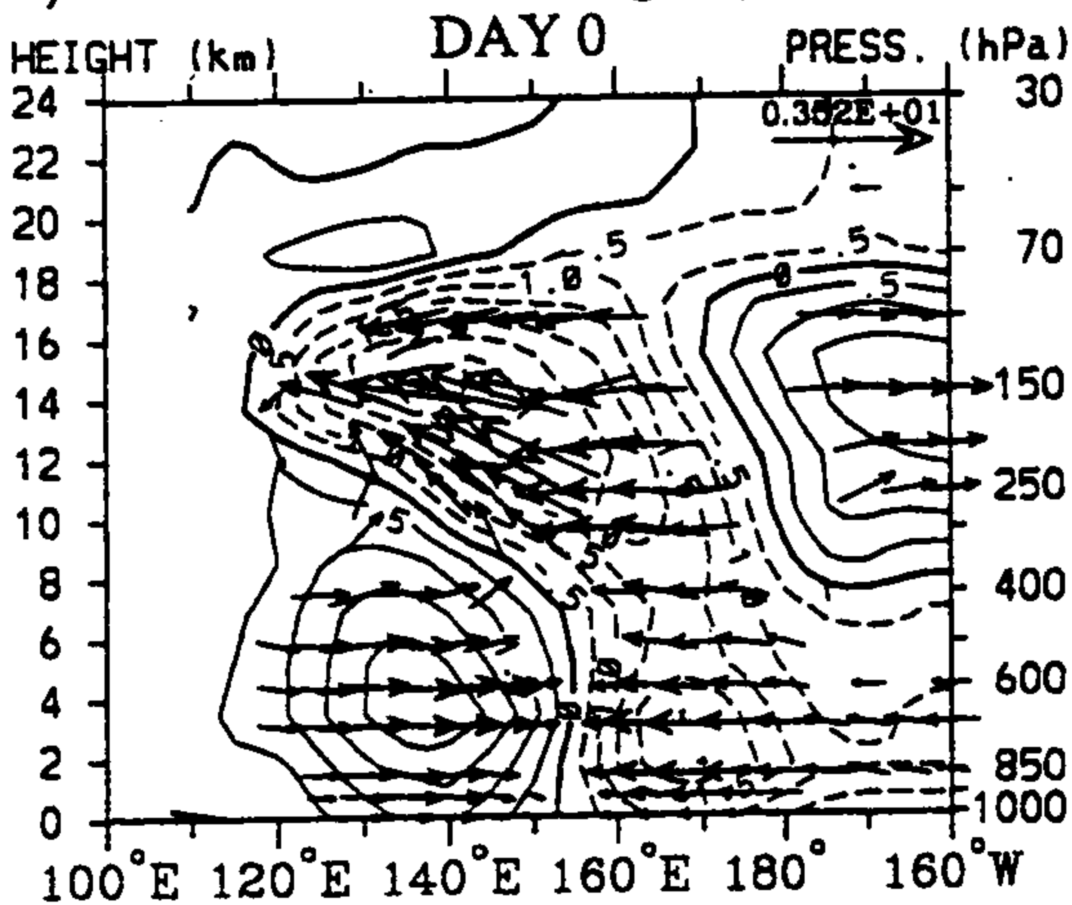

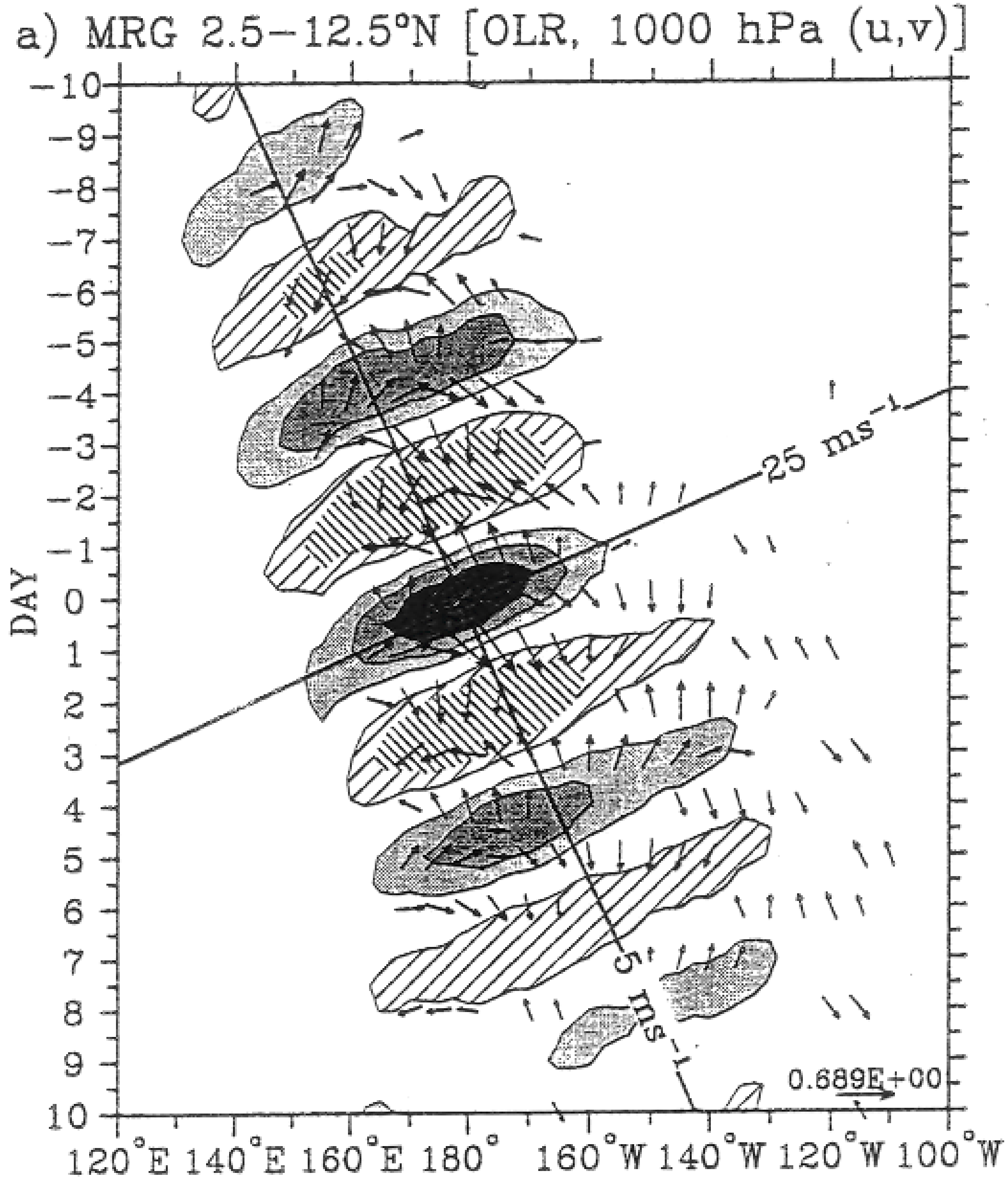

a) MRG 2.5–12.5°N [OLR, 1000 hPa (u,v)]
DAY
-10
-9
-8
-7
-6
-5
-4
-3
-2
-1
0
1
2
3
4
5
6
7
8
9
10
25 ms⁻¹
5 ms⁻¹
0.689E+00
120°E
140°E
160°E
180°
160°W
140°W
120°W
100°W

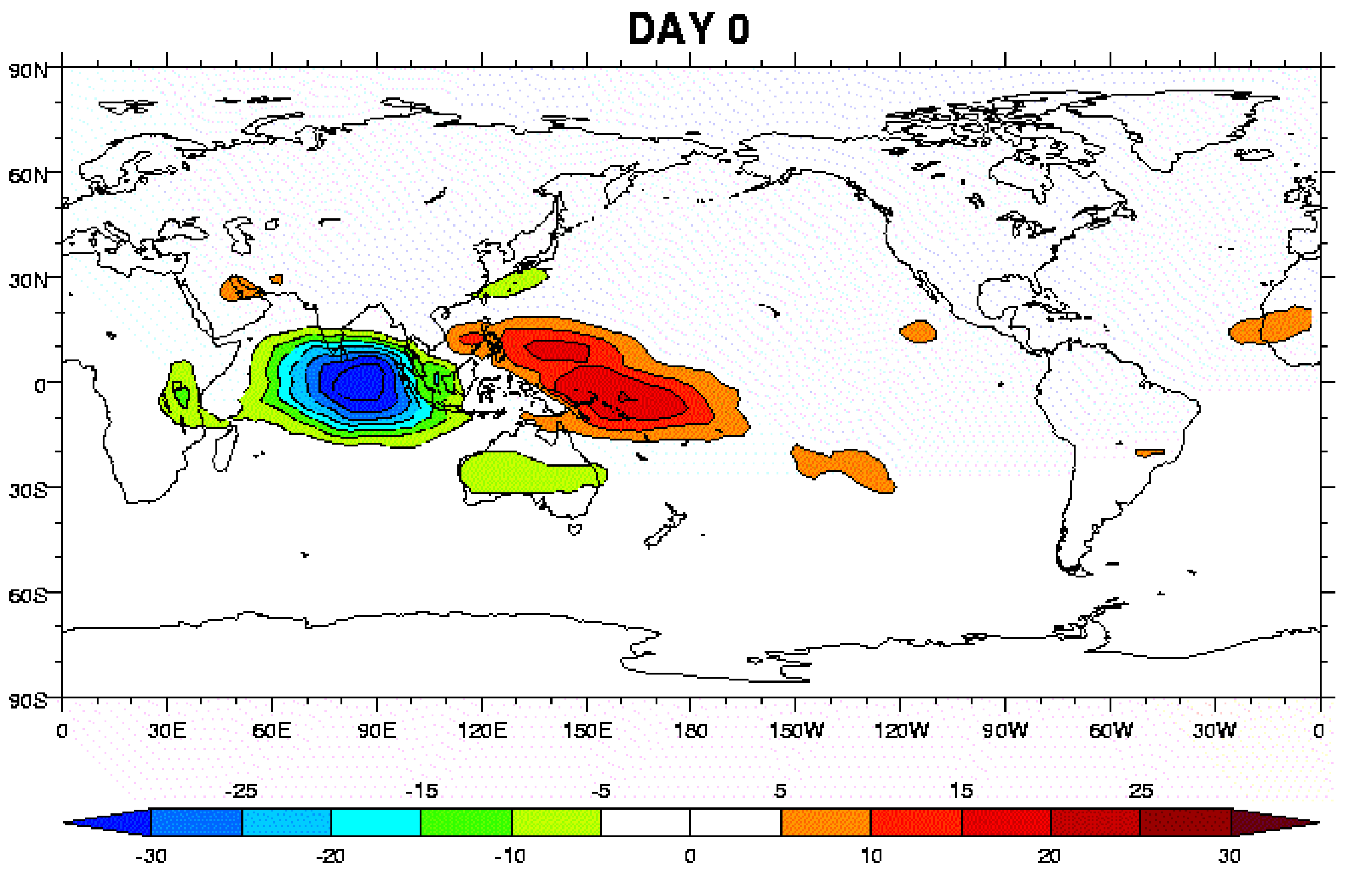
DAY 0
90N
60N
30N
0
30S
60S
90S
0
30E
60E
90E
120E
150E
180
150W
120W
90W
60W
30W
0
-25
-15
-5
5
15
25
-30
-20
-10
0
10
20
30

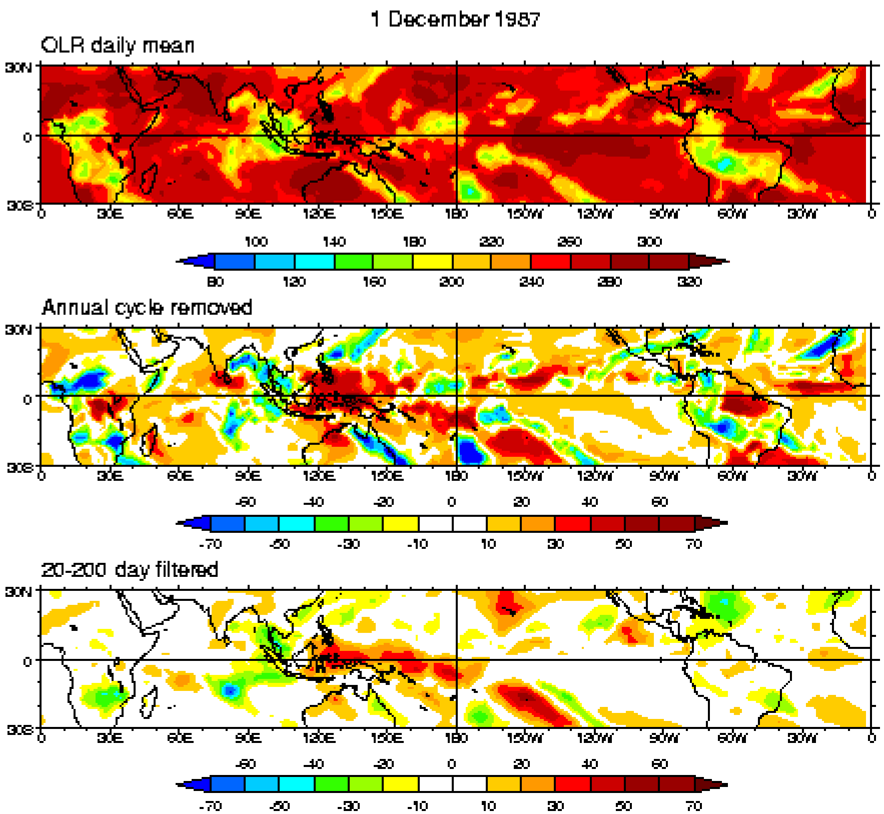
1 December 1987
OLR daily mean
100 140 180 220 260 300
80 120 160 200 240 280 320
Annual cycle removed
-60 -40 -20 0 20 40 60
-70 -50 -30 -10 10 30 50 70
20-200 day filtered
-60 -40 -20 0 20 40 60
-70 -50 -30 -10 10 30 50 70

Perturbations in surface properties and OLR/precip confined to Indian Ocean and western Pacific, but upper tropopsheric wind signals are global

**European Center forecast 200 hPa velocity potential, 4 January to 13 February, 2005**

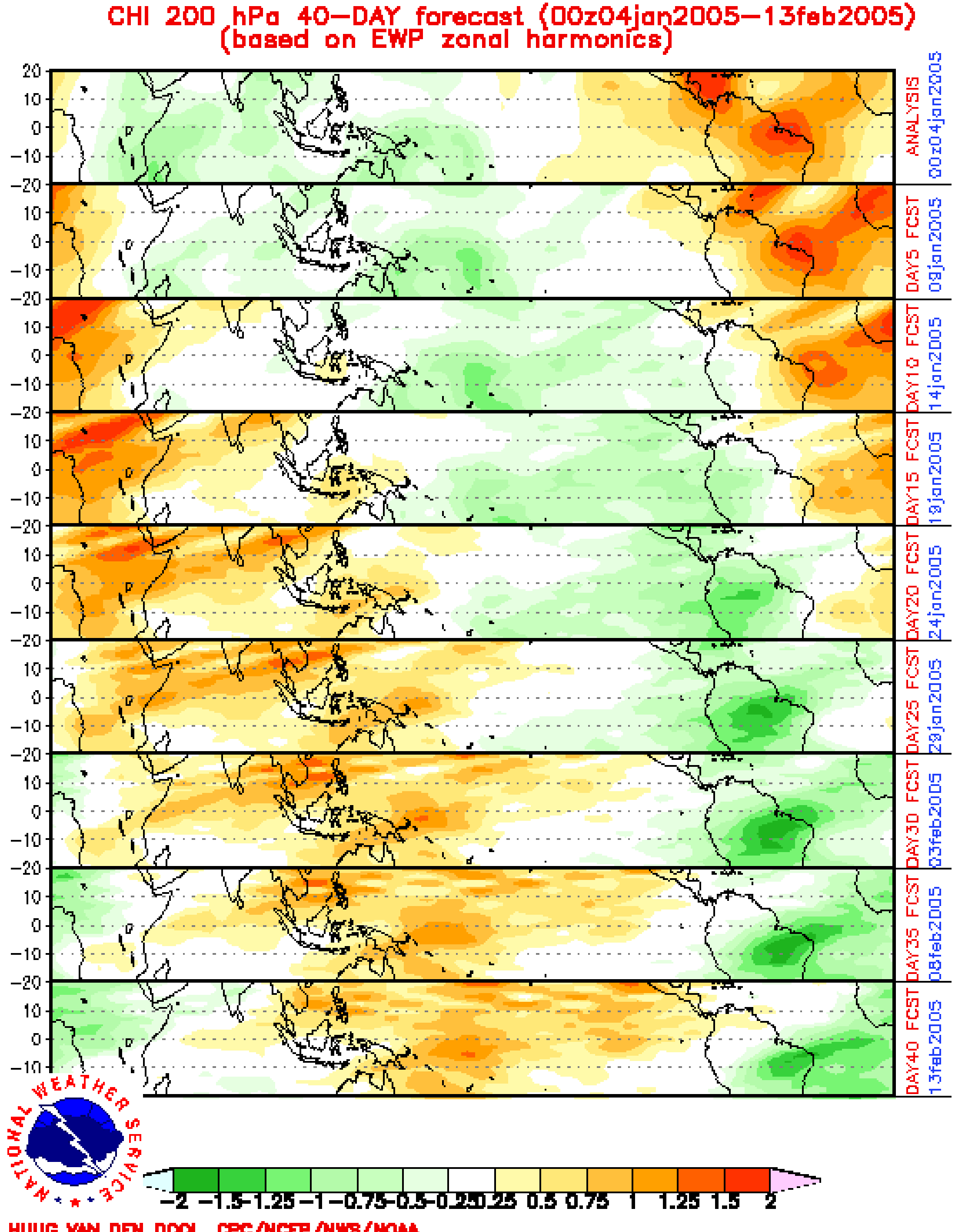

# Observational analyses courtesy of:

*George N. Kiladis*
*NOAA Aeronomy Laboratory, Boulder, Colorado*

*Katherine H. Straub*
*Susquehanna University*

*Patrick T. Haertel*
*University of North Dakota*

# OLR power spectrum, 15ºS-15ºN, 1979–2001 (Symmetric)

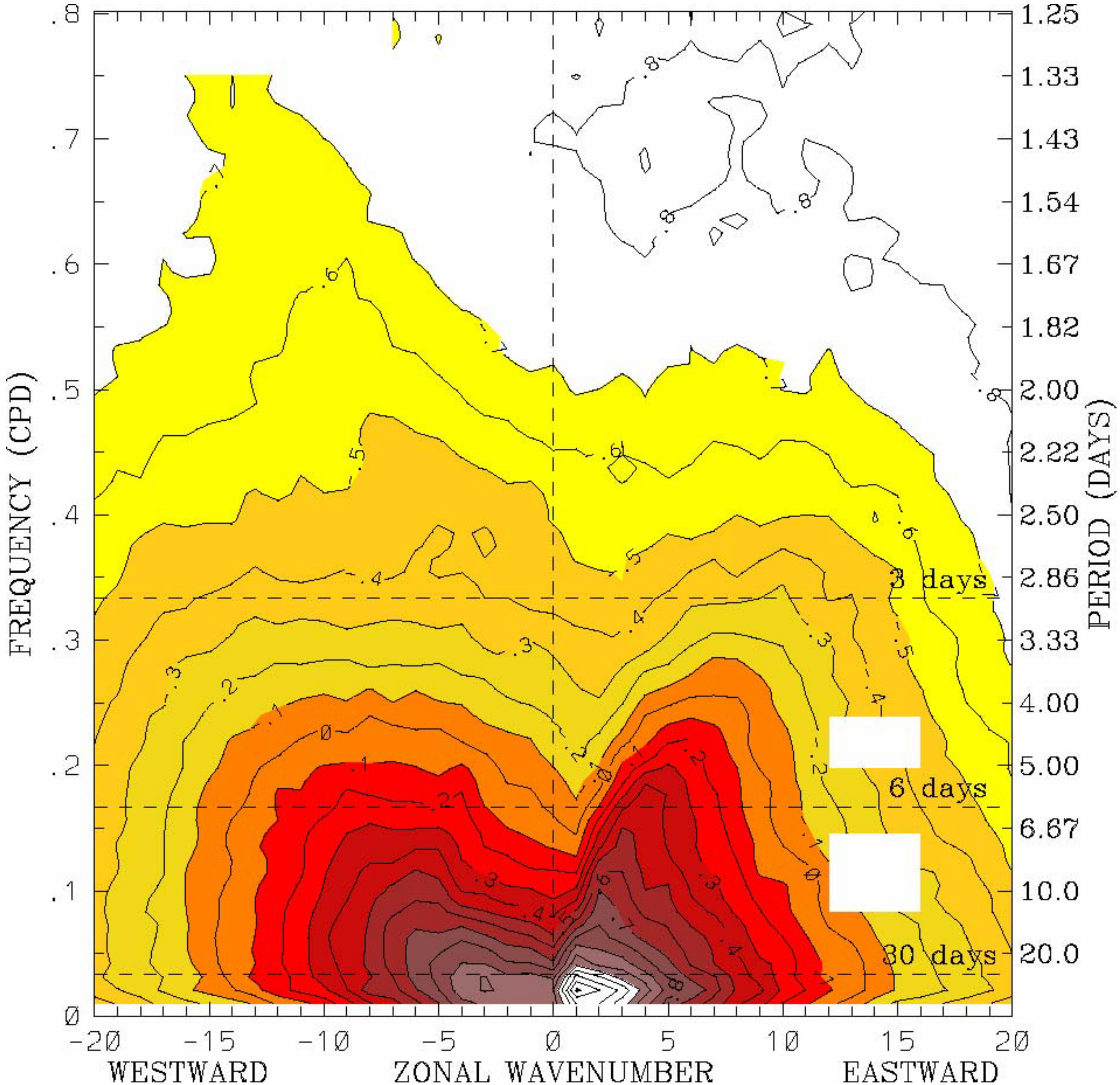


from Wheeler and Kiladis, 1999

# OLR power spectrum, 15ºS-15ºN, 1979–2001 (Antisymmetric)

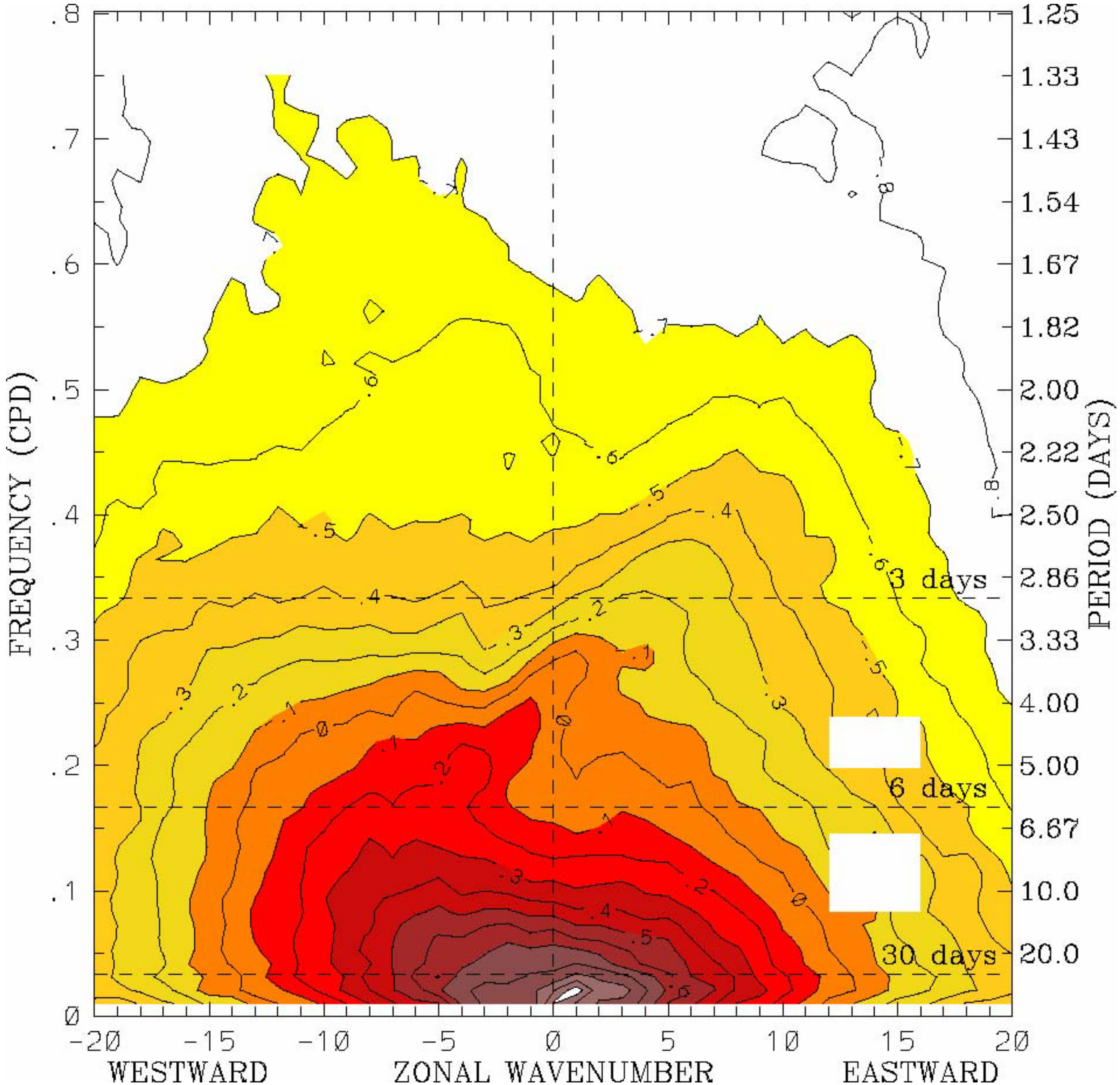


from Wheeler and Kiladis, 1999

# OLR background spectrum, 15ºS-15ºN, 1979–2001

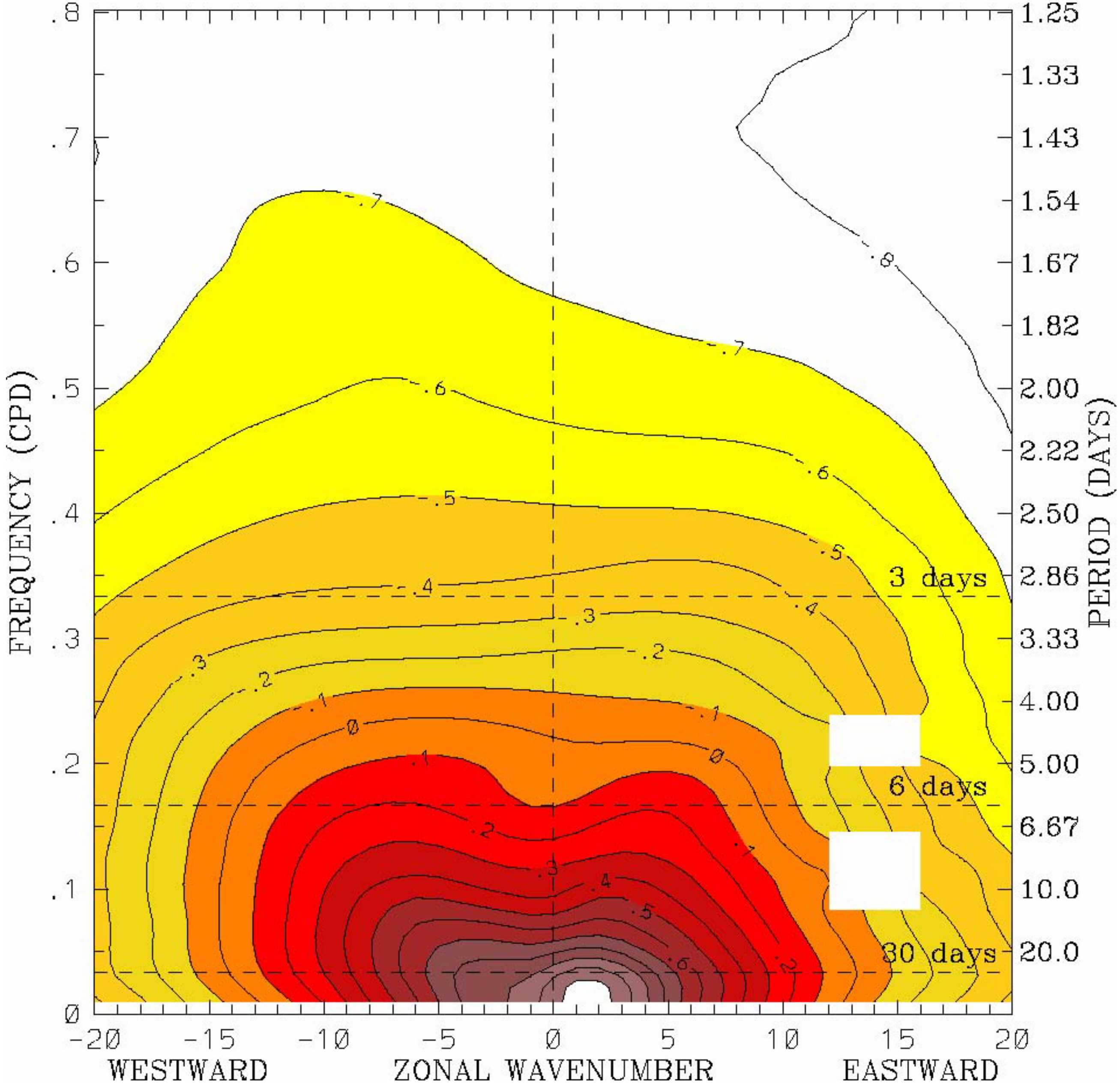


from Wheeler and Kiladis, 1999

# OLR power spectrum, 1979–2001 (Symmetric)

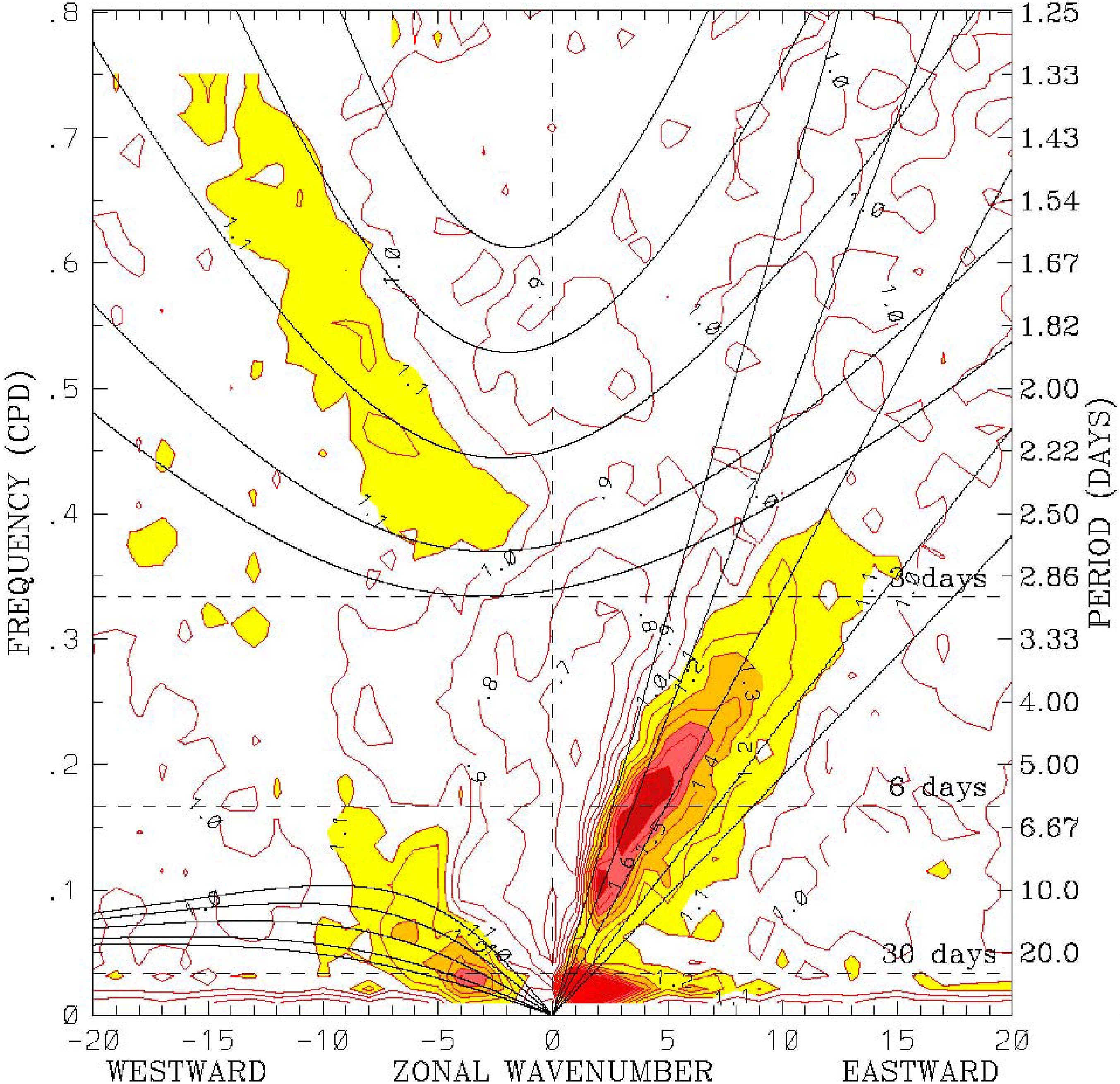


from
Wheeler and Kiladis, 1999

# OLR power spectrum, 1979–2001 (Symmetric)

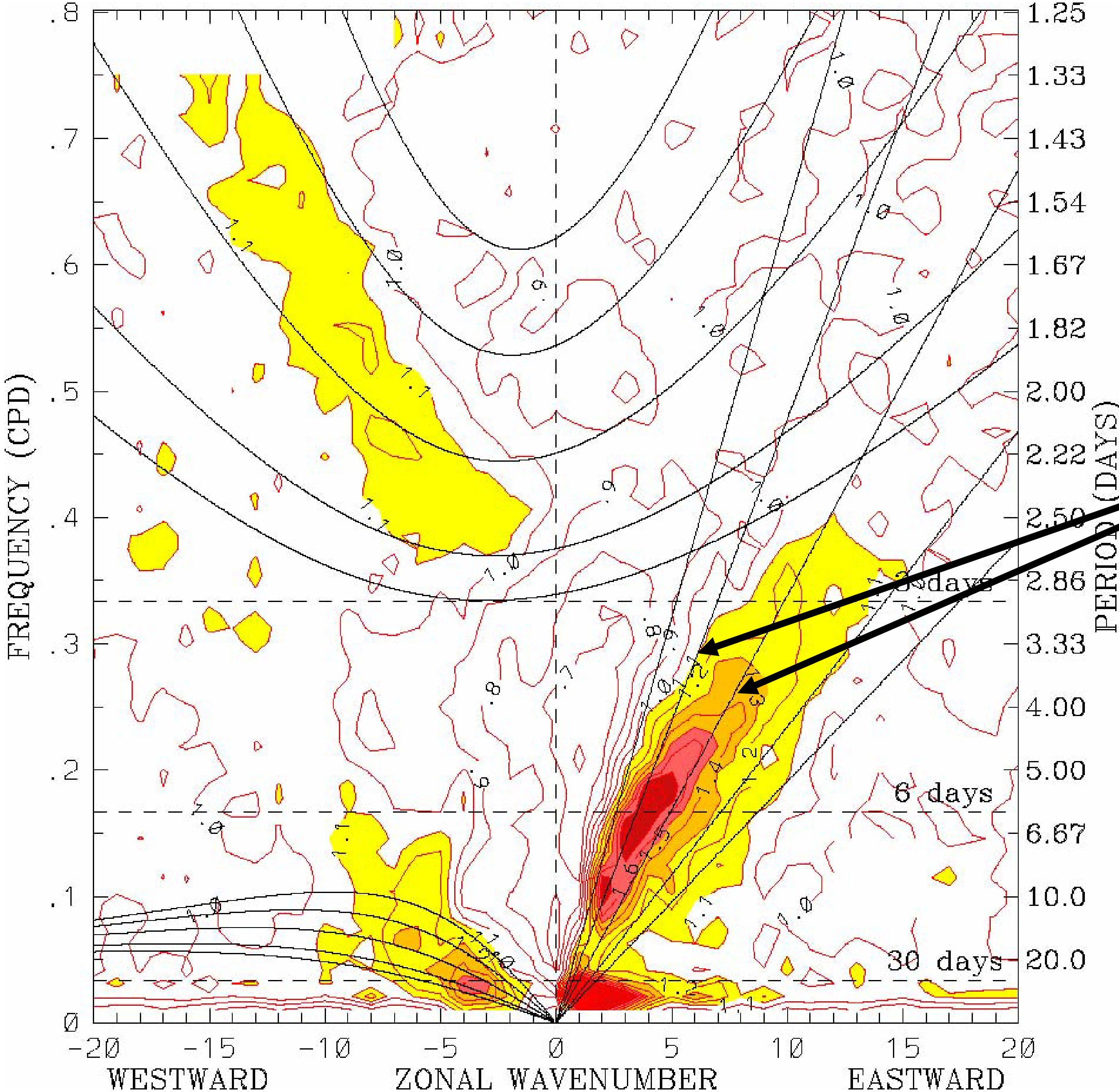


**Kelvin wave Phase Speed: 15 m $s^{-1}$**

from
Wheeler and Kiladis, 1999

# OLR power spectrum, 1979–2001 (Symmetric)

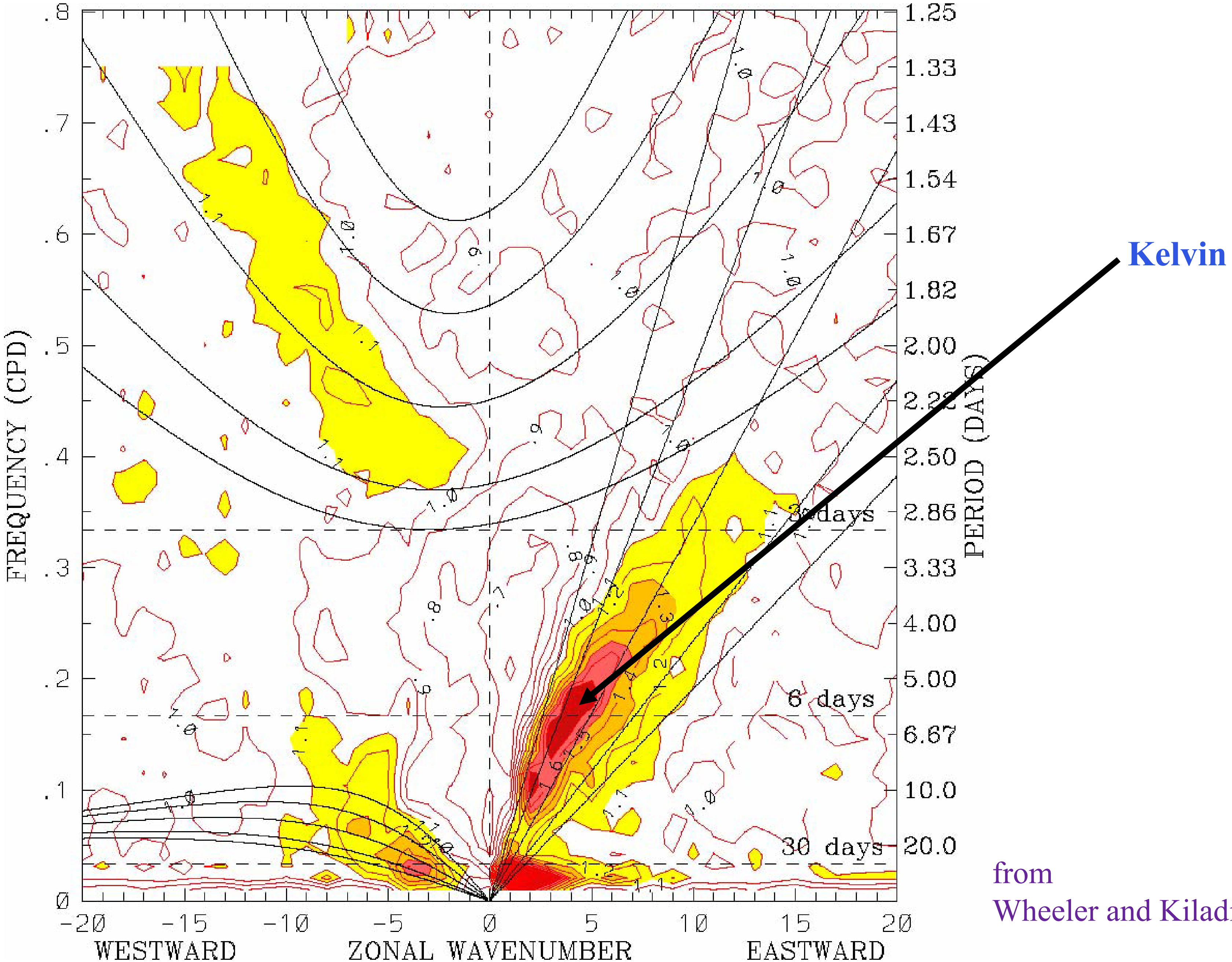


from
Wheeler and Kiladis, 1999

# OLR power spectrum, 1979–2001 (Symmetric)

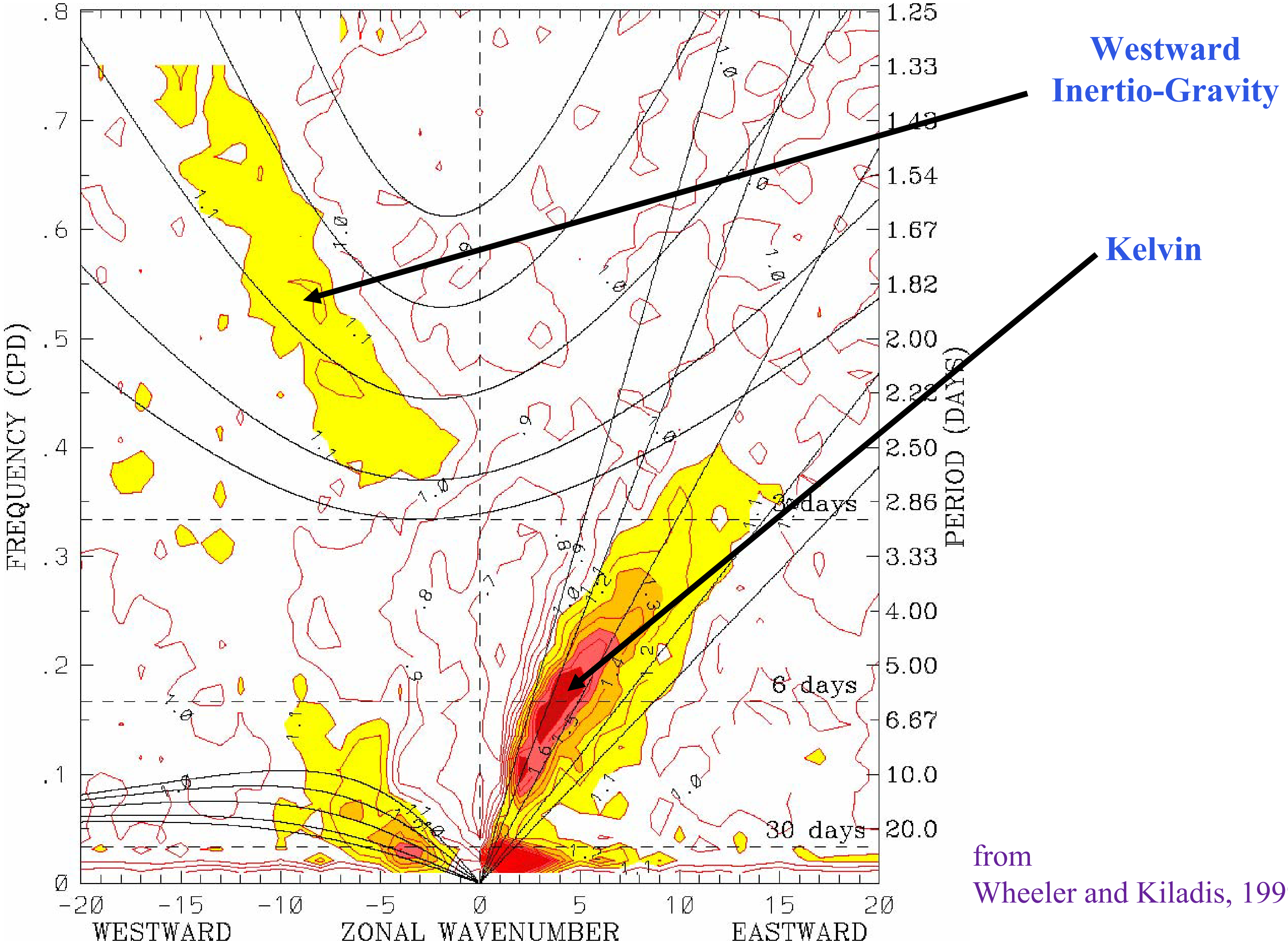


from
Wheeler and Kiladis, 1999

# OLR power spectrum, 1979–2001 (Symmetric)

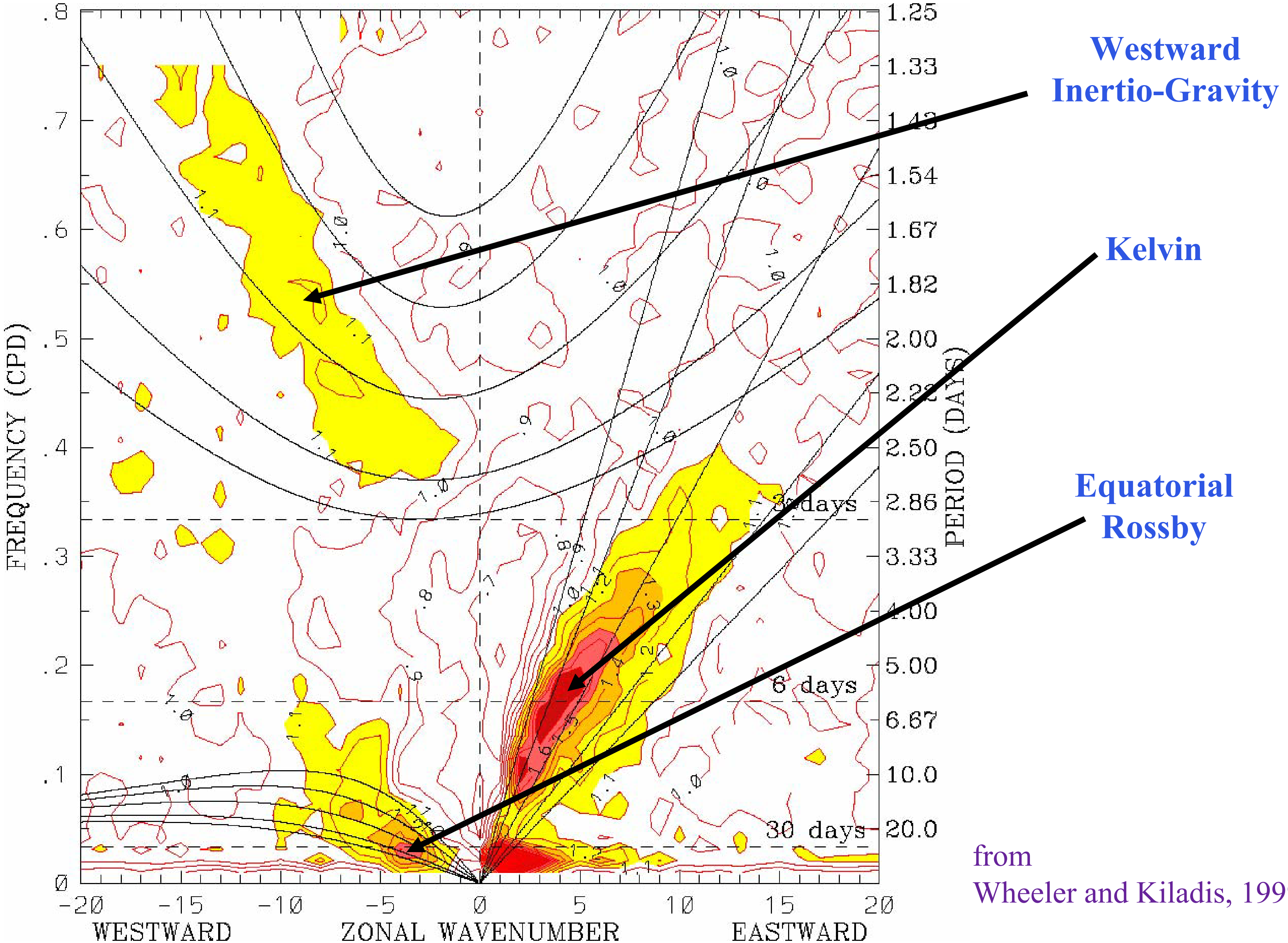


from
Wheeler and Kiladis, 1999

# OLR power spectrum, 1979–2001 (Symmetric)

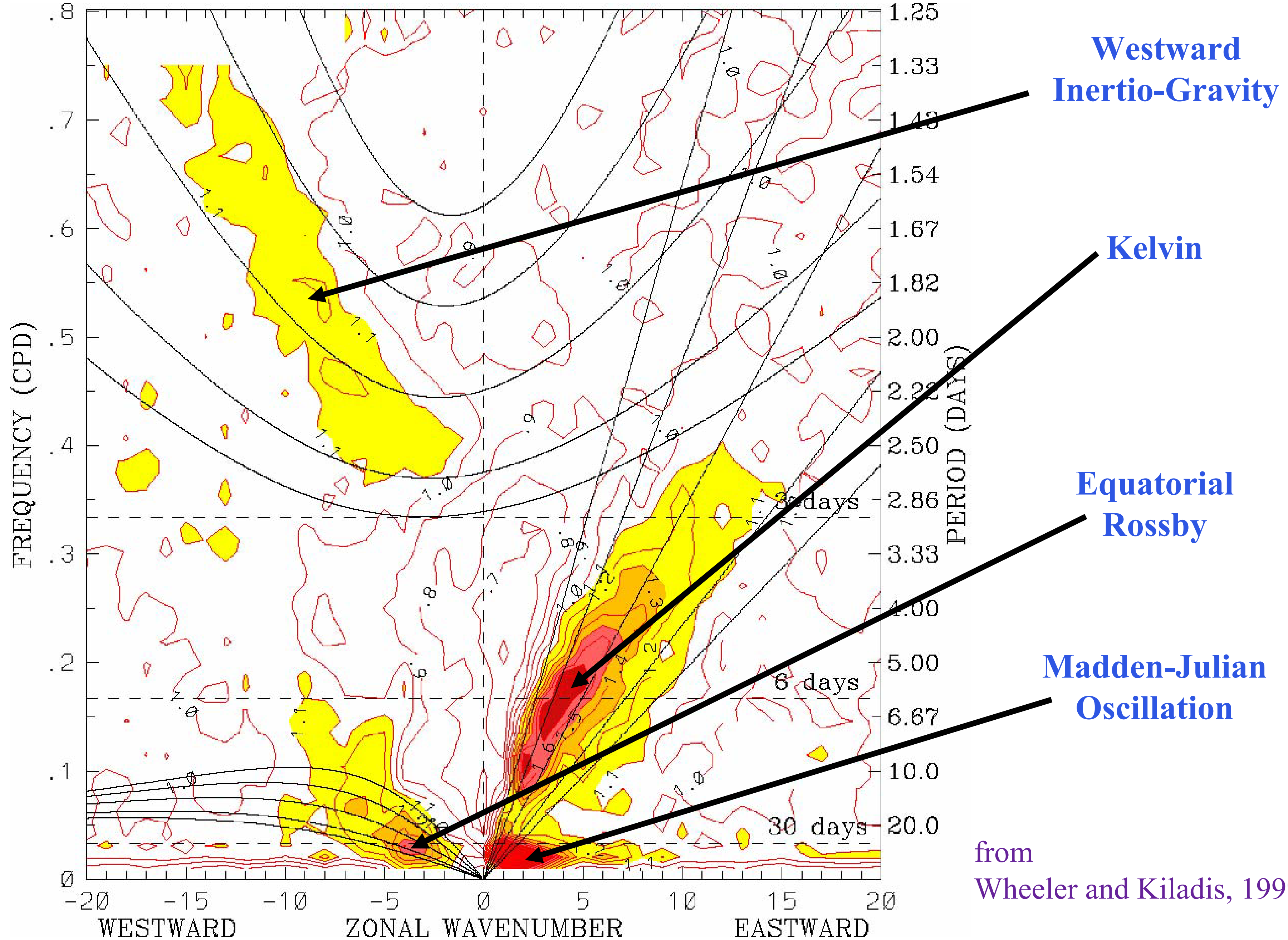


from Wheeler and Kiladis, 1999

# OLR power spectrum, 1979–2001 (Antisymmetric)

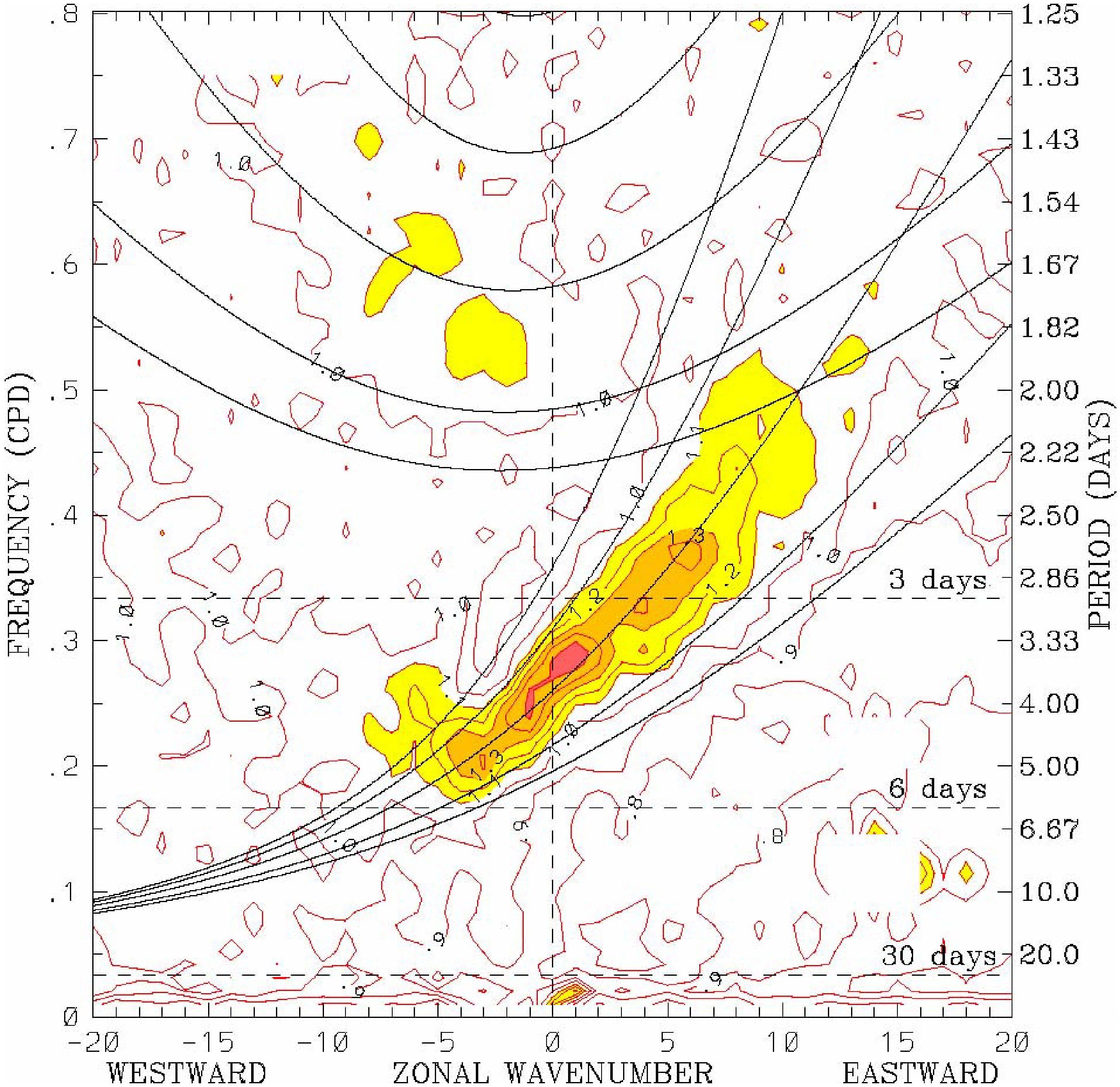


from
Wheeler and Kiladis, 1999

# OLR power spectrum, 1979–2001 (Antisymmetric)

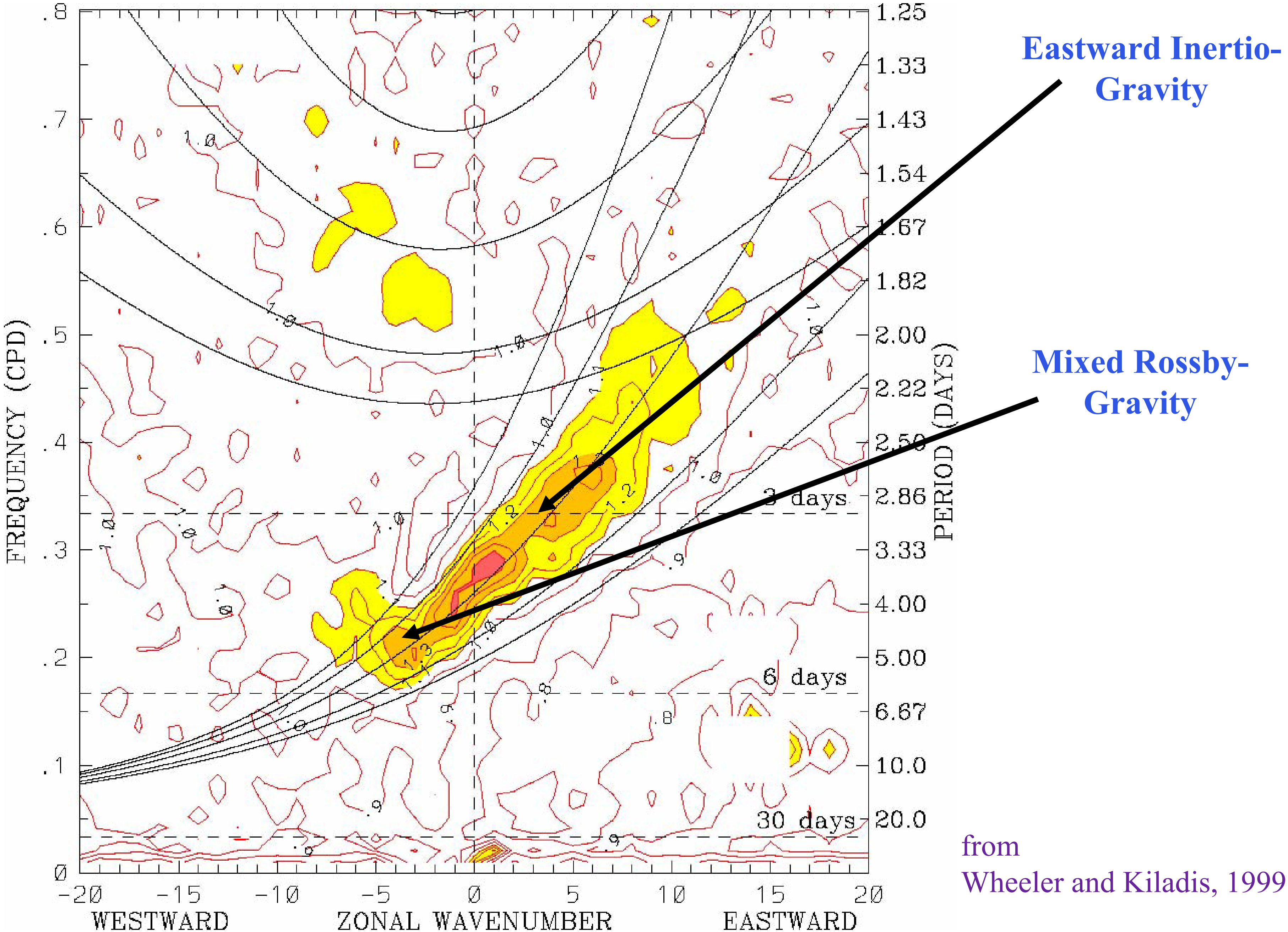


from
Wheeler and Kiladis, 1999

# OLR power spectrum, 1979–2001 (Symmetric)

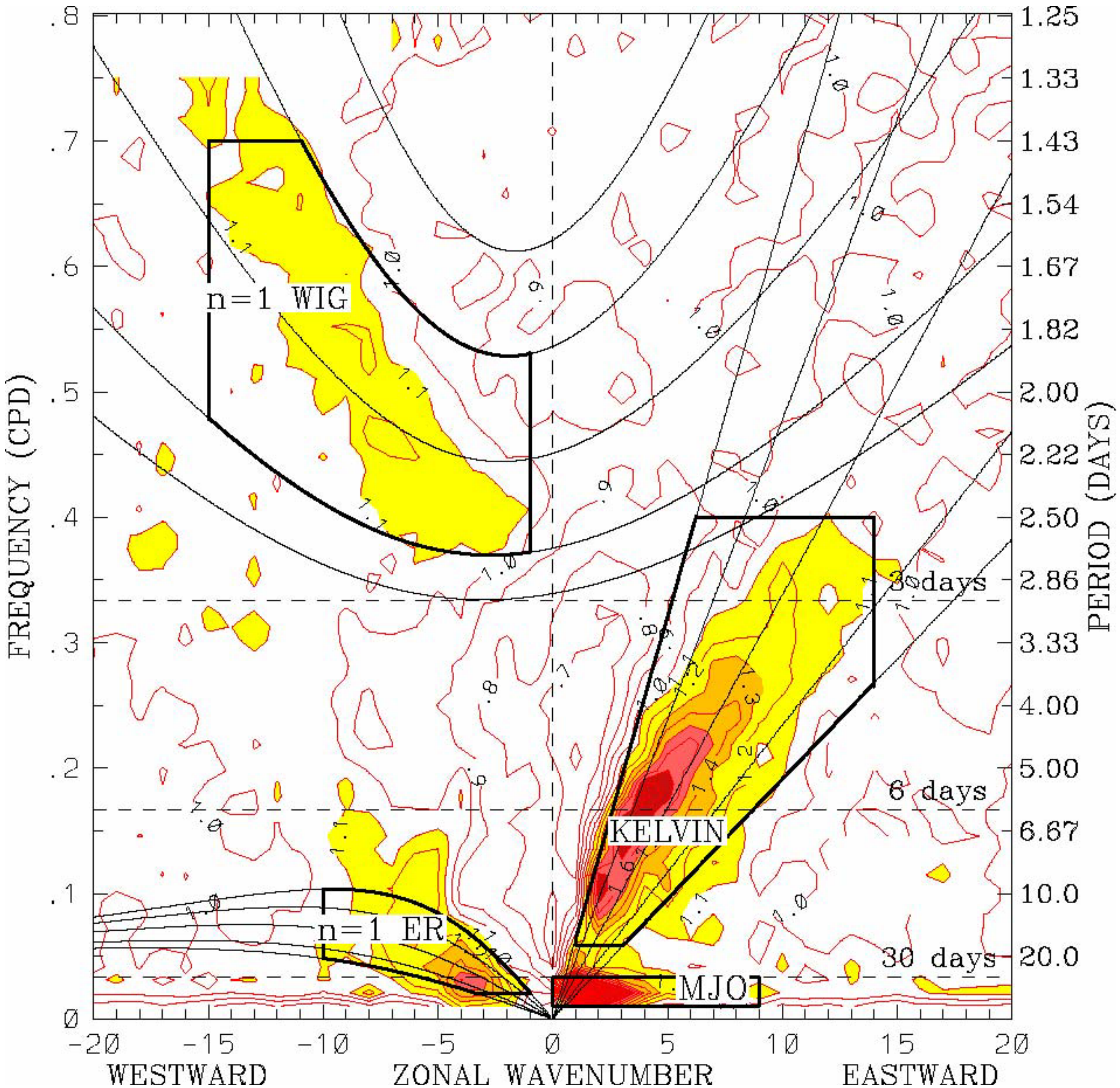

# OBSERVATIONS OF KELVIN WAVES AND THE MJO

## Time–longitude diagram of CLAUS Tb (5S–equator), February 1987

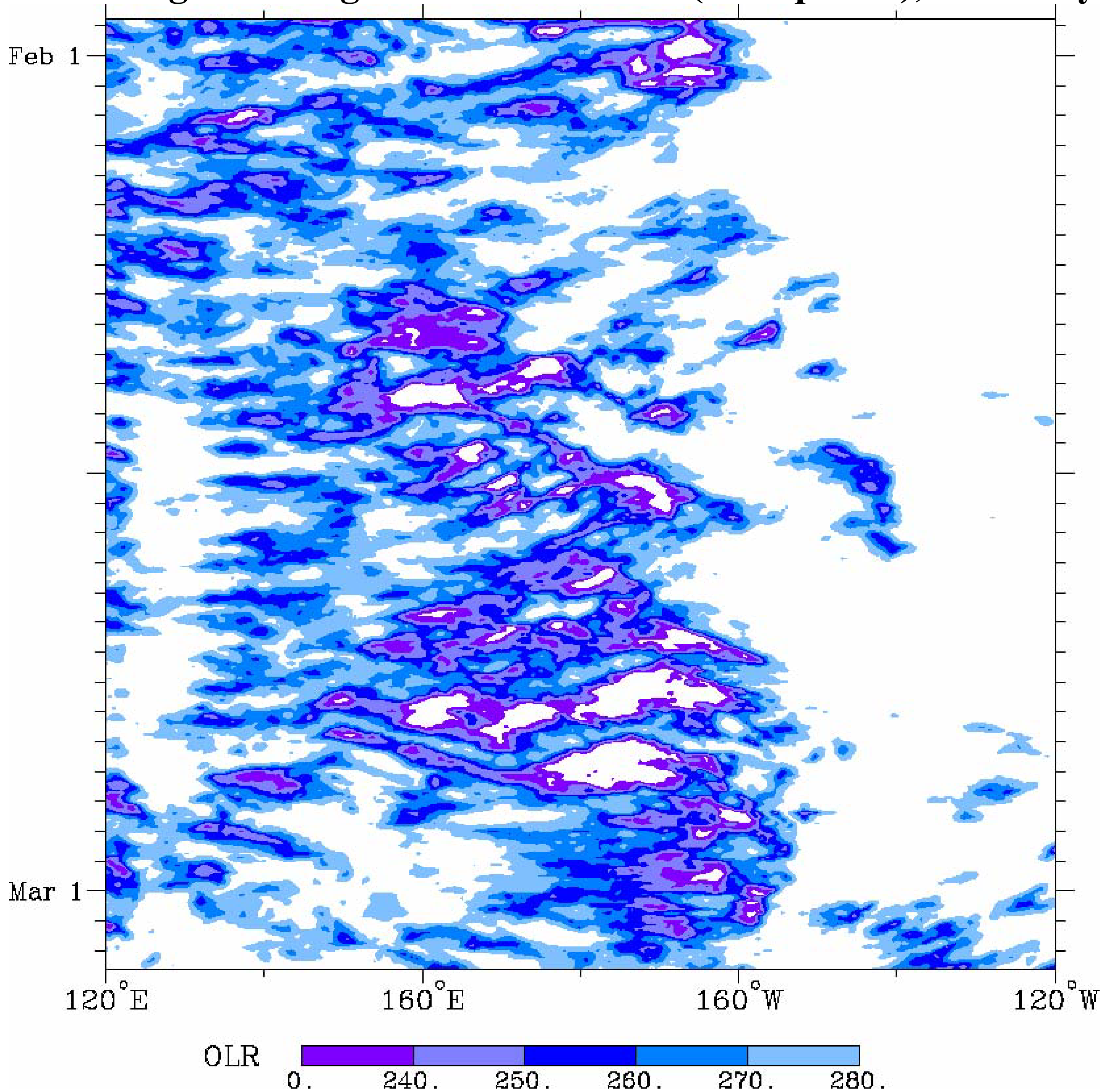

# OBSERVATIONS OF TWO DAY (WIG), KELVIN WAVES AND THE MJO

**Time–longitude diagram of CLAUS Tb (2.5S–2.5N), October–December 1992**

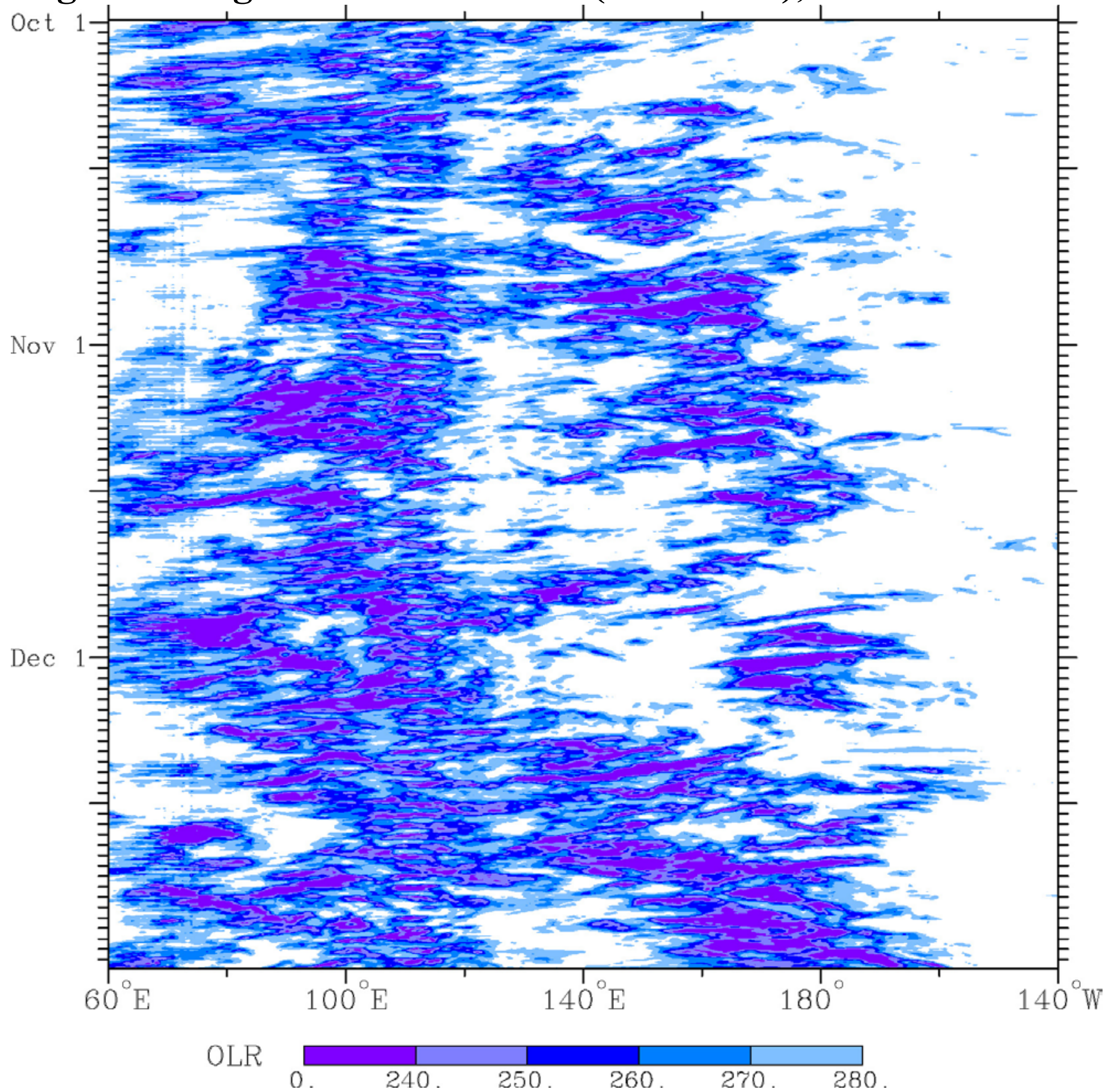

# OBSERVATIONS OF TWO DAY (WIG), KELVIN WAVES AND THE MJO

**Time–longitude diagram of CLAUS Tb (2.5S–2.5N), October–December 1992**

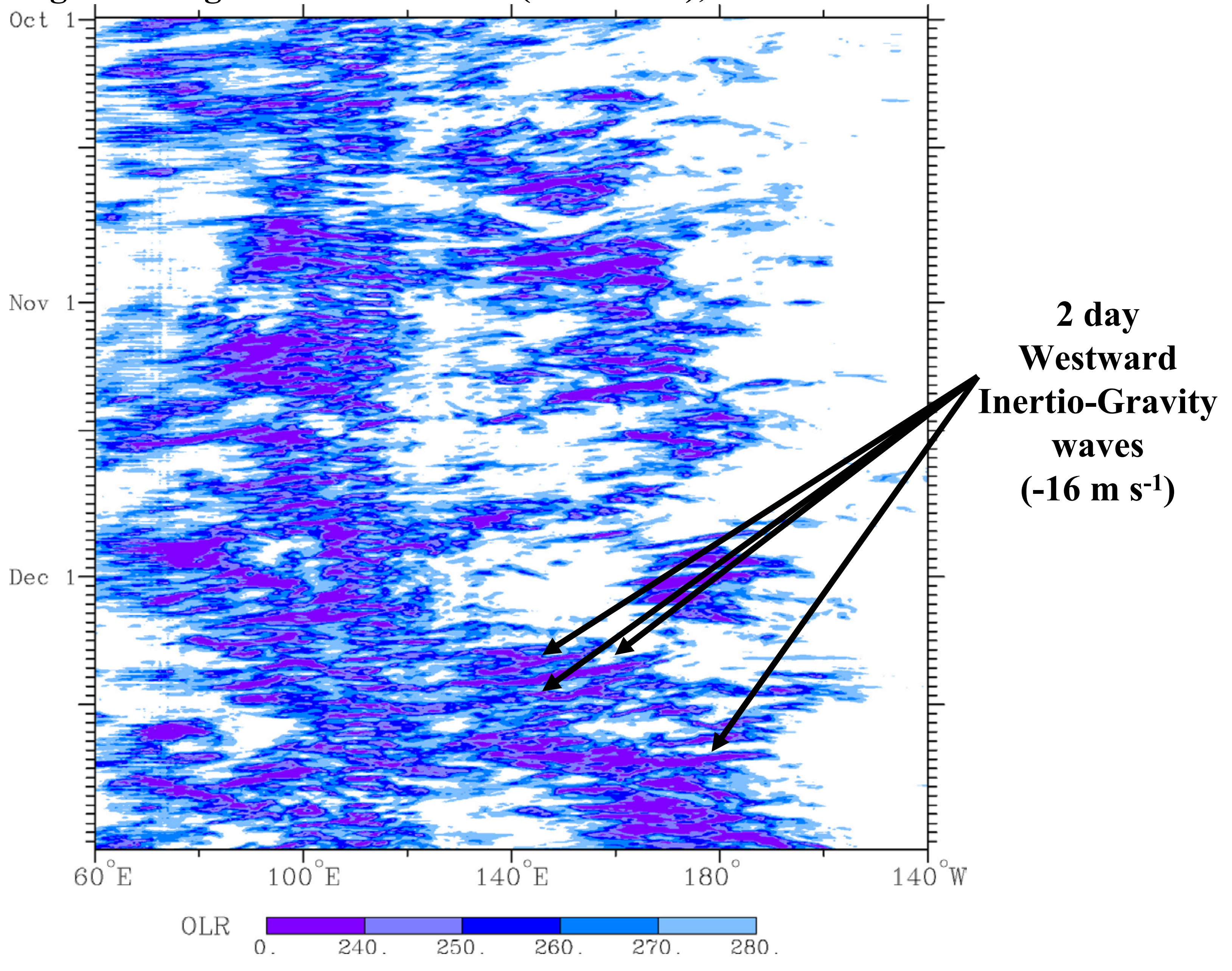

# OBSERVATIONS OF TWO DAY (WIG), KELVIN WAVES AND THE MJO

**Time–longitude diagram of CLAUS Tb (2.5S–2.5N), October–December 1992**

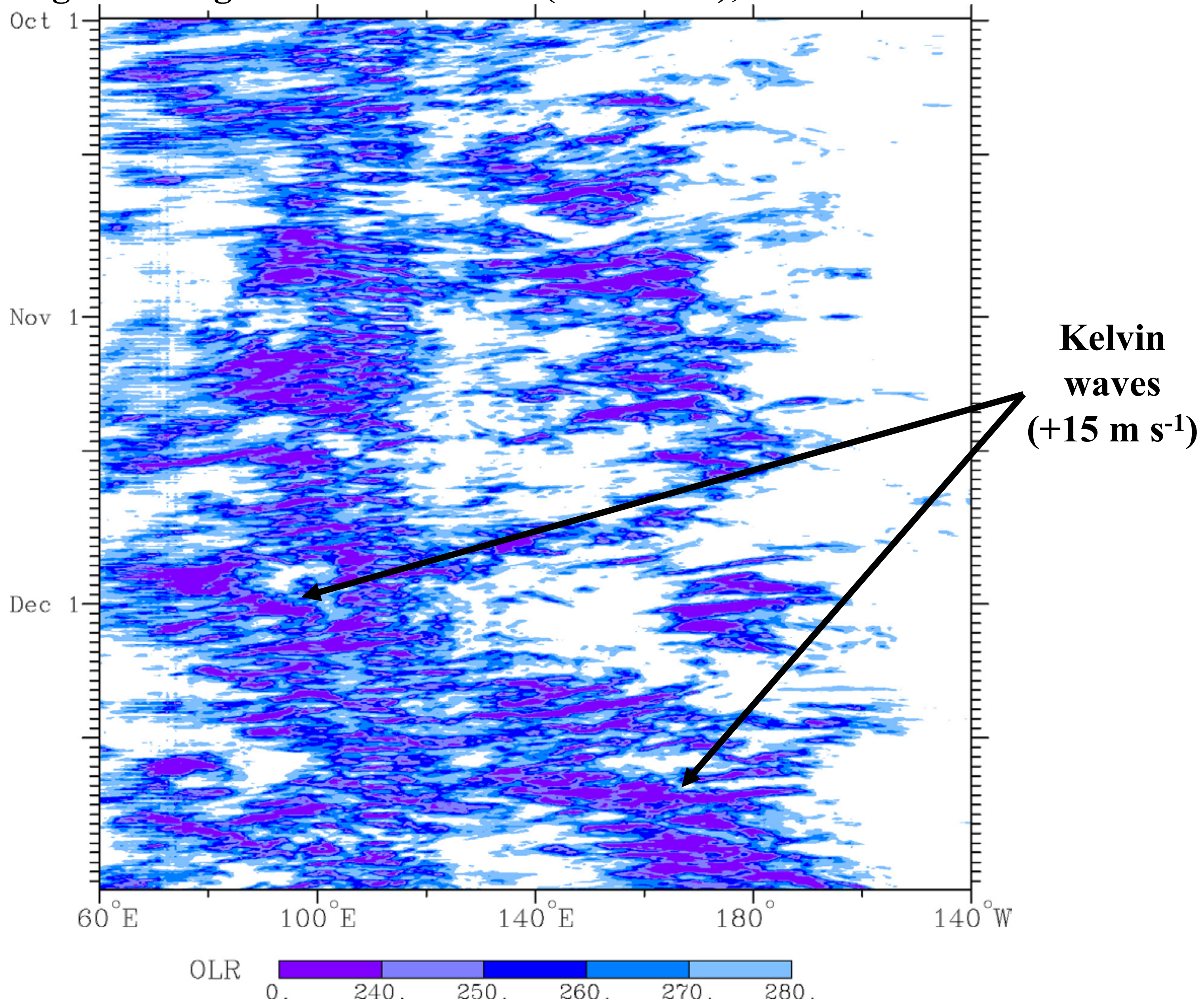

# OBSERVATIONS OF KELVIN WAVES AND THE MJO

## Time–longitude diagram of CLAUS Tb (2.5S–7.5N), January–April 1987

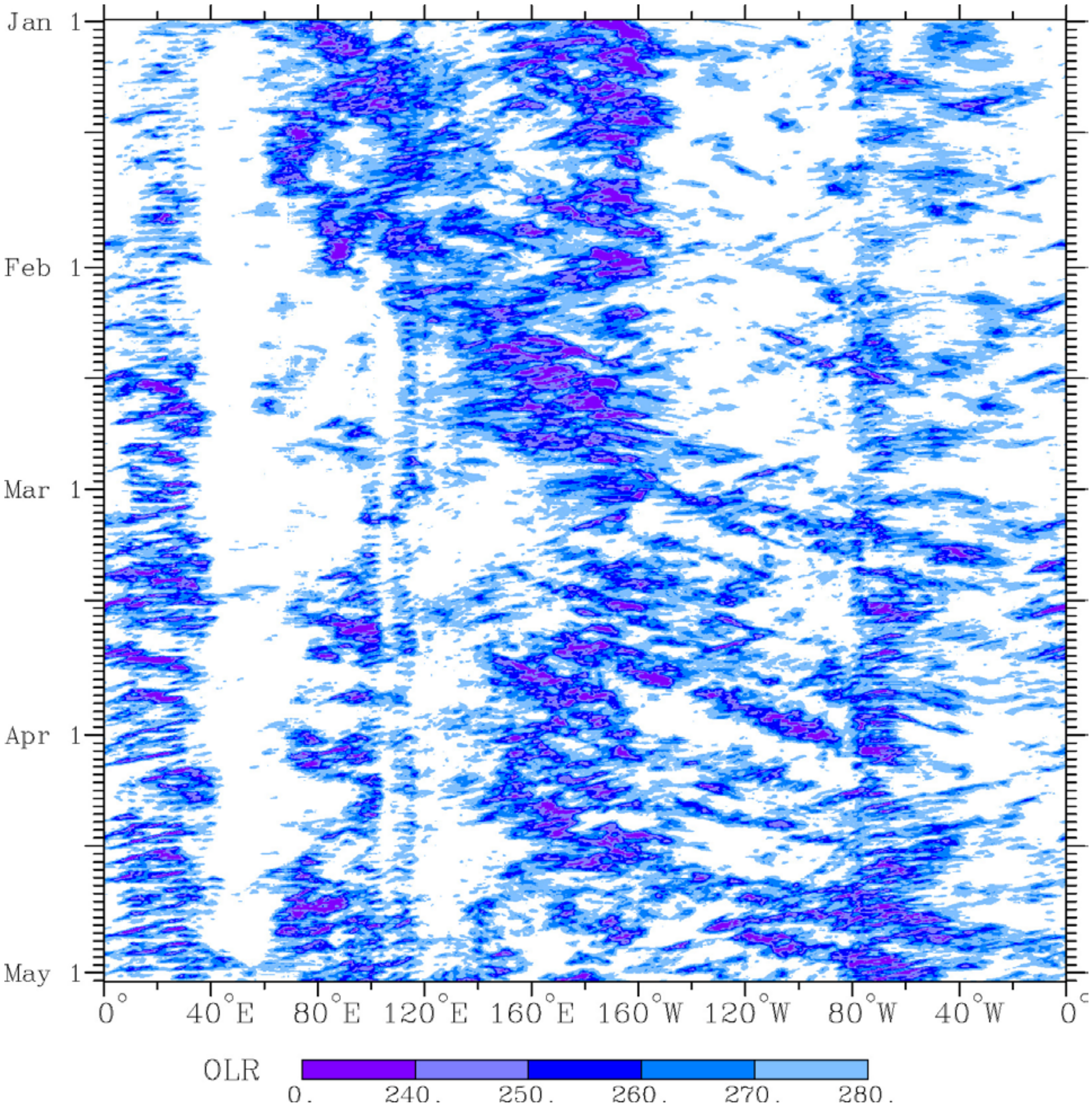

# OBSERVATIONS OF KELVIN WAVES AND THE MJO

**Time–longitude diagram of CLAUS Tb (2.5S–7.5N), January–April 1987**

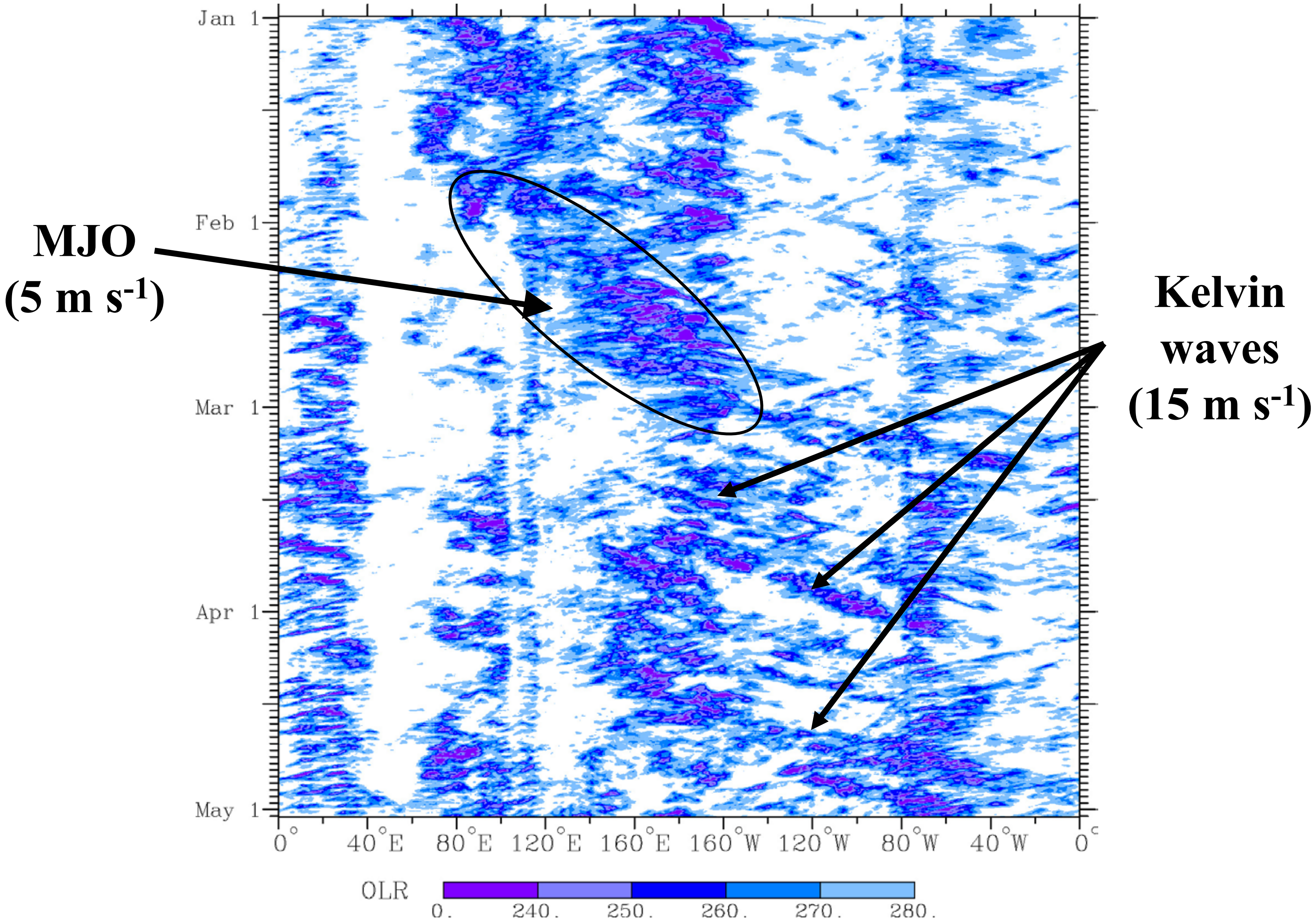

# OBSERVATIONS OF KELVIN AND MRG WAVES

## Time–longitude diagram of CLAUS Tb (2.5S–7.5N), May 1987

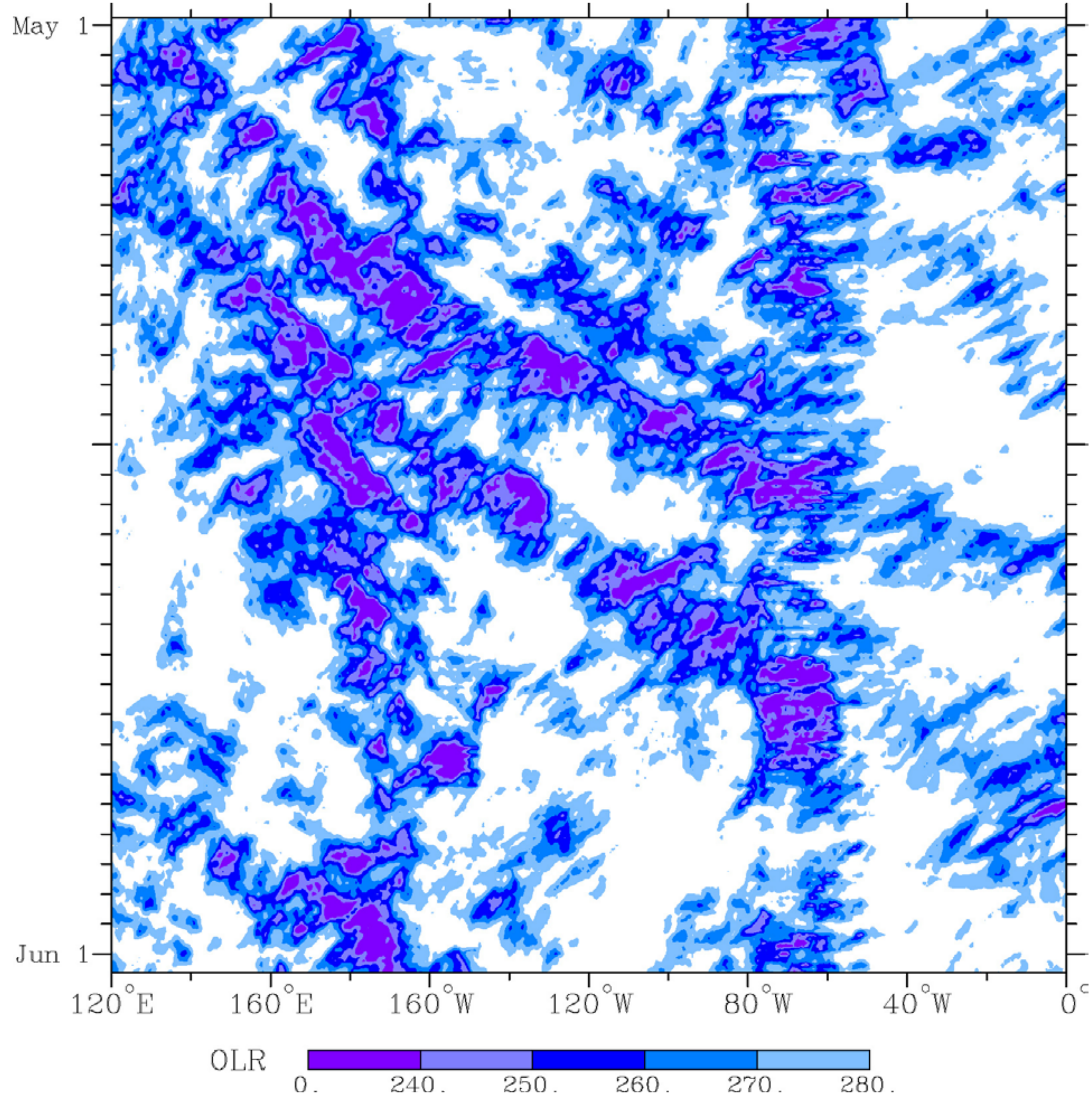

# 1998 OLR 2.5ºS-2.5º N

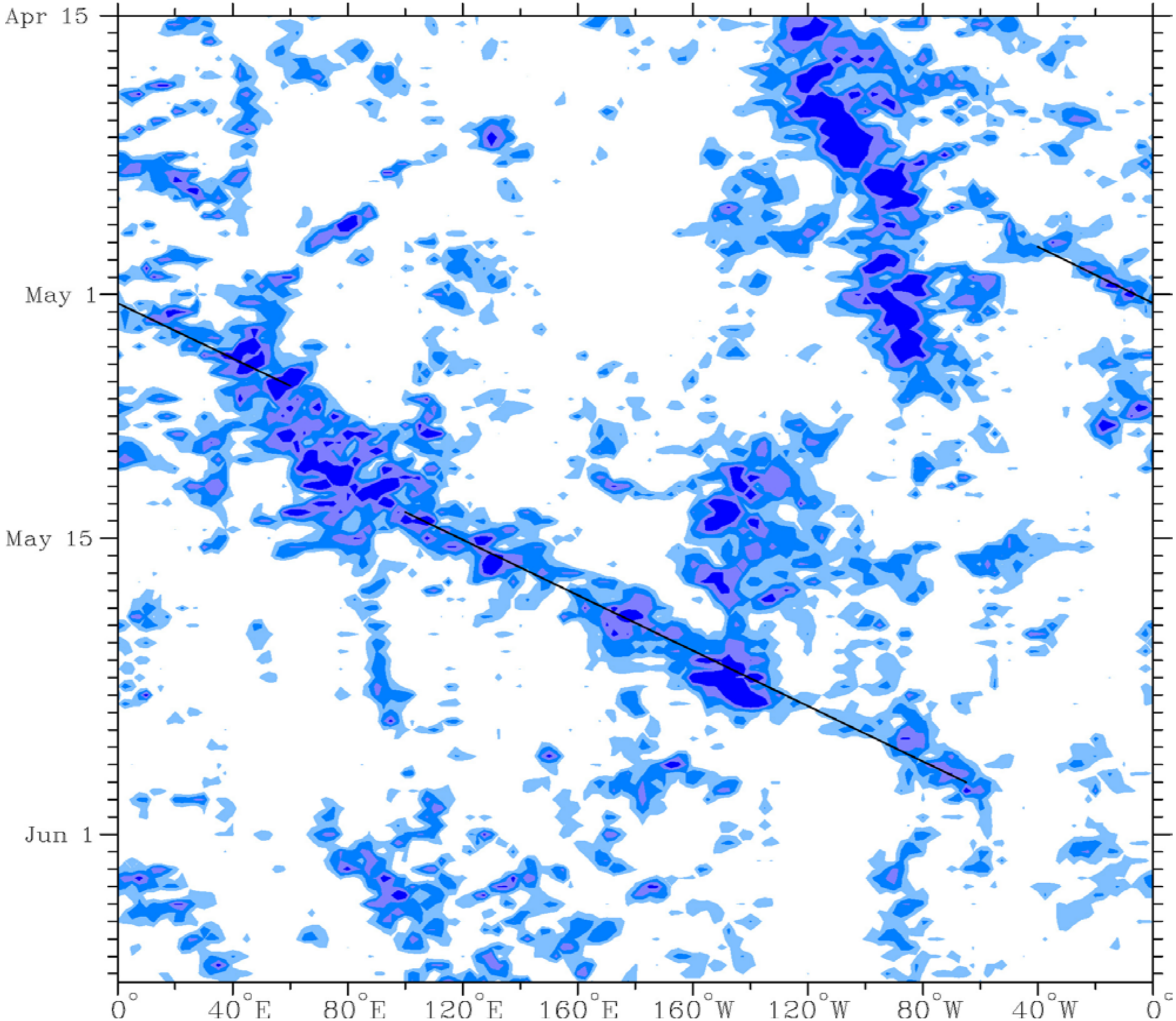


OLR shading starts at - 10 W $m^{-2}$ at 20 W $m^{-2}$ intervals, negative only

# *Regression Model*

## Simple Linear Model:

$$y = ax + b$$

**where: x= predictor (filtered OLR)**
**y= predictand (OLR, circulation)**

# Convective Fraction from TRMM TMI Regressed against MJO-filtered OLR at Eq, 80°E (scaled -40 W m$^2$) for 1998-2003

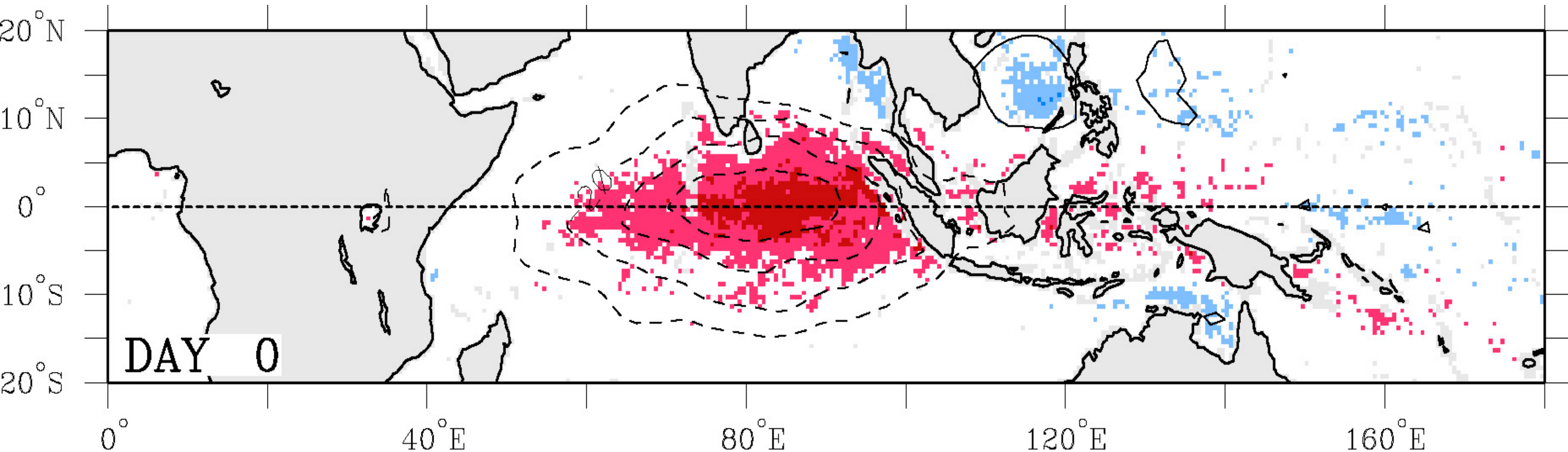


OLR (contours, 10 W m$^{-2}$)
Convective Fraction (shading, ± 2 and 5%), red positive

# Convective Fraction from TRMM TMI Regressed against Kelvin-filtered OLR at 7.5°N, 172.5°W (scaled -40 W $m^2$) for 1998-2003

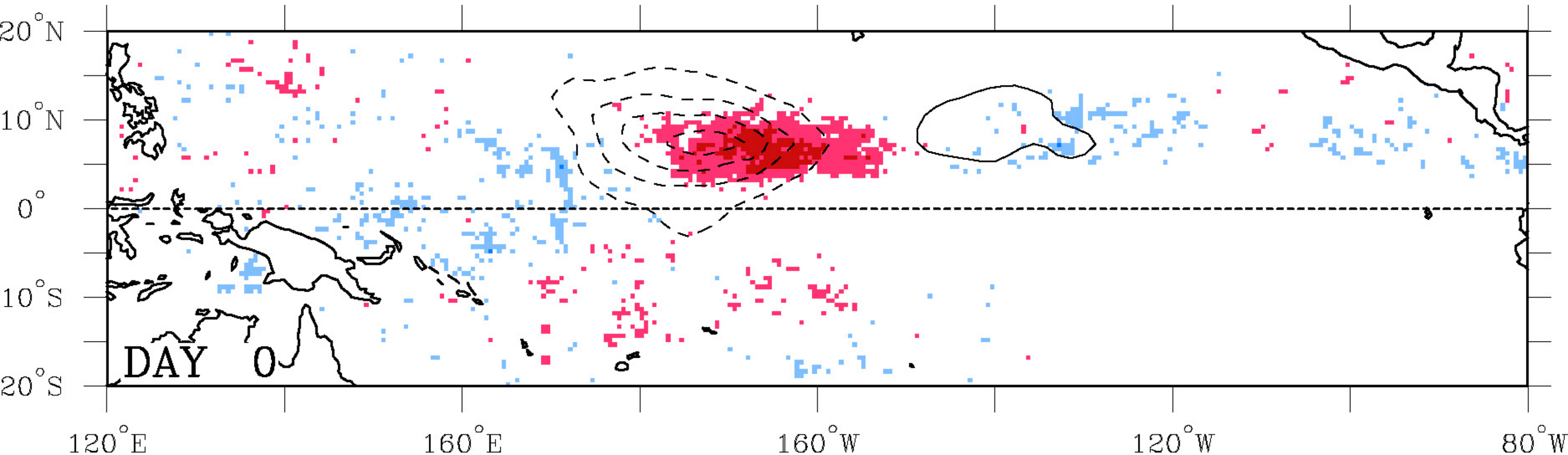


OLR (contours, 10 W $m^{-2}$)
Convective Fraction (shading, ± 2 and 5%), red positive

# Convective Fraction from TRMM TMI Regressed against MRG-filtered OLR at 7.5°N, 172.5°W (scaled -40 W m$^2$) for 1998-2003

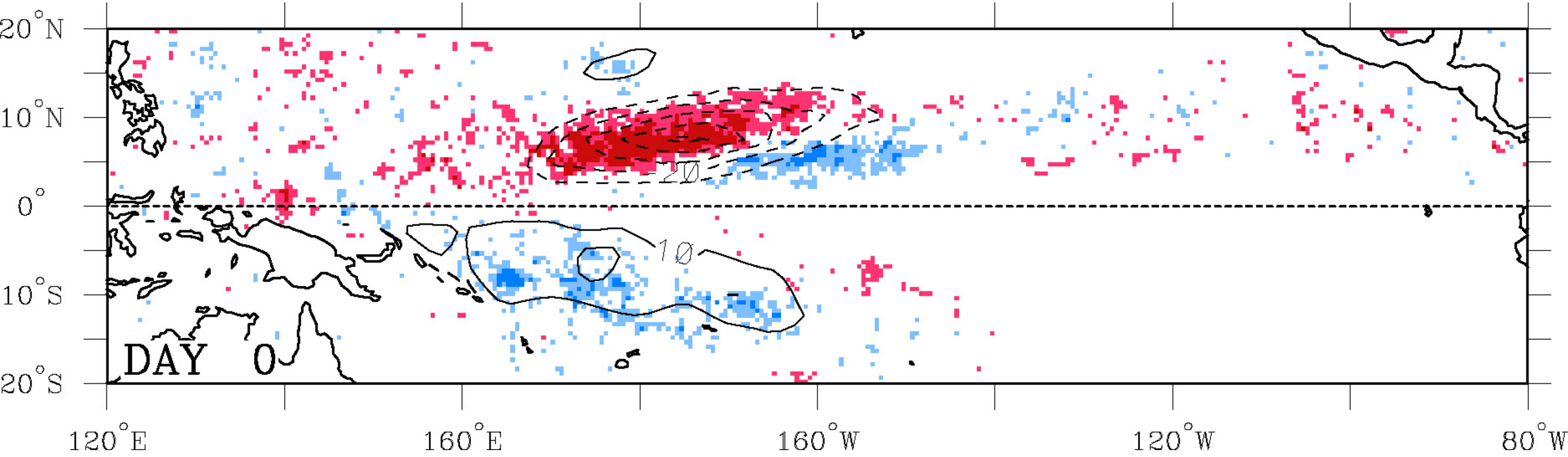


OLR (contours, 10 W m$^{-2}$)

Convective Fraction (shading, ± 2 and 5%), red positive

# Morphology of a Tropical Mesoscale Convective Complex in the eastern Atlantic during GATE (from Zipser et al. 1981)

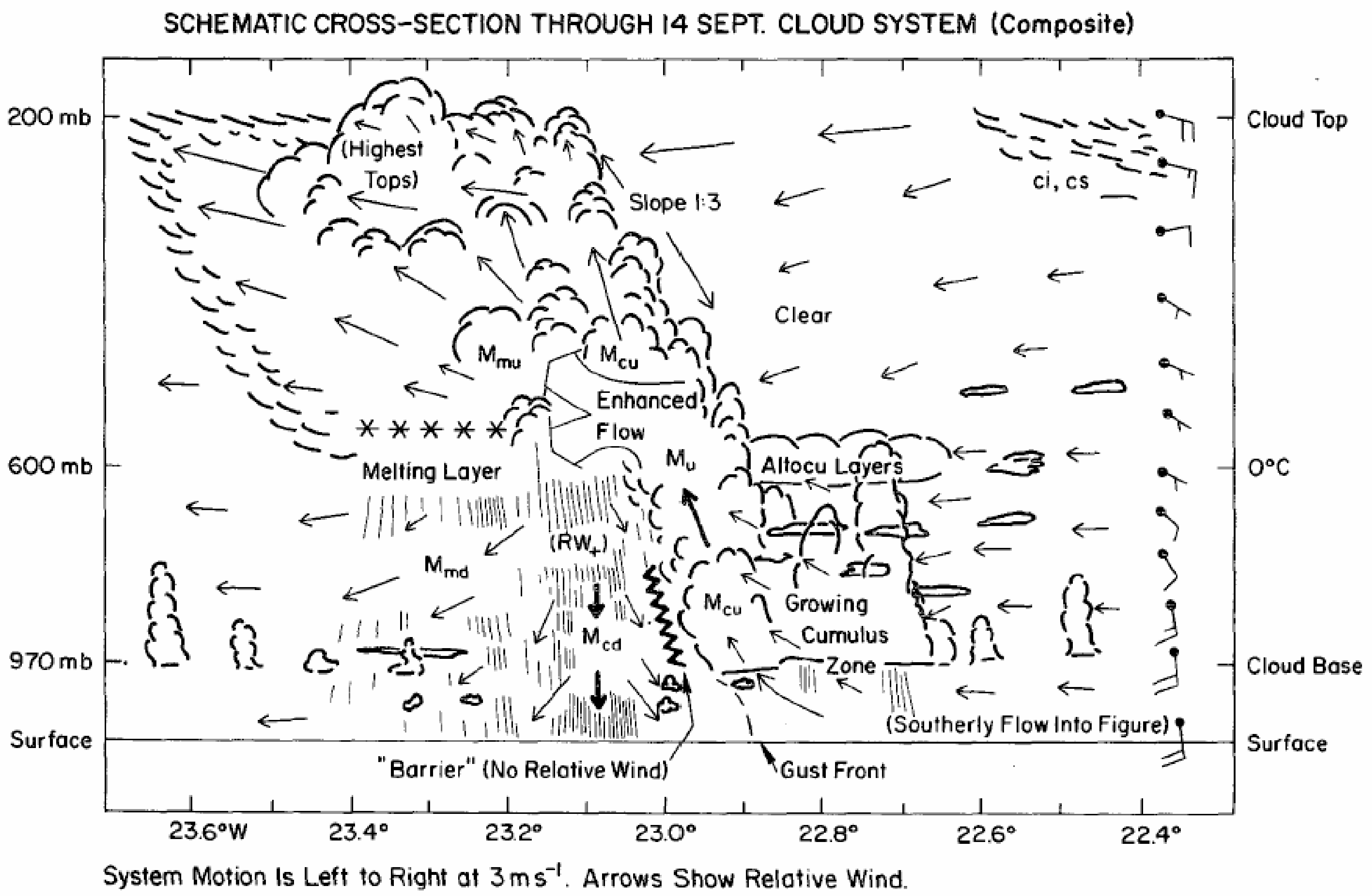

# Two day wave cloud morphology (from Takayabu et al. 1996)

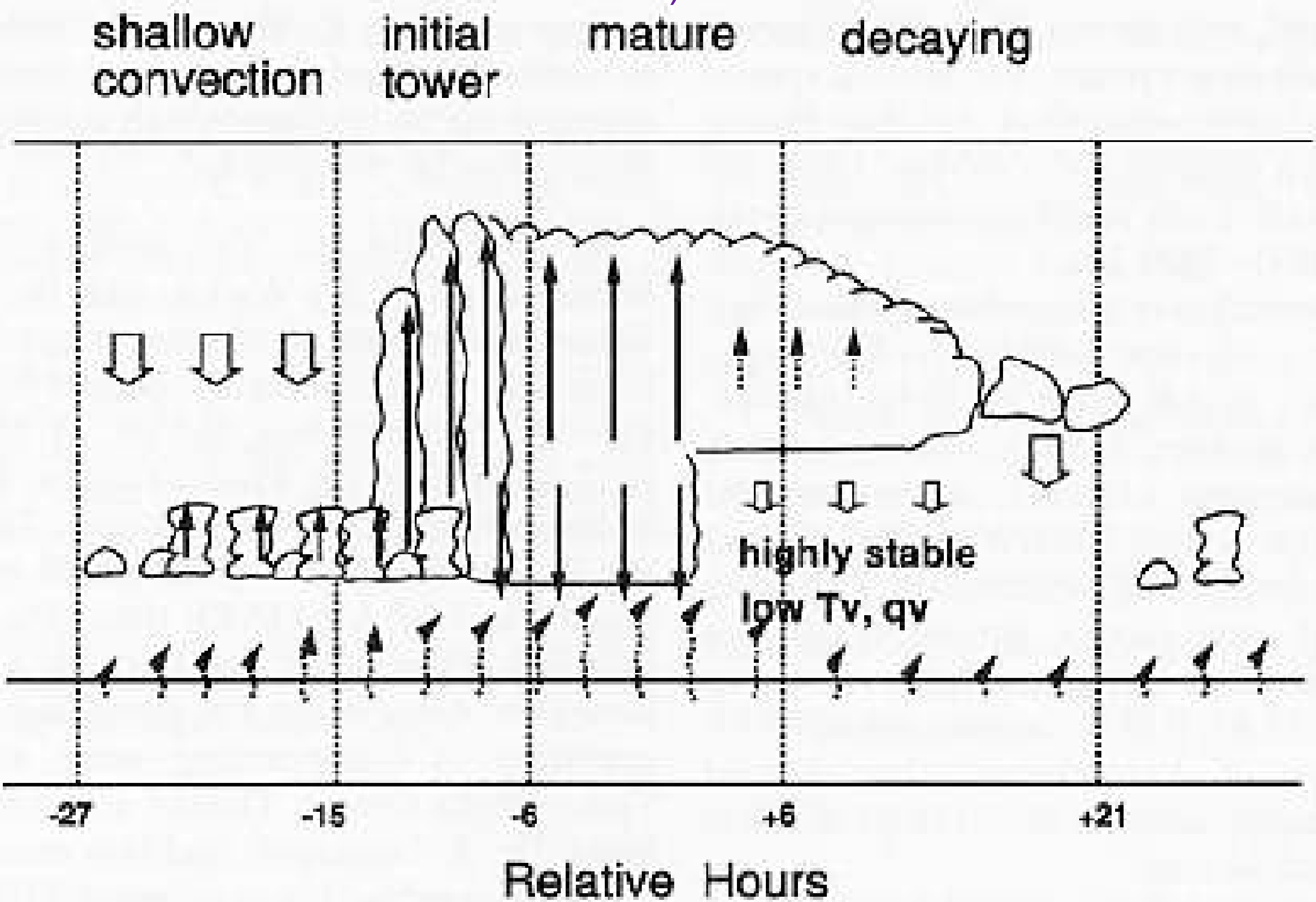

# Observed Kelvin wave morphology (from Straub and Kiladis 2003)

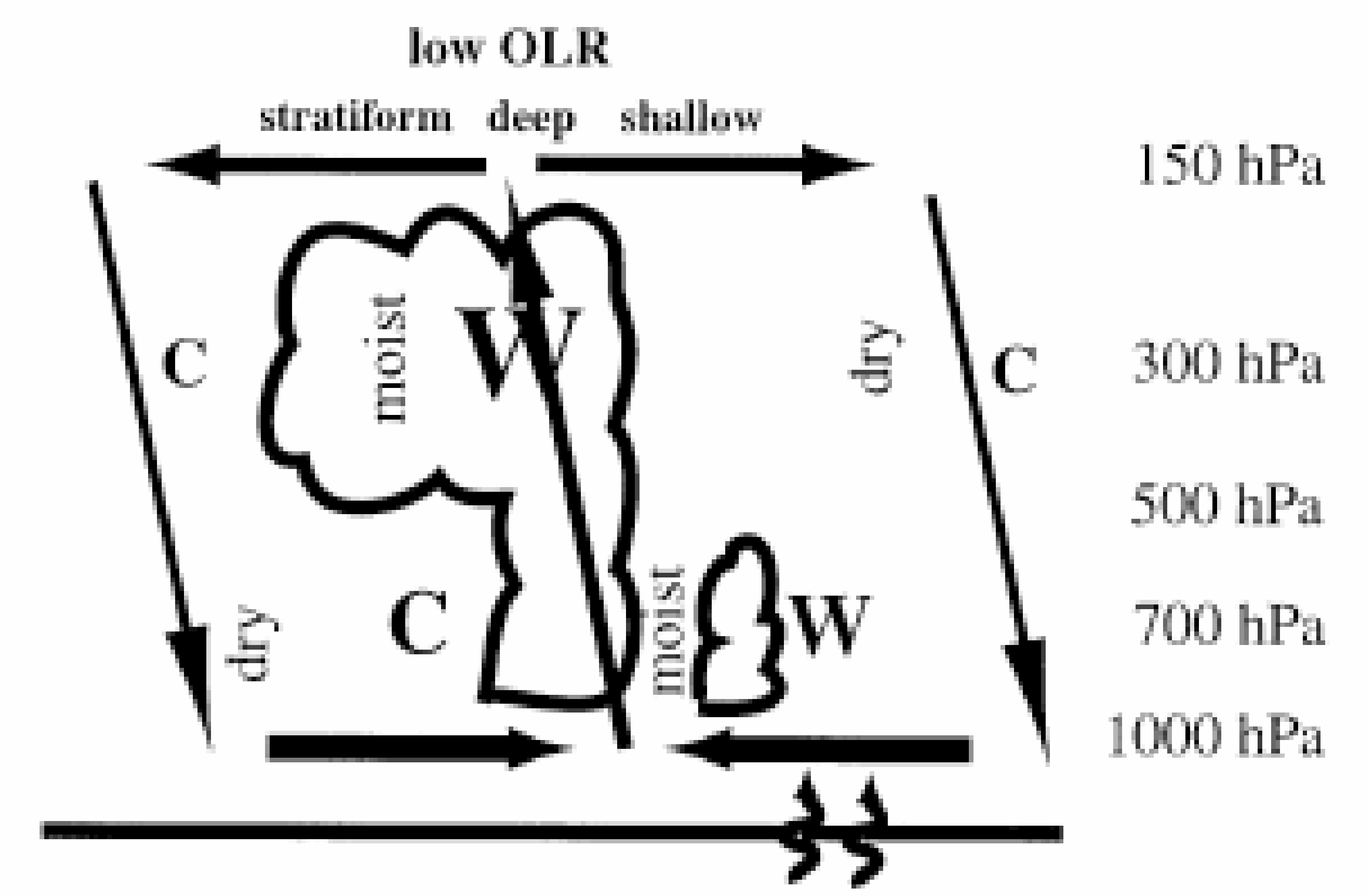

# Morphology of MJO (from Wang 2005)

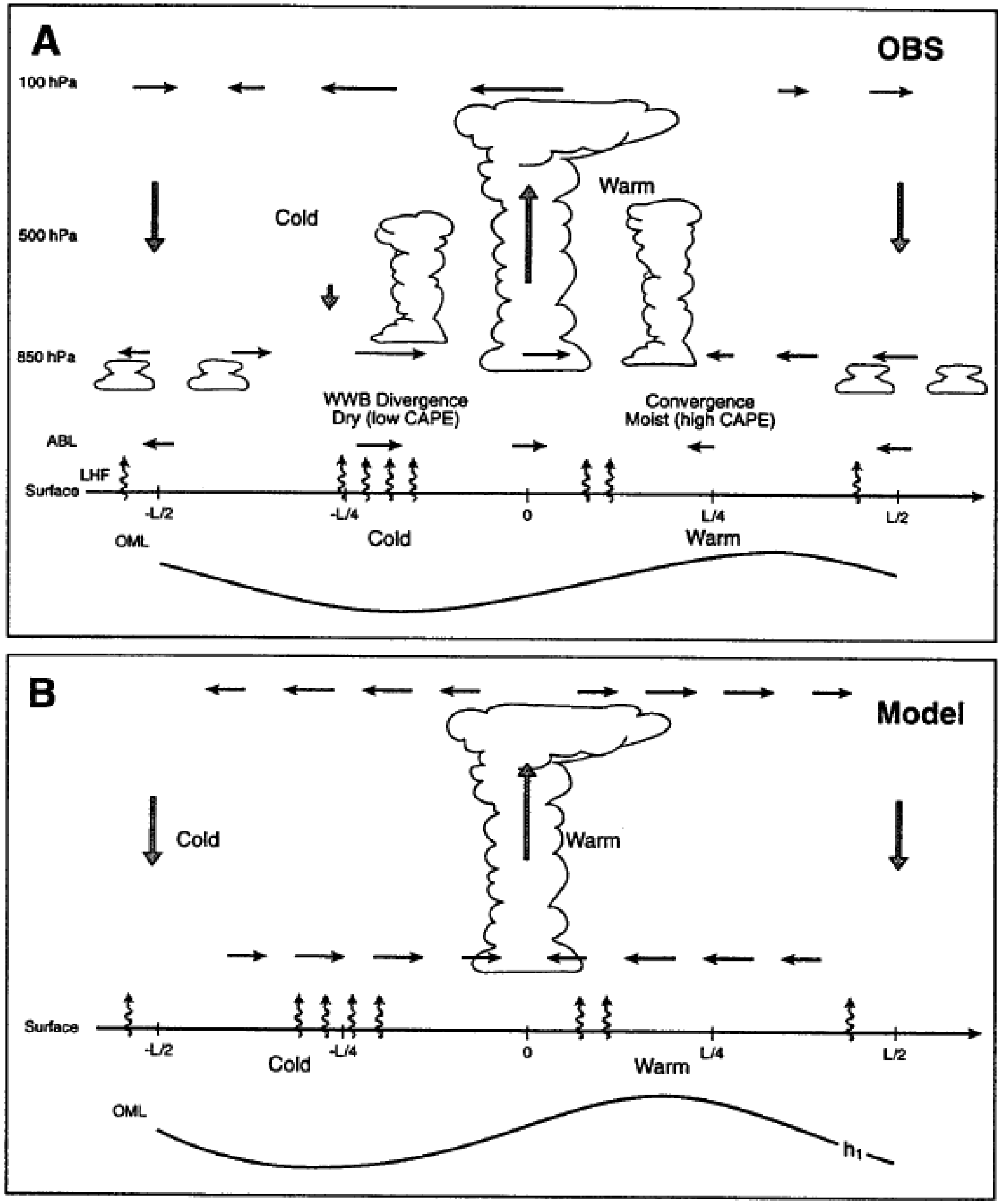

# *Equatorial Wave Structure*

*Consistent with a progression of shallow to deep convection, followed by stratiform precipitation for the Kelvin, Westward Inertio-gravity (2-day) Waves, and Easterly Waves*

*This was also observed during COARE for the MJO (e.g. Lin and Johnson 1996; Johnson et al. 1999; Lin et al. 2004)*

***This evolution is similar to that occurring on the Mesoscale Convective Complex scale***

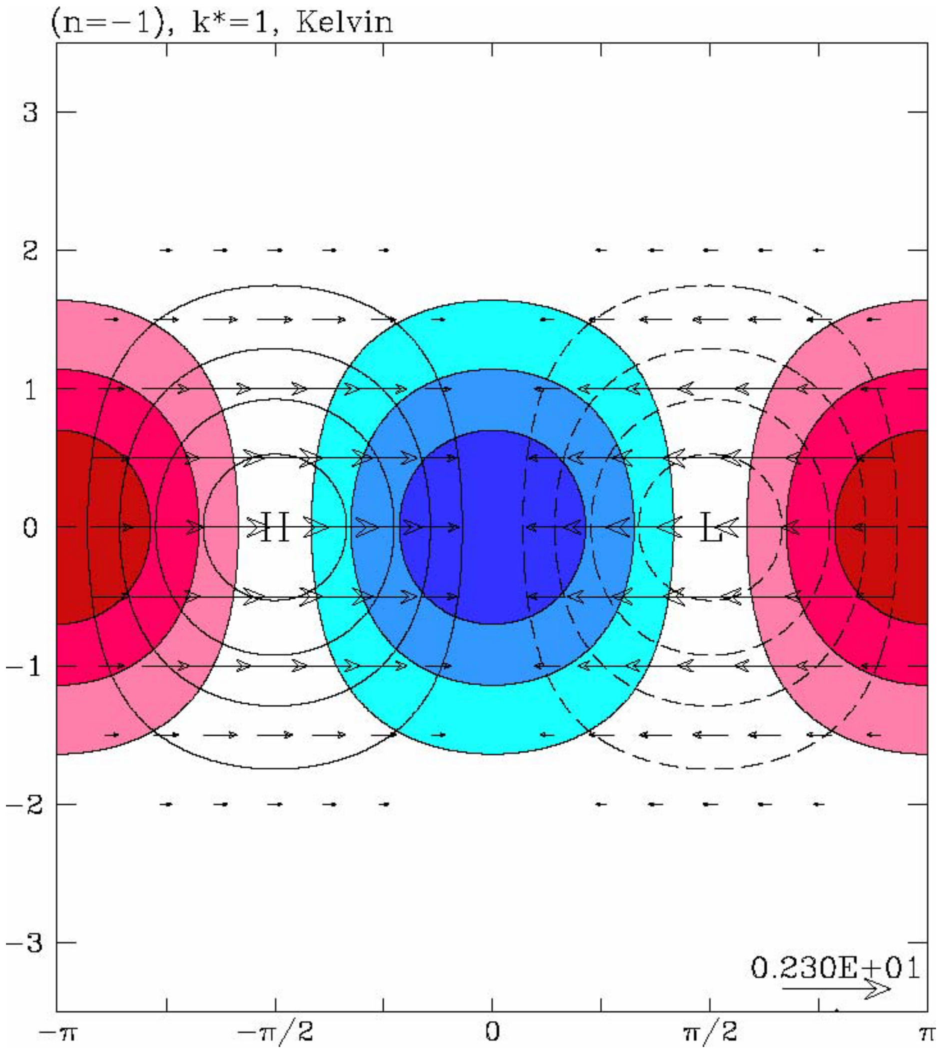

(n=−1), k*=1, Kelvin
3
2
1
0
−1
−2
−3
H
L
0.230E+01
−π
−π/2
0
π/2
π

# ECMWF reanalysis regression

**OLR (shading), 1000-hPa Z (contours), 1000-hPa winds (vectors)**

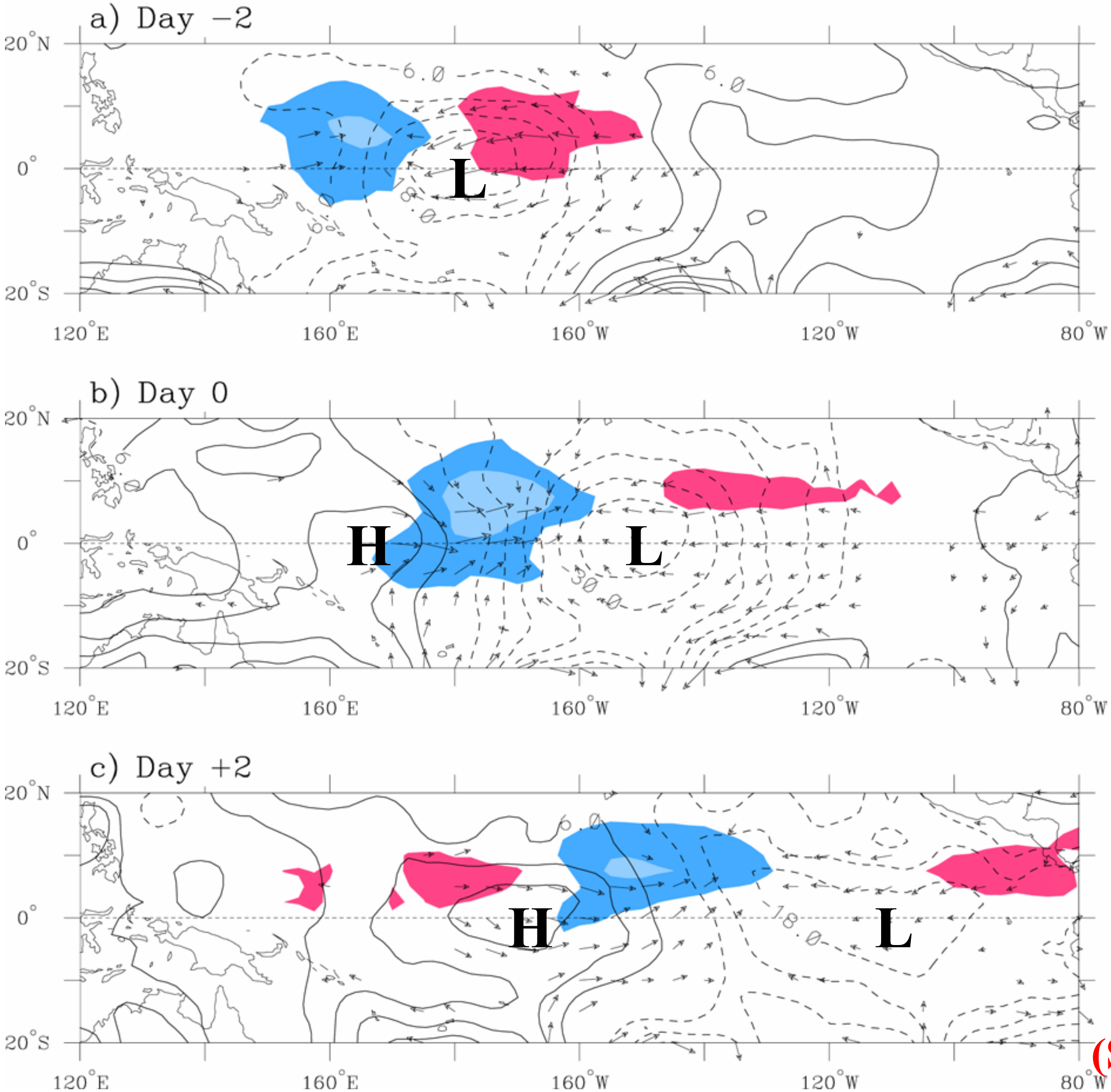


**Dynamical fields are symmetric with respect to the equator; convection is centered in NH along ITCZ**

(Straub and Kiladis, 2002)

# Kelvin wave in Majuro radiosonde data: 1979-1999 (Straub and Kiladis, 2003)

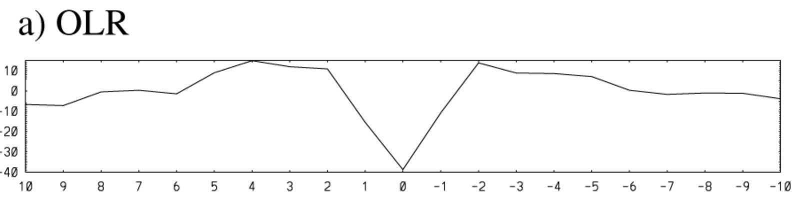


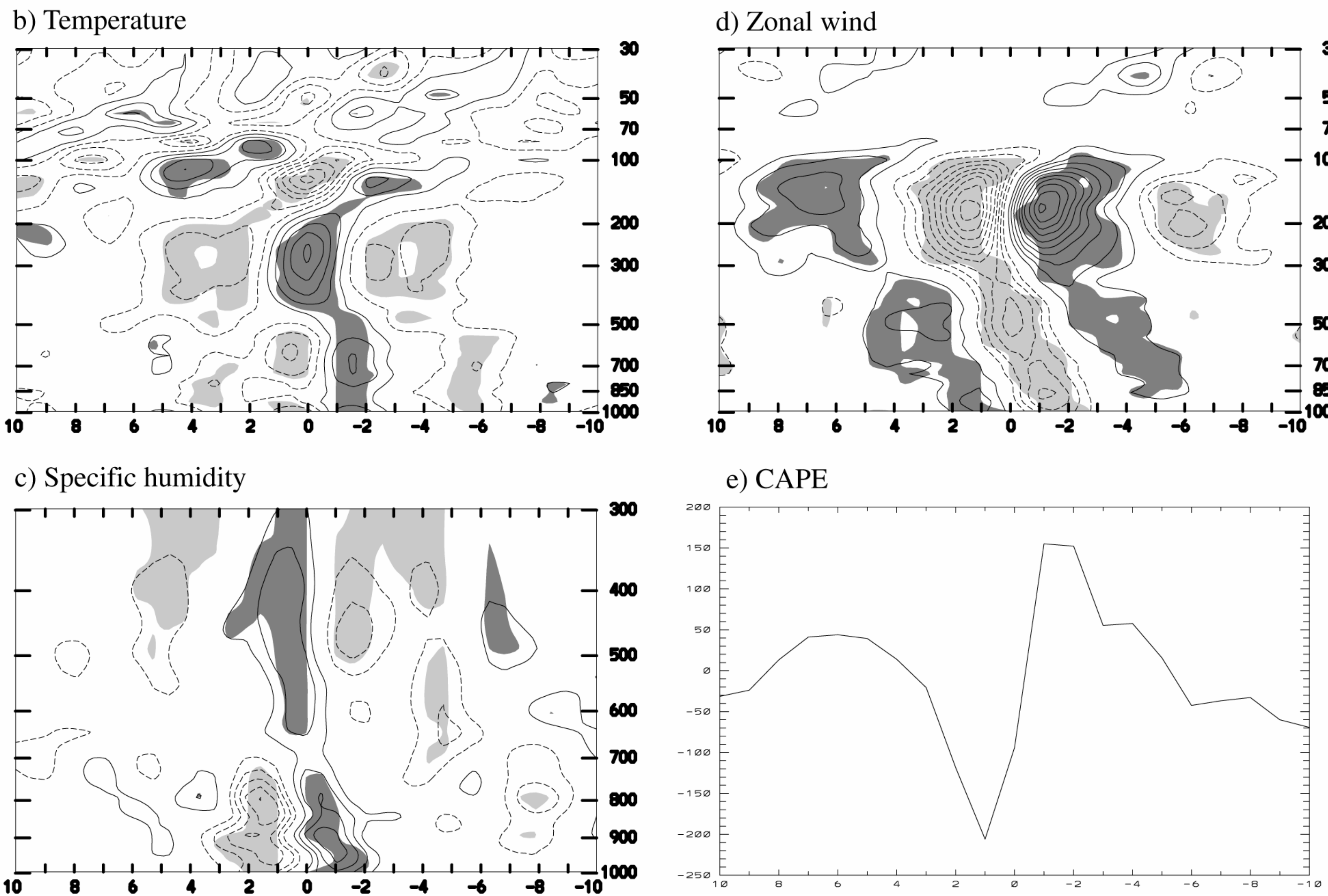

# Zonal Wind Anomaly over the IFA

Two day waves during COARE,
from Haertel and Kiladis, 2004

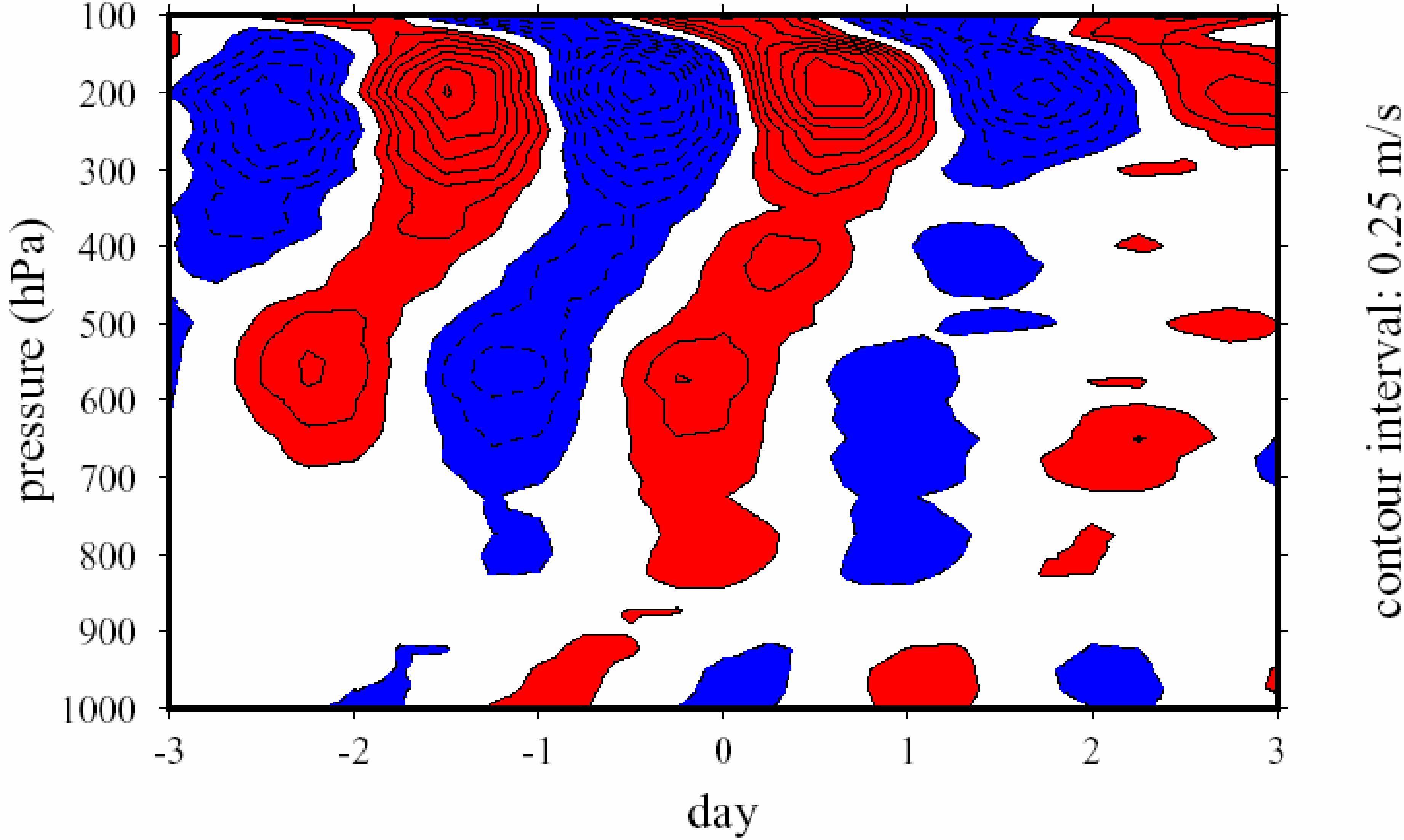

# Temperature Anomaly over the IFA

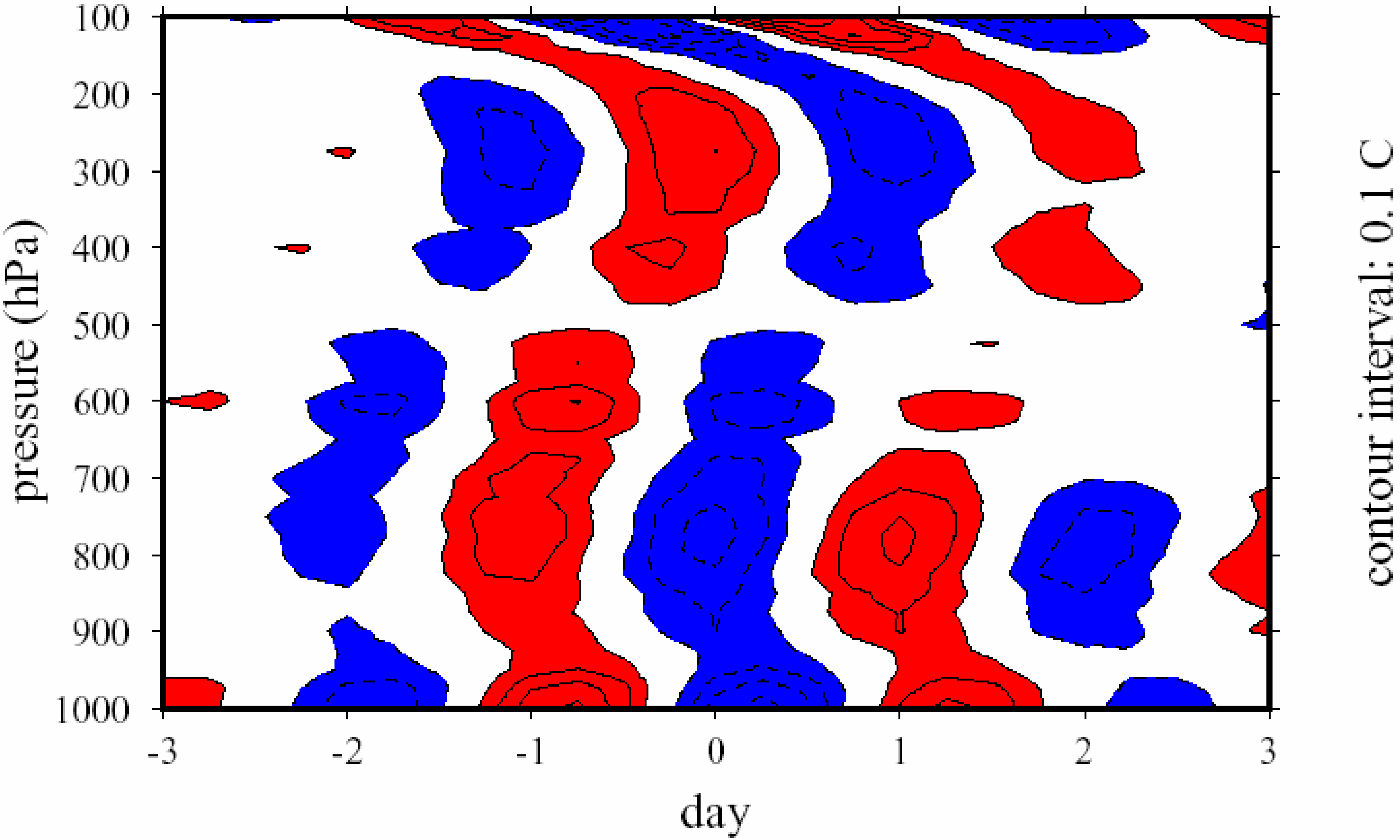

# Moisture Anomaly over the IFA

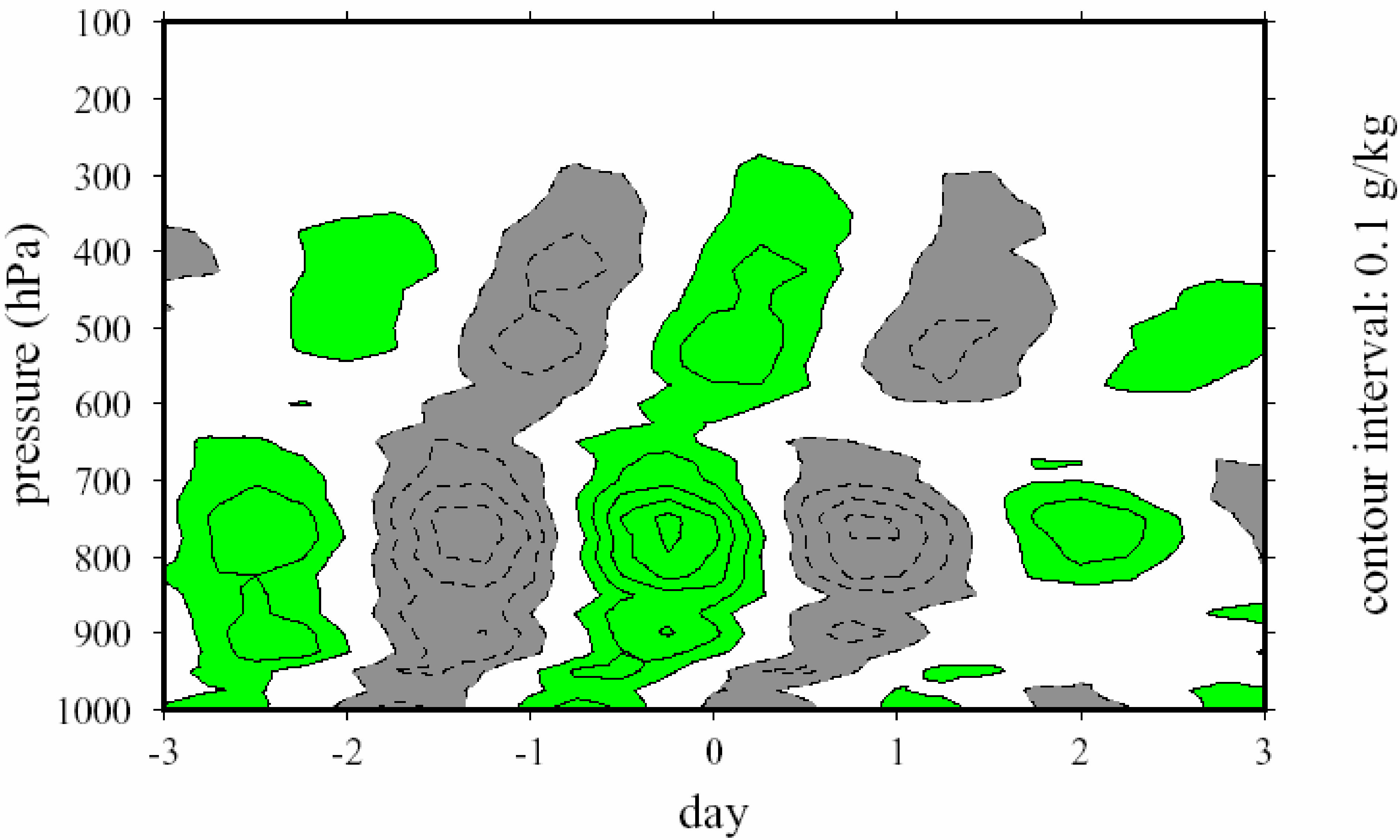

# Heating Anomaly over the IFA

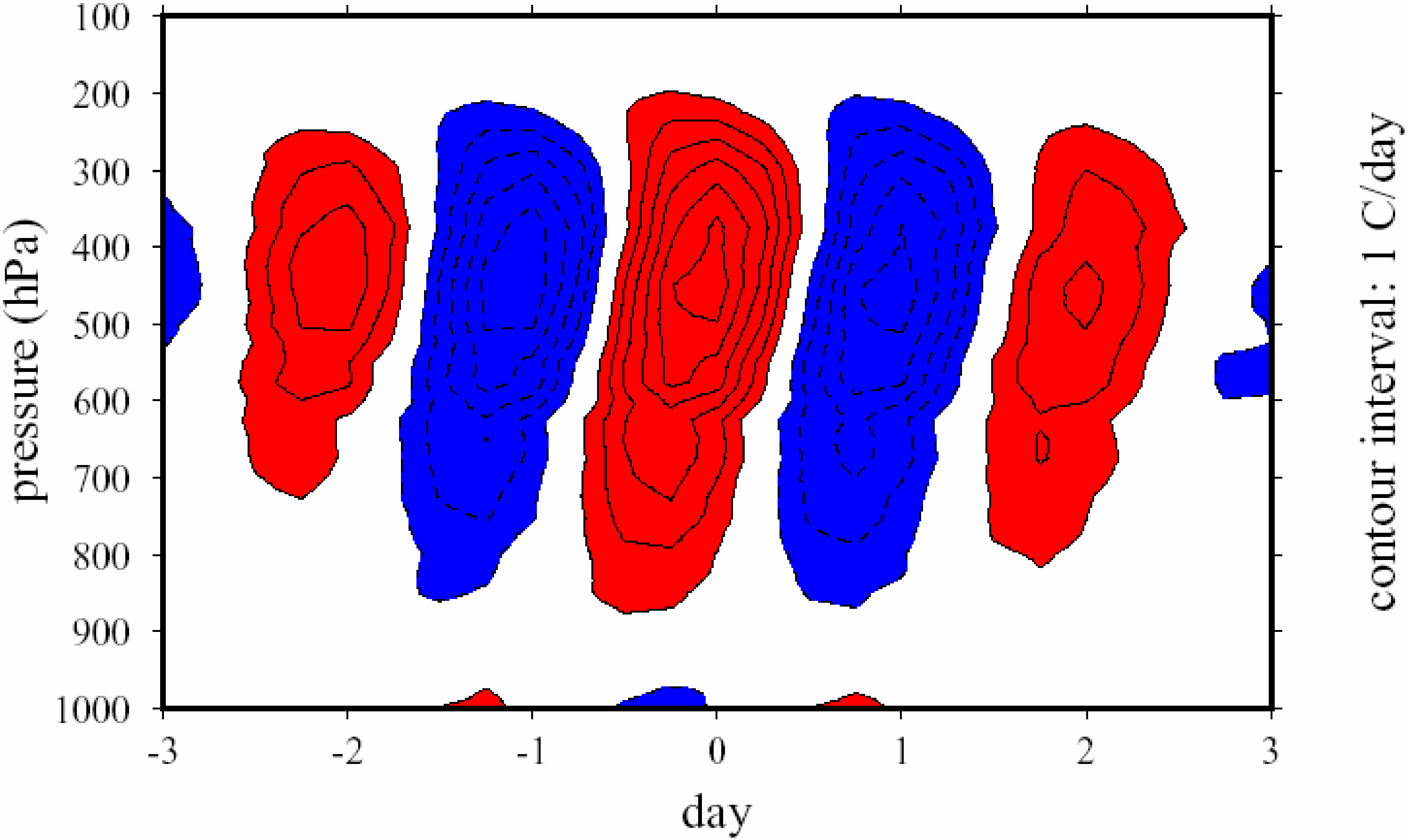

# OLR and 850 hPa Flow Regressed against MJO-filtered OLR (scaled -40 W m$^2$) at eq, 155°E, 1979-1993

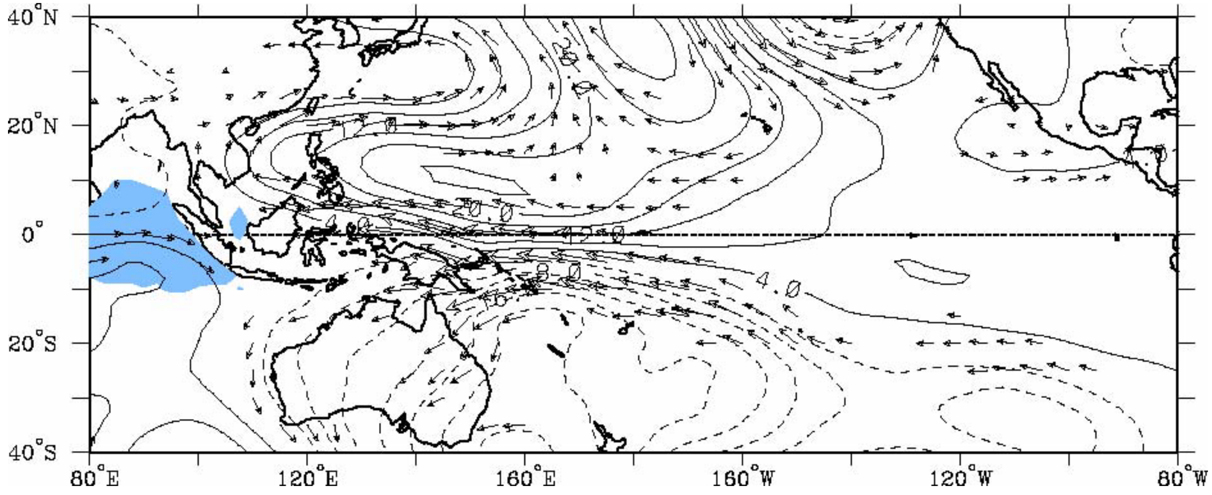


Day-16

Streamfunction (contours 4 X $10^5$ m$^2$ s$^{-1}$)

Wind (vectors, largest around 2 m s$^{-1}$)

OLR (shading starts at +/- 6 W s$^{-2}$), negative blue

# OLR and 850 hPa Flow Regressed against MJO-filtered OLR (scaled -40 W m$^2$) at eq, 155°E, 1979-1993

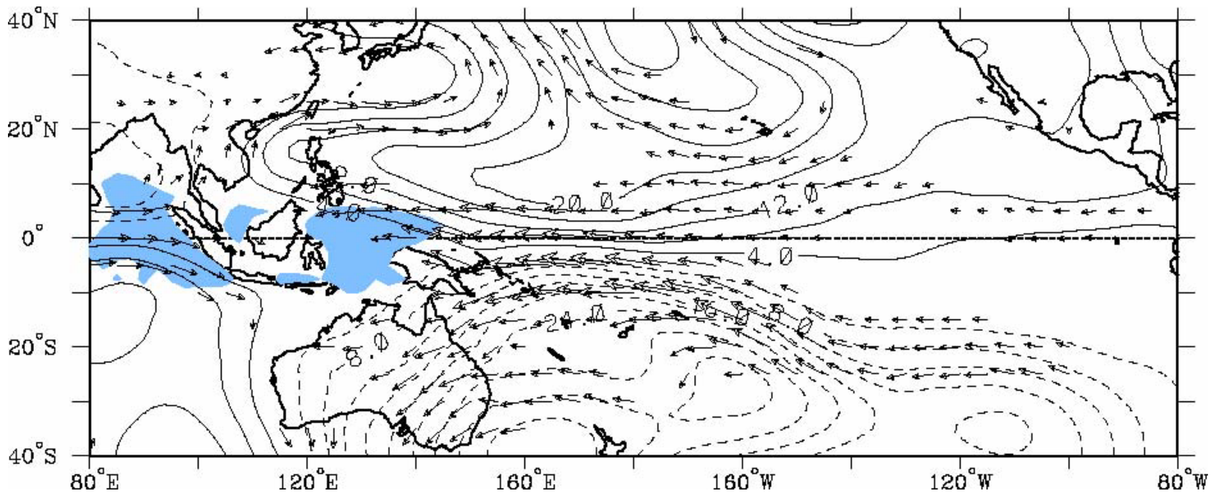


Day-12

Streamfunction (contours 4 X 10$^5$ m$^2$ s$^{-1}$)

Wind (vectors, largest around 2 m s$^{-1}$)

OLR (shading starts at +/- 6 W s$^{-2}$), negative blue

# OLR and 850 hPa Flow Regressed against MJO-filtered OLR (scaled -40 W $m^2$) at eq, 155°E, 1979-1993

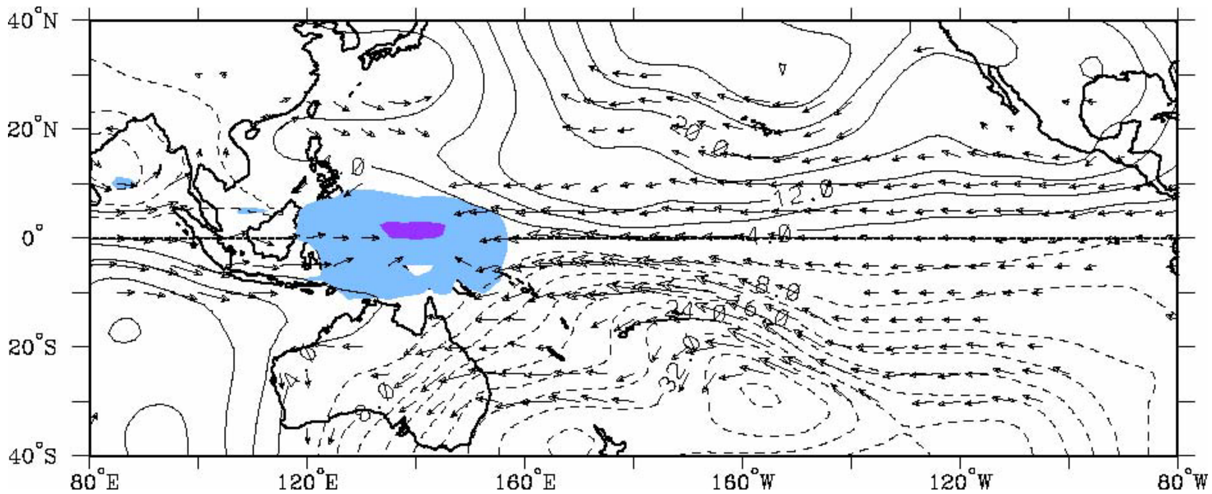


Day-8

Streamfunction (contours 4 X $10^5$ $m^2$ $s^{-1}$)

Wind (vectors, largest around 2 m $s^{-1}$)

OLR (shading starts at +/- 6 W $s^{-2}$), negative blue

# OLR and 850 hPa Flow Regressed against MJO-filtered OLR (scaled -40 W m$^2$) at eq, 155°E, 1979-1993

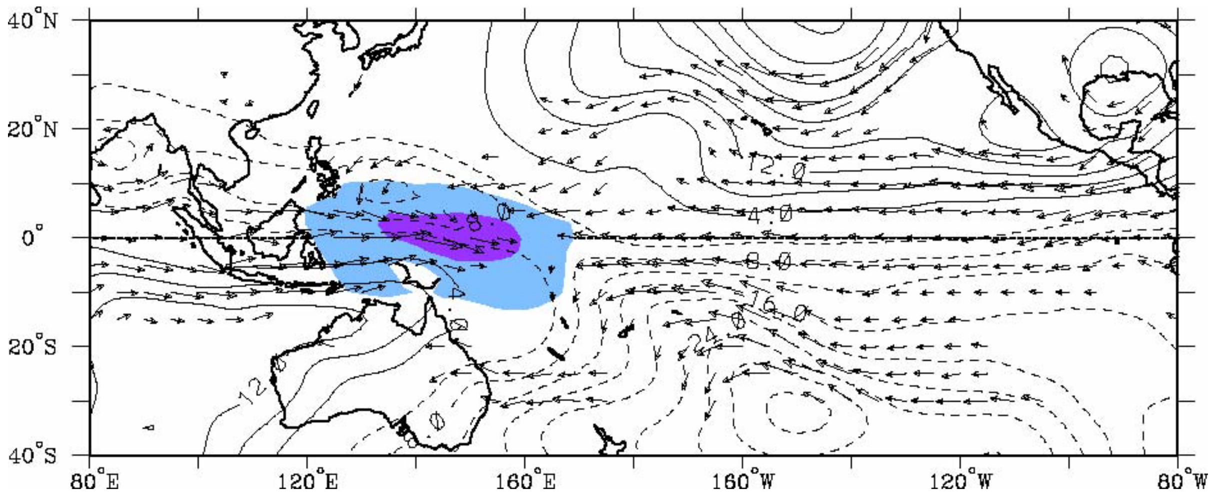


Day-4

Streamfunction (contours 4 X 10$^5$ m$^2$ s$^{-1}$)

Wind (vectors, largest around 2 m s$^{-1}$)

OLR (shading starts at +/- 6 W s$^{-2}$), negative blue

# OLR and 850 hPa Flow Regressed against MJO-filtered OLR (scaled -40 W $m^2$) at eq, 155°E, 1979-1993

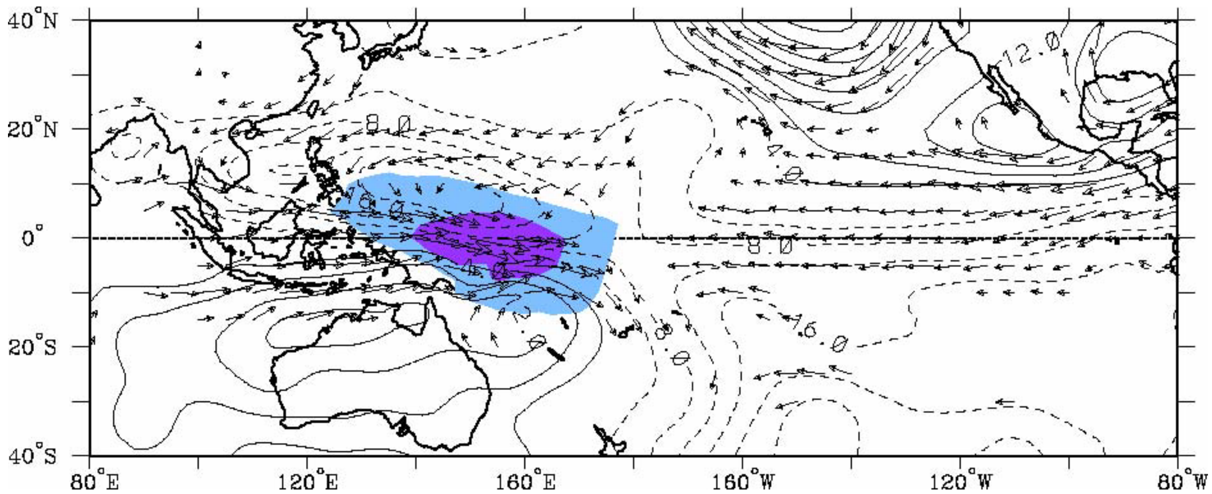


Day 0

Streamfunction (contours 4 X $10^5$ $m^2$ $s^{-1}$)

Wind (vectors, largest around 2 m $s^{-1}$)

OLR (shading starts at +/- 6 W $s^{-2}$), negative blue

# OLR and 850 hPa Flow Regressed against MJO-filtered OLR (scaled -40 W m$^2$) at eq, 155°E, 1979-1993

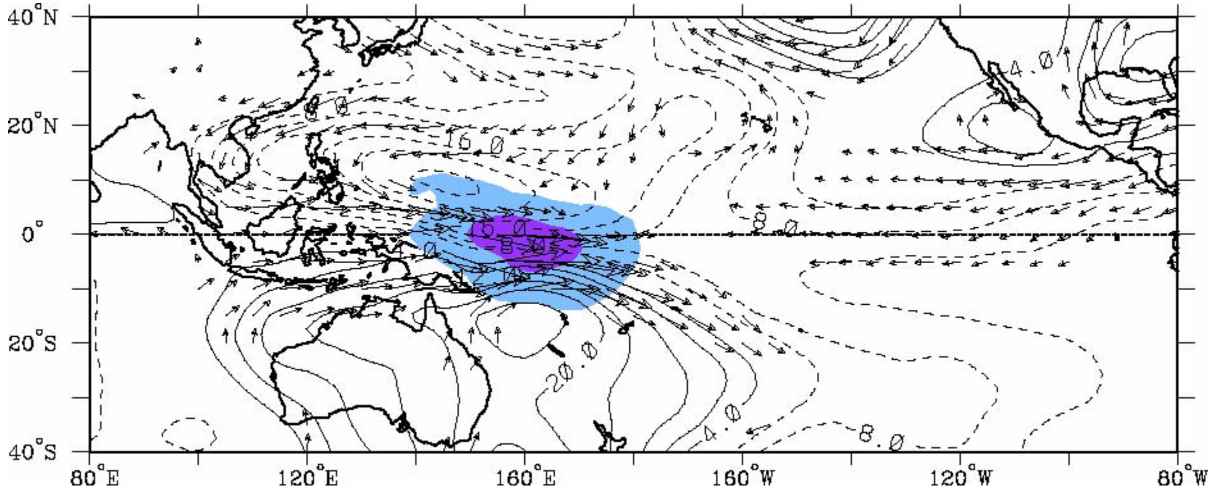


Day+4

Streamfunction (contours 4 X $10^5$ $m^2$ $s^{-1}$)

Wind (vectors, largest around 2 m $s^{-1}$)

OLR (shading starts at +/- 6 W $s^{-2}$), negative blue

# OLR and 850 hPa Flow Regressed against MJO-filtered OLR (scaled -40 W m$^2$) at eq, 155°E, 1979-1993

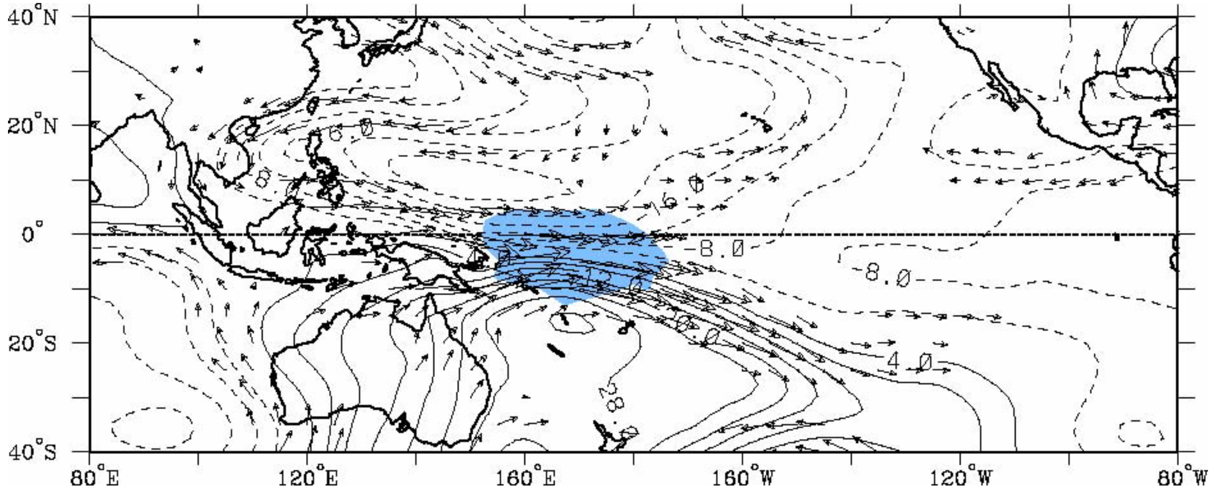


Day+8

Streamfunction (contours 4 X 10$^5$ m$^2$ s$^{-1}$)

Wind (vectors, largest around 2 m s$^{-1}$)

OLR (shading starts at +/- 6 W s$^{-2}$), negative blue

# OLR and 850 hPa Flow Regressed against MJO-filtered OLR (scaled -40 W m$^2$) at eq, 155°E, 1979-1993

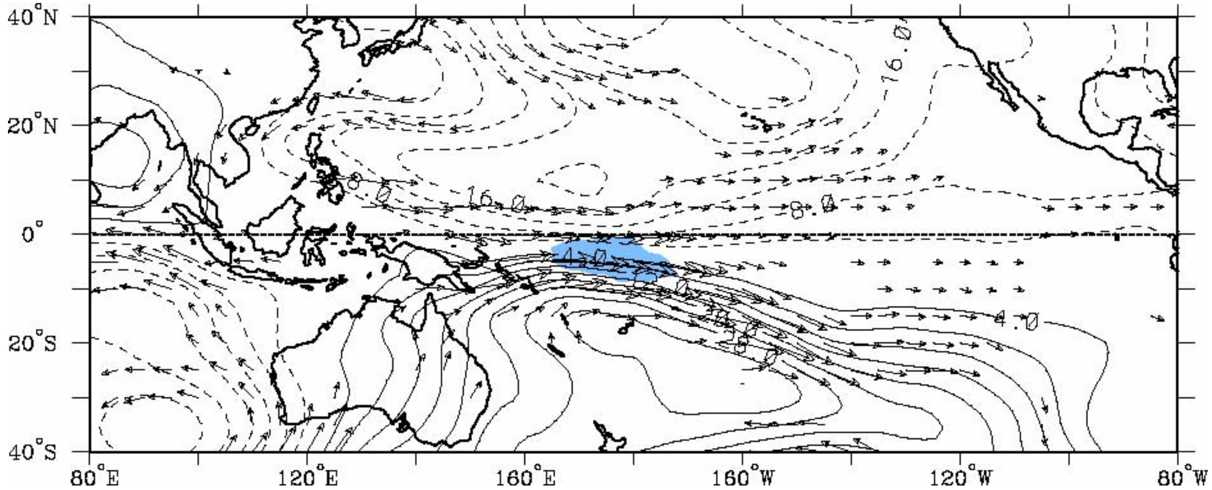


Day+12

Streamfunction (contours 4 X 10$^5$ m$^2$ s$^{-1}$)

Wind (vectors, largest around 2 m s$^{-1}$)

OLR (shading starts at +/- 6 W s$^{-2}$), negative blue

# Zonal Wind at Honiara (10°S, 160°E) Regressed against MJO-filtered OLR (scaled -40 W $m^2$) for 1979-1999

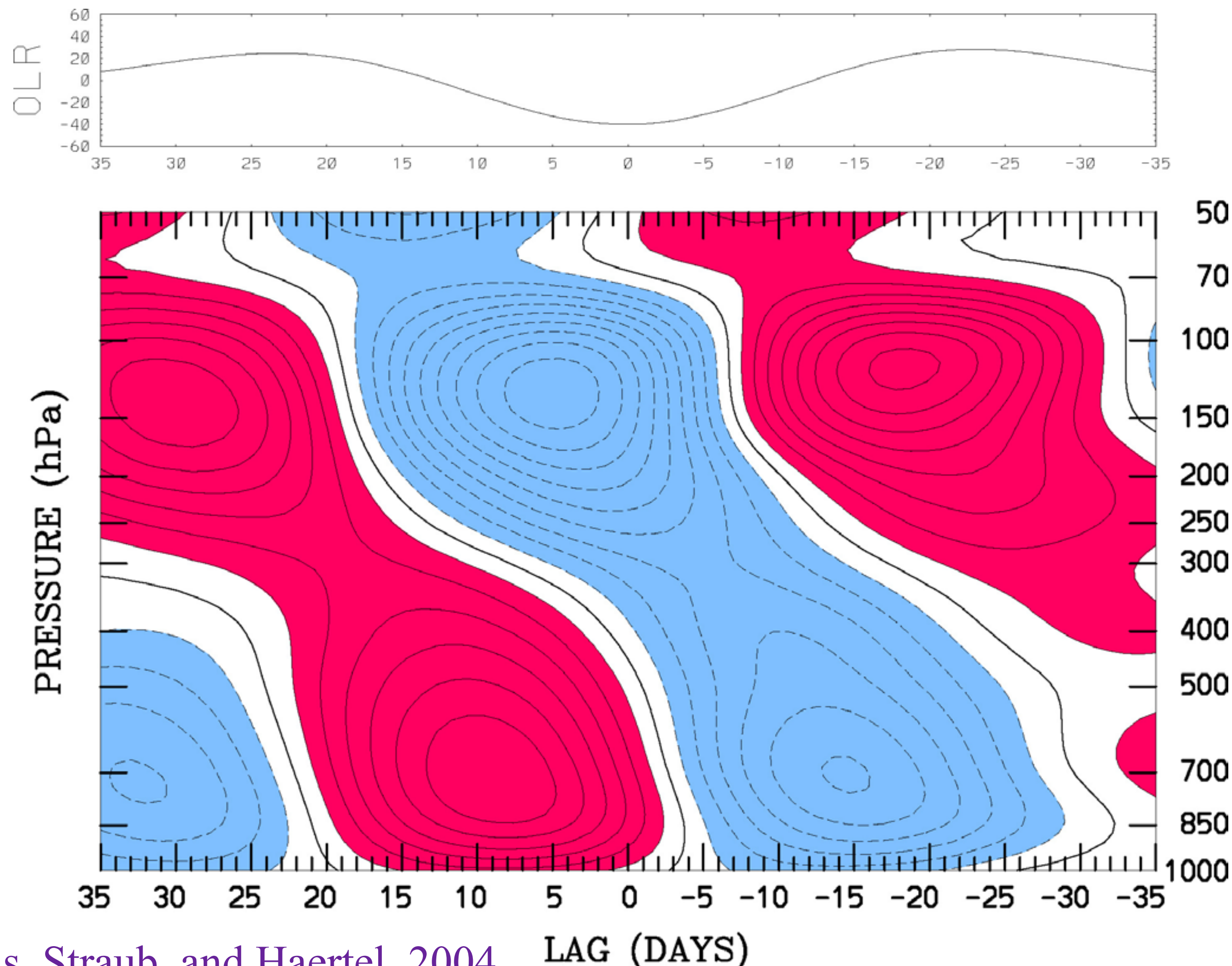


OLR

Pressure (hPa)

from Kiladis, Straub, and Haertel, 2004

OLR (top, $Wm^{-2}$)

U Wind (contours, .5 m $s^{-1}$), red positive

# Zonal Wind at Seychelles (5°S, 55°E) Regressed against MJO-filtered OLR (scaled -40 W m$^2$) for 1979-1999

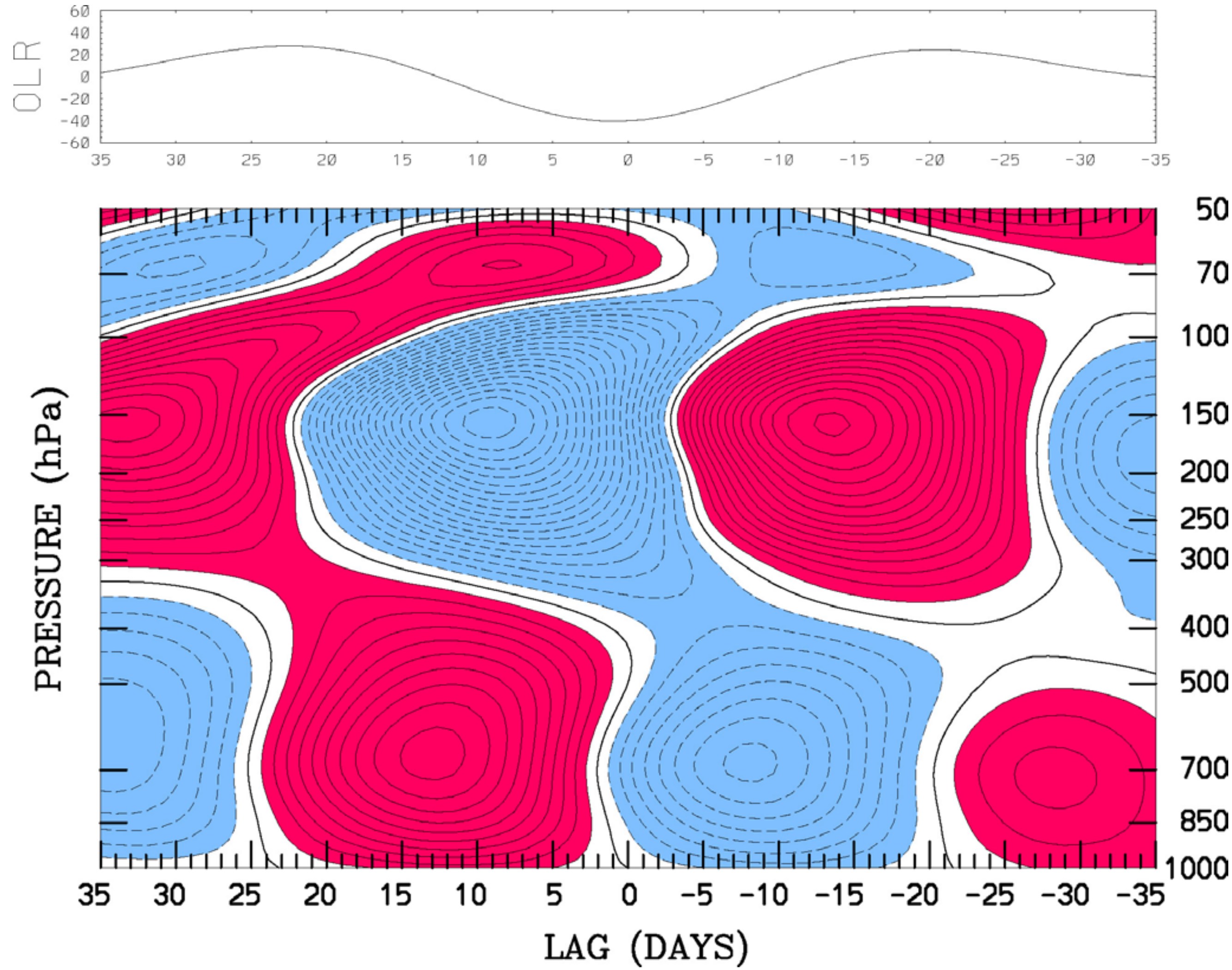


OLR

Pressure (hPa)

OLR (top, Wm$^{-2}$)

U Wind (contours, .5 m s$^{-1}$), red positive

# Zonal Wind at Diego Garcia (7.5°S, 72°E) Regressed against MJO-filtered OLR (scaled -40 W m²) for 1979-1999

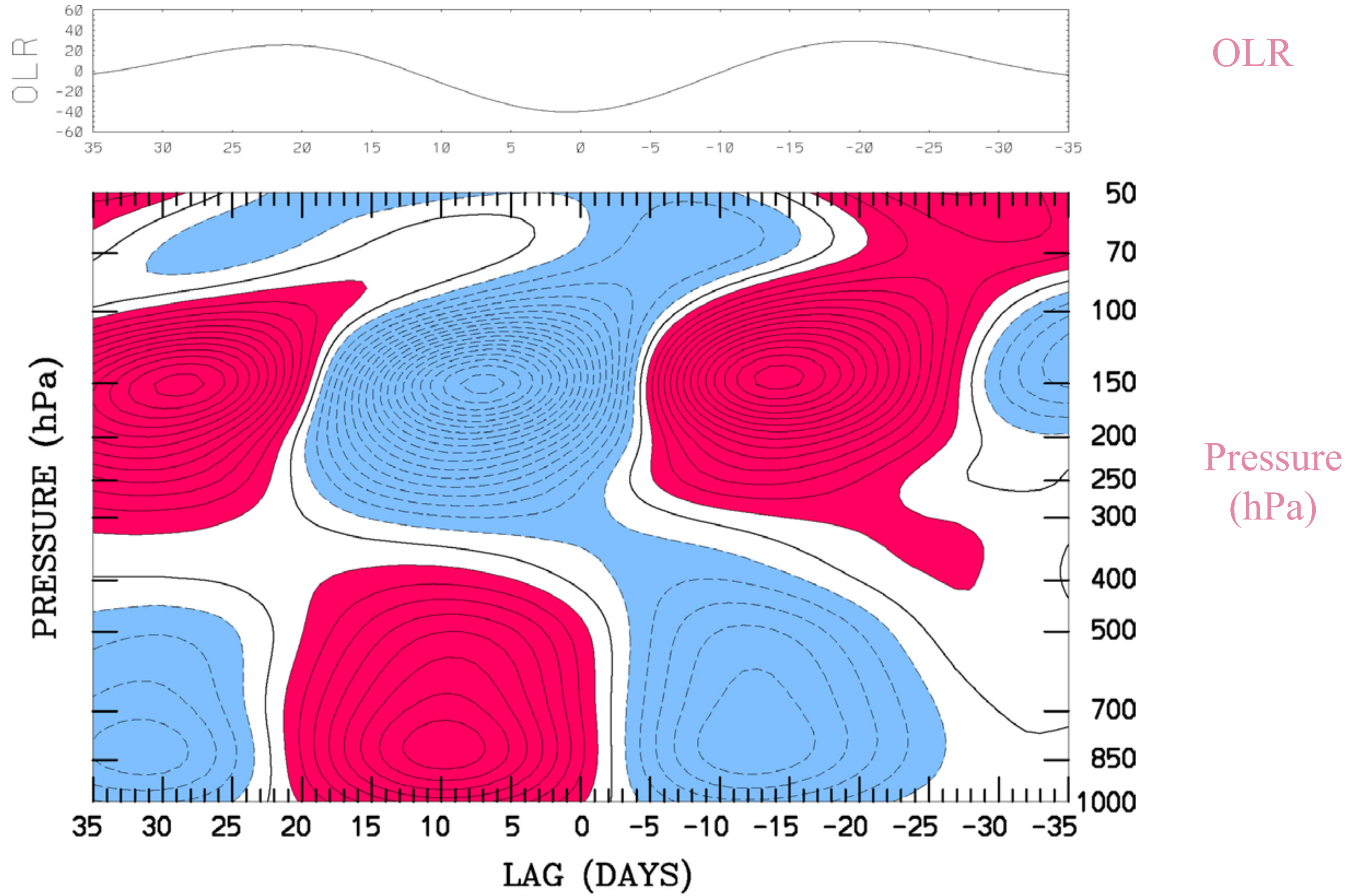


OLR (top, $Wm^{-2}$)

U Wind (contours, .5 m $s^{-1}$), red positive

# Temperature at Tarawa (Eq, 172.5°E) Regressed against MJO-filtered OLR (scaled -40 W $m^2$) for 1979-1999

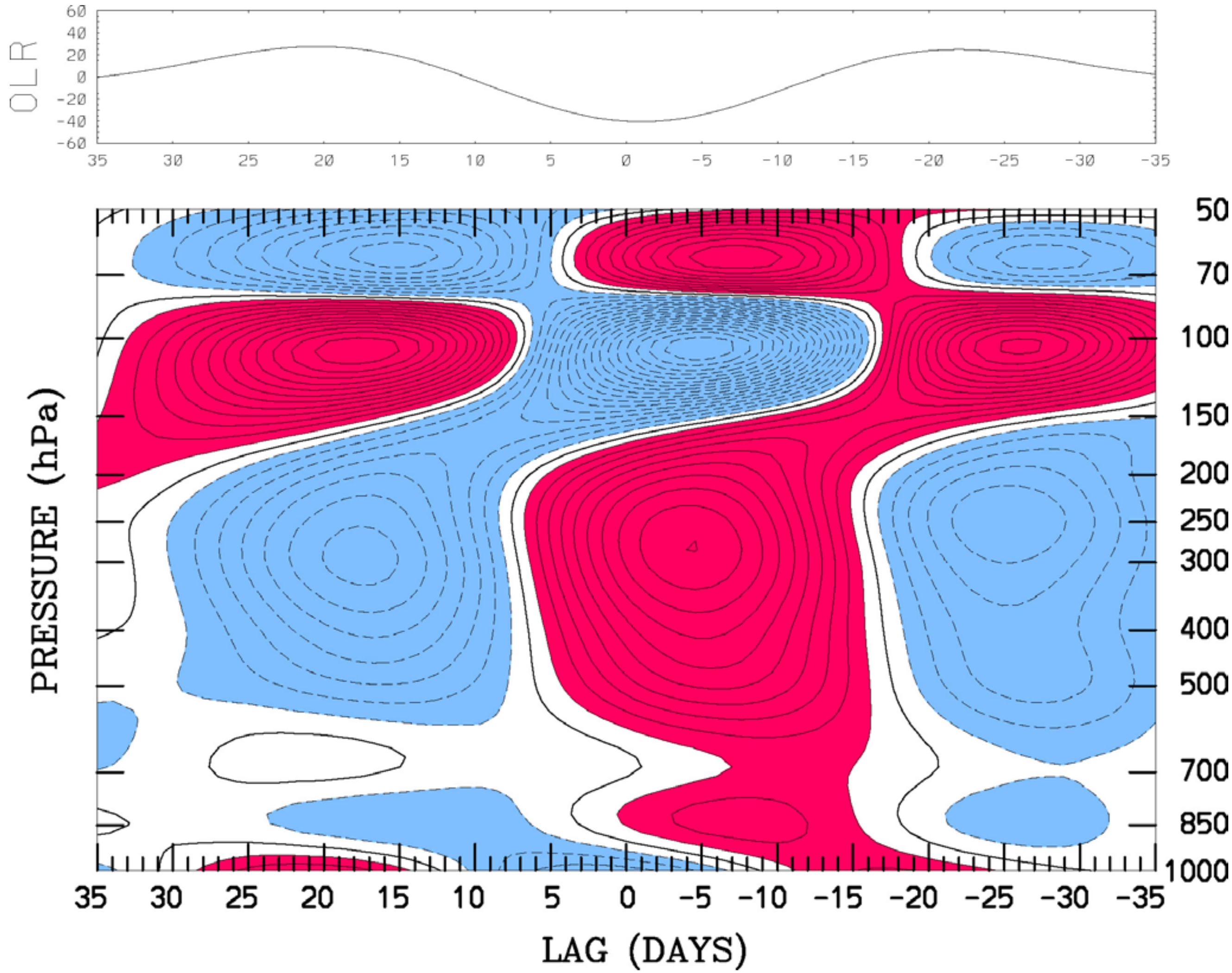


OLR

Pressure (hPa)

OLR (top, $Wm^{-2}$)

Temperature (contours, .1 °C), red positive

# Temperature at Honiara (10°S, 160.0°E) Regressed against MJO-filtered OLR (scaled -40 W m2) for 1979-1999

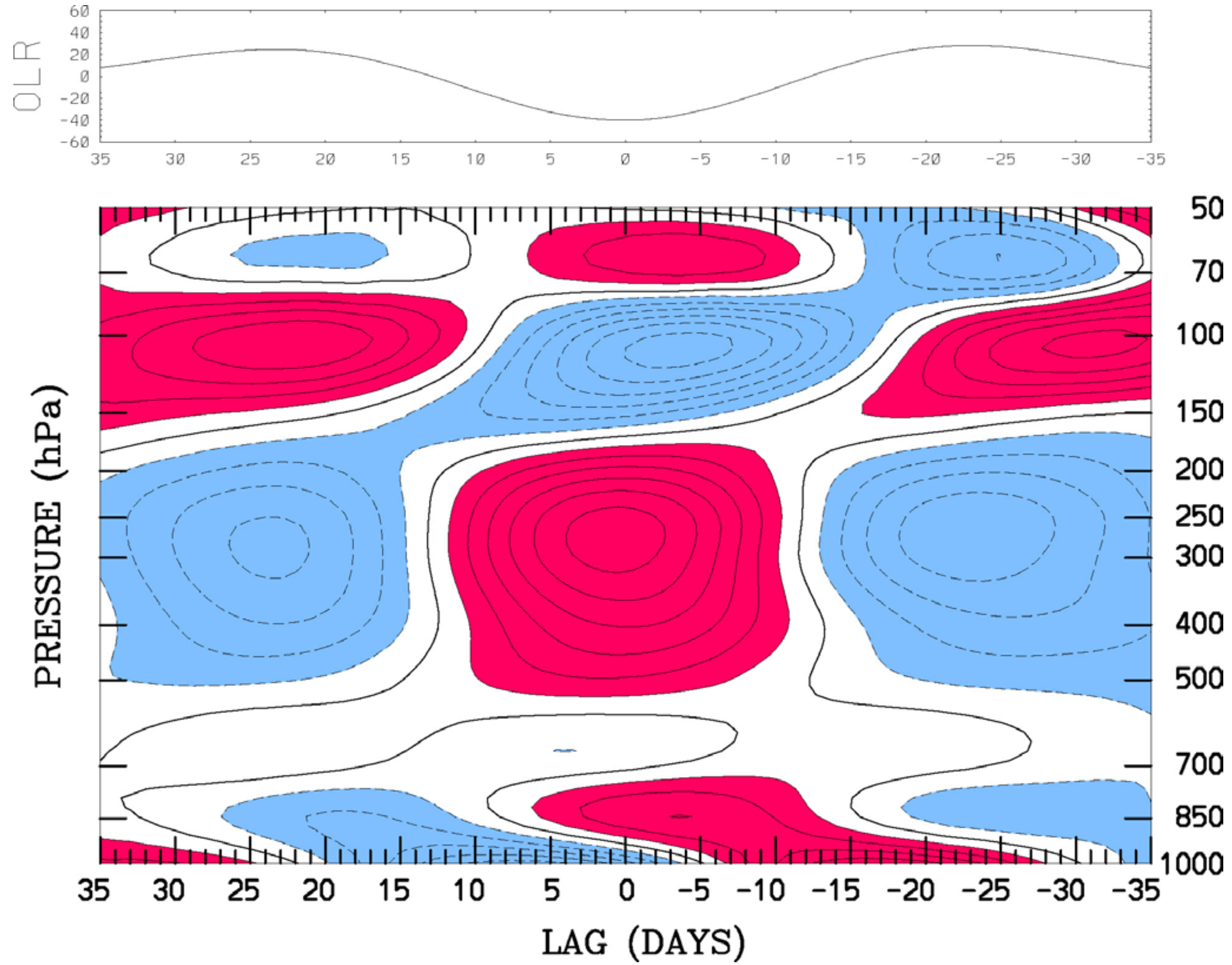


OLR

Pressure (hPa)

OLR (top, $Wm^{-2}$)

Temperature (contours, .1 °C), red positive

# Temperature at Diego Garcia (7.5°S, 72°E) Regressed against MJO-filtered OLR (scaled -40 W $m^2$) for 1979-1999

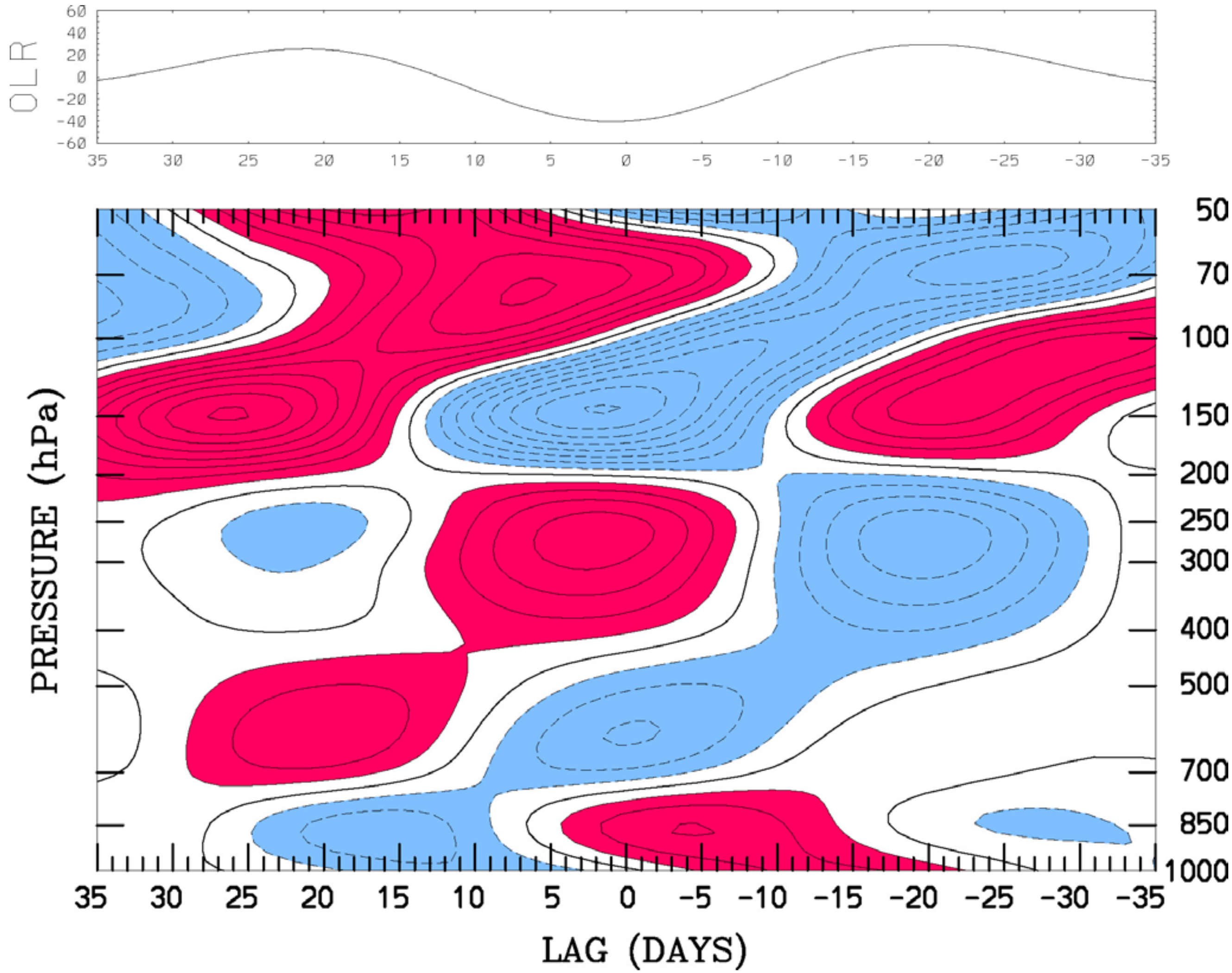


OLR

Pressure (hPa)

OLR (top, $Wm^{-2}$)

Temperature (contours, .1 °C), red positive

# Temperature at Seychelles (5°S, 55°E) Regressed against MJO-filtered OLR (scaled -40 W $m^2$) for 1979-1999

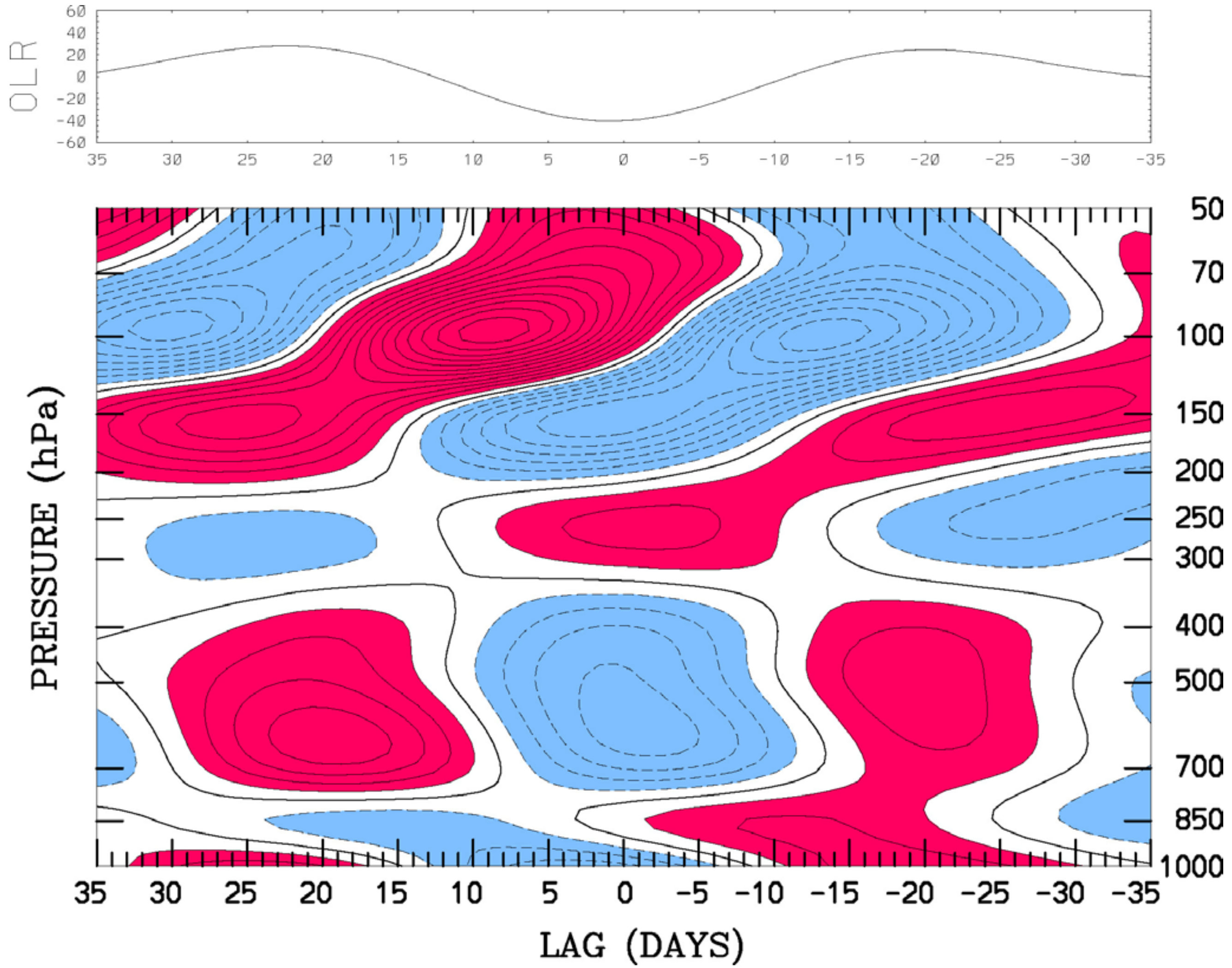


OLR

Pressure (hPa)

OLR (top, $Wm^{-2}$)

Temperature (contours, .1 °C), red positive

# Specific Humidity at Diego Garcia (7.5°S, 72°E) Regressed against MJO-filtered OLR (scaled -40 W m$^2$) for 1979-1999

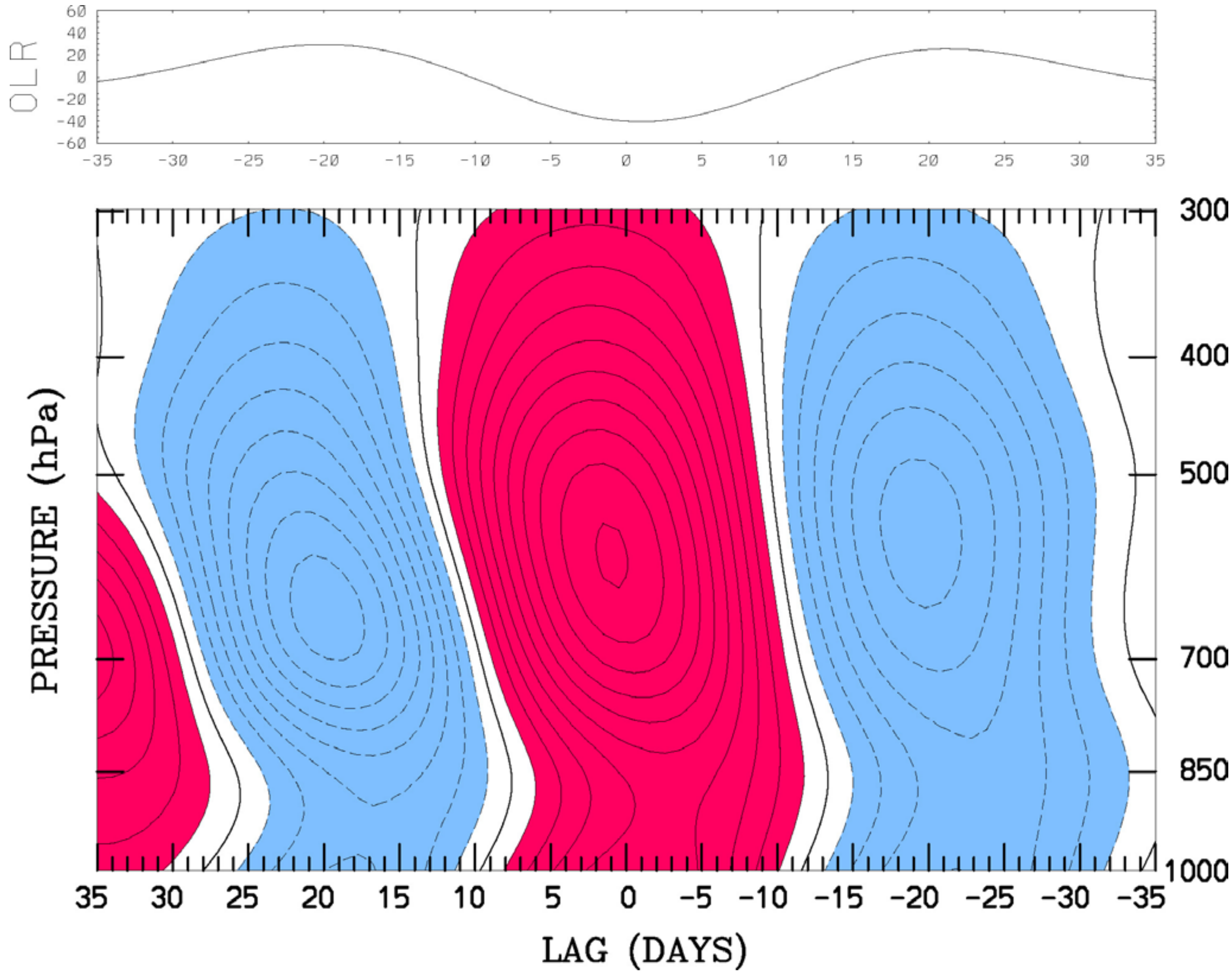


OLR

Pressure (hPa)

OLR (top, Wm$^{-2}$)

Specific Humidity (contours, 1 X 10$^{-1}$ g kg$^{-1}$), red positive

# Specific Humidity at Medan (2.5°N, 97.5°E) Regressed against MJO-filtered OLR (scaled -40 W m$^2$) for 1979-1999

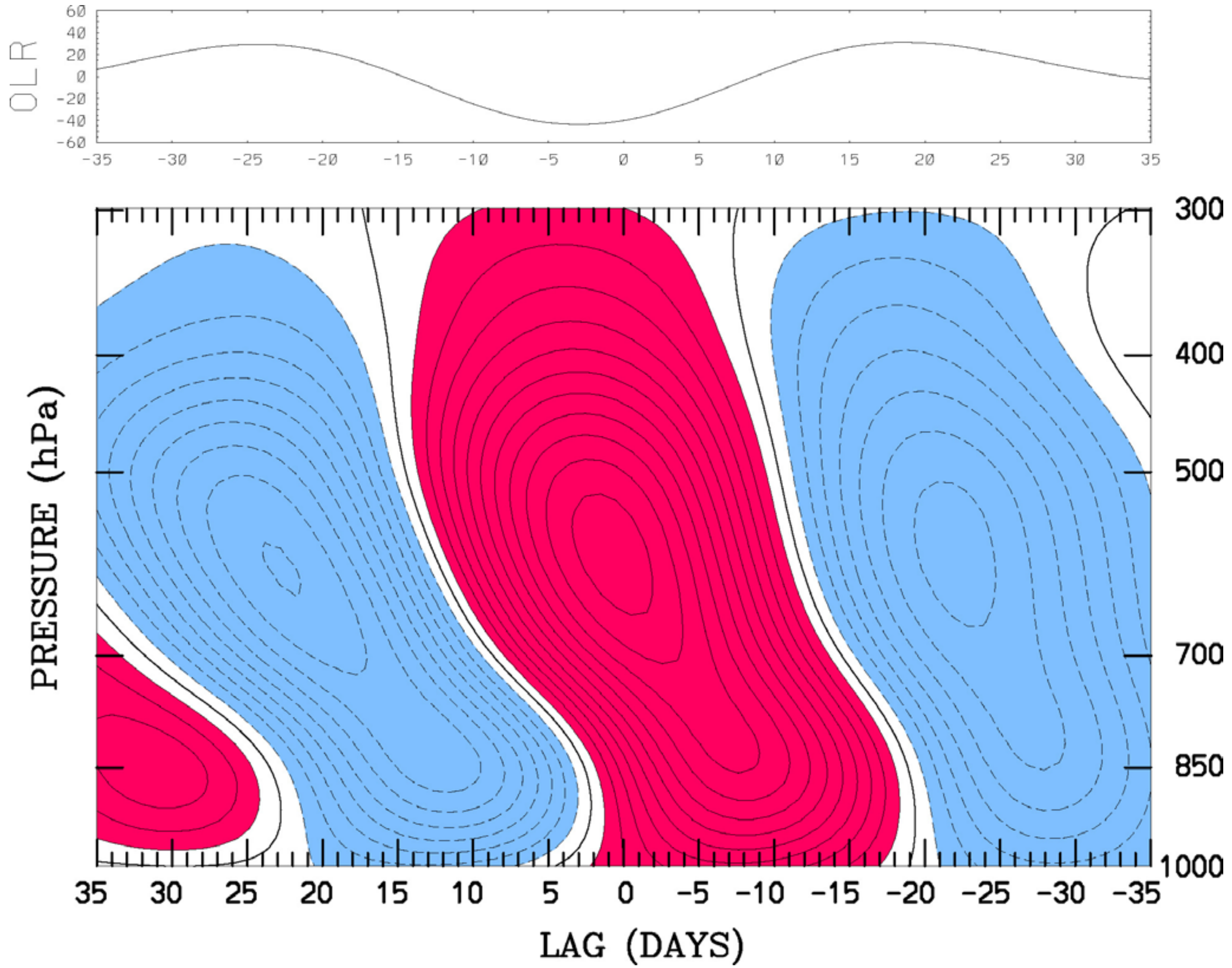


OLR

Pressure (hPa)

OLR (top, Wm$^{-2}$)

Specific Humidity (contours, 1 X 10$^{-1}$ g kg$^{-1}$), red positive

# Specific Humidity at Tarawa (Eq, 172.5°E) Regressed against MJO-filtered OLR (scaled -40 W m2) for 1979-1999

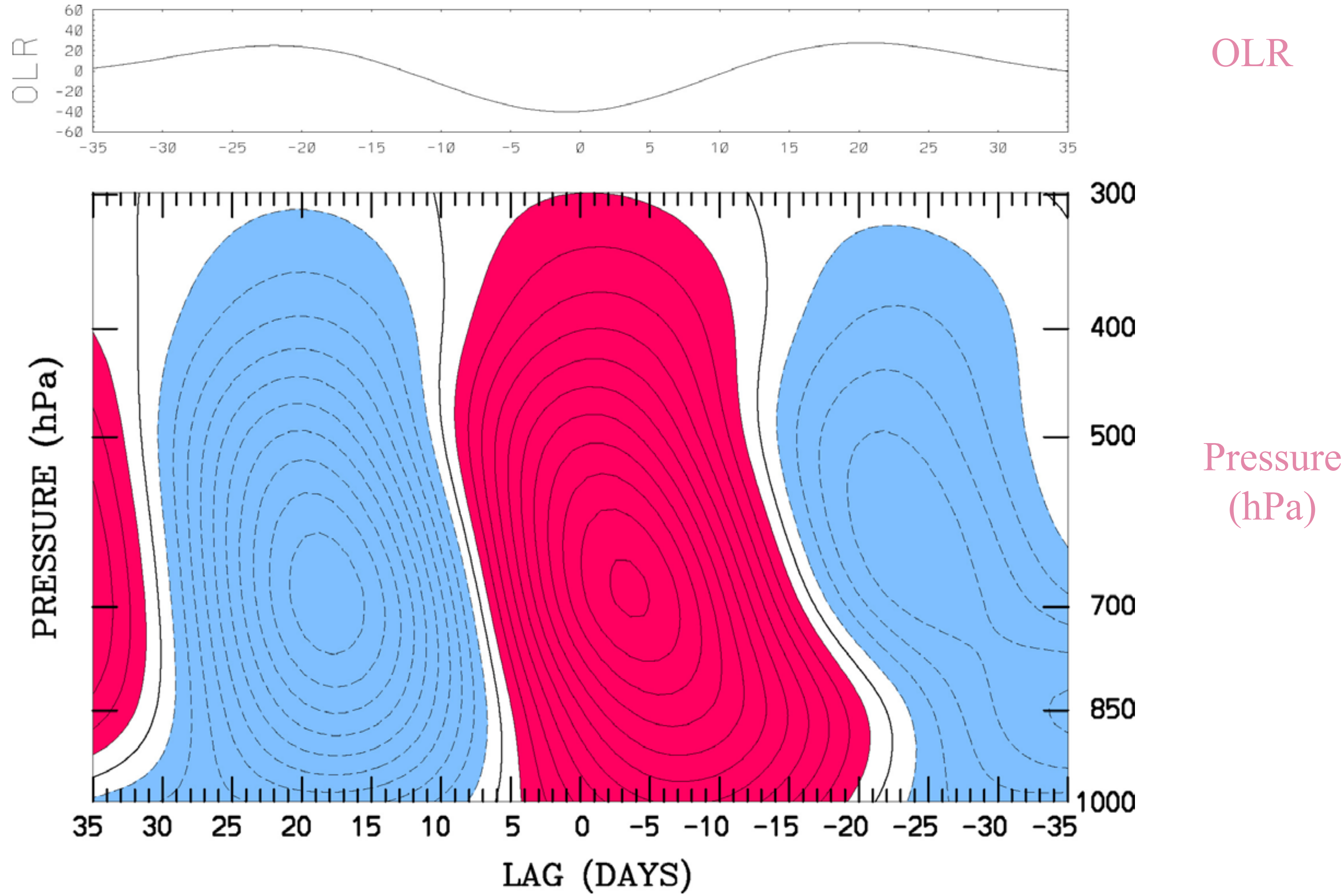


OLR (top, $Wm^{-2}$)

Specific Humidity (contours, $1 \times 10^{-1}$ g $kg^{-1}$), red positive

# Specific Humidity at Truk (7.5°N, 152.5°E) Regressed against MJO-filtered OLR (scaled -40 W m$^2$) for 1979-1999

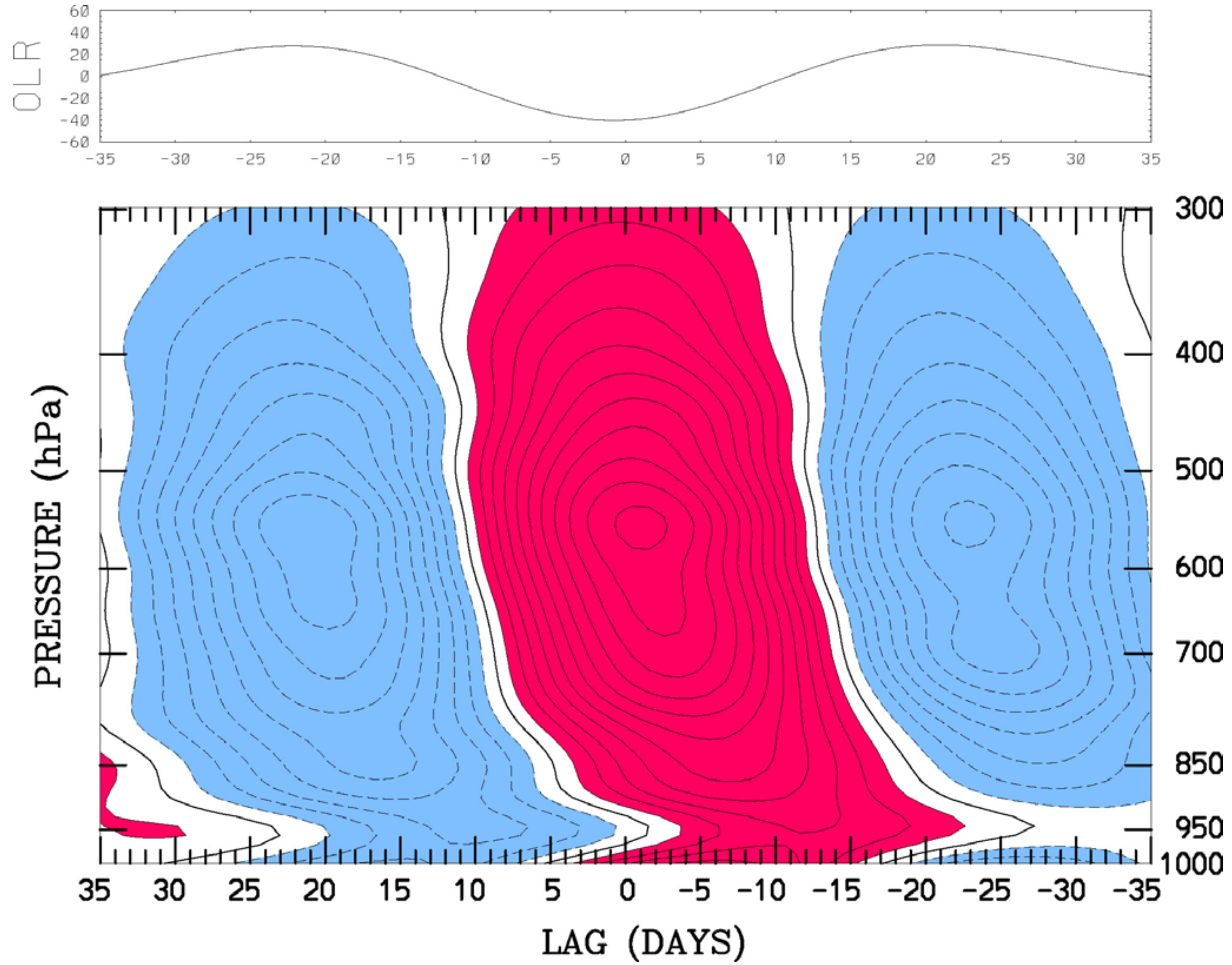


OLR

Pressure (hPa)

OLR (top, Wm$^{-2}$)

Specific Humidity (contours, 1 X 10$^{-1}$ g kg$^{-1}$), red positive

# Q1 Regressed against MJO-filtered OLR over the IFA during COARE

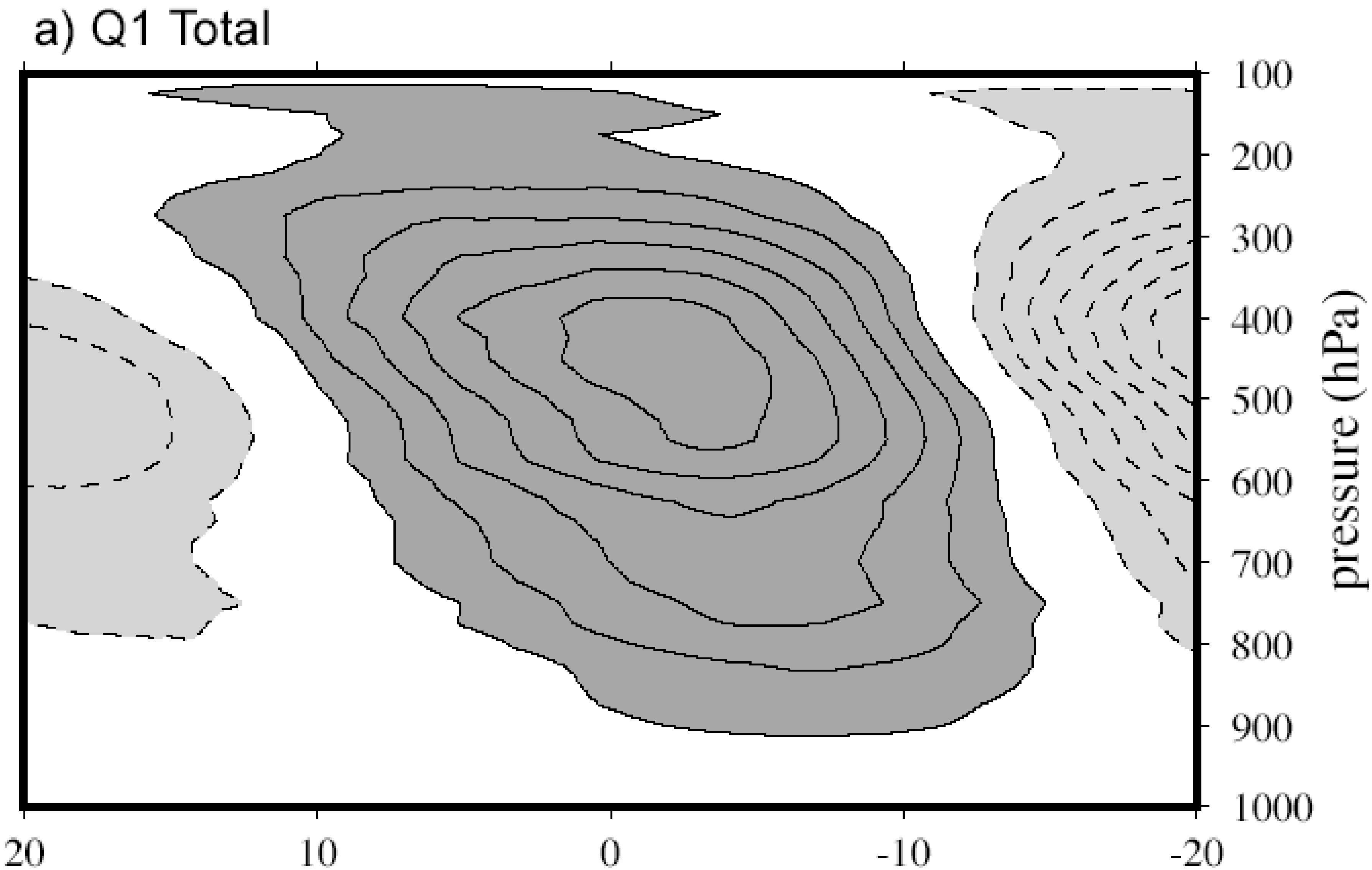

# Q1 Regressed against MJO-filtered OLR over the IFA during COARE

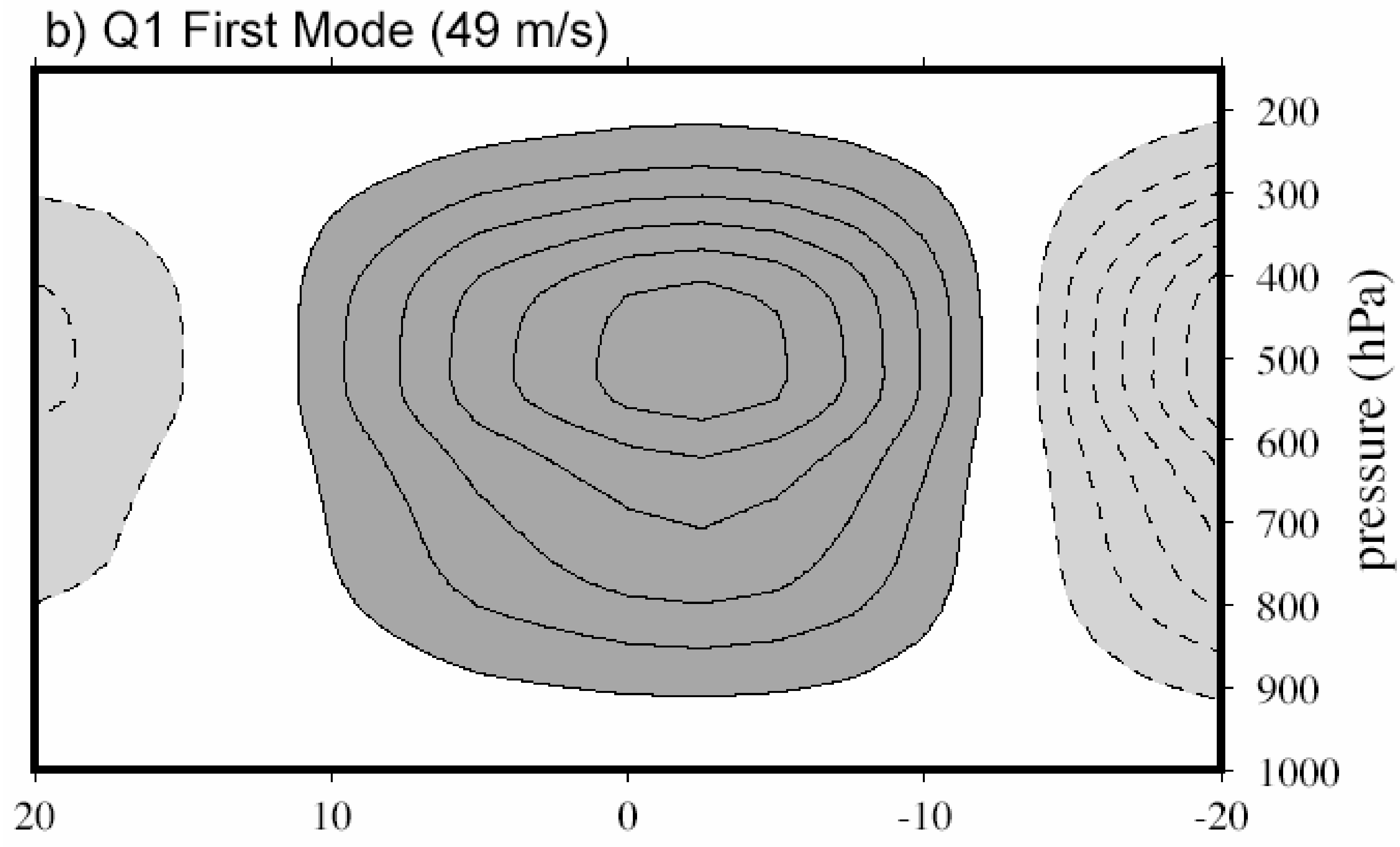

# Q1 Regressed against MJO-filtered OLR over the IFA during COARE

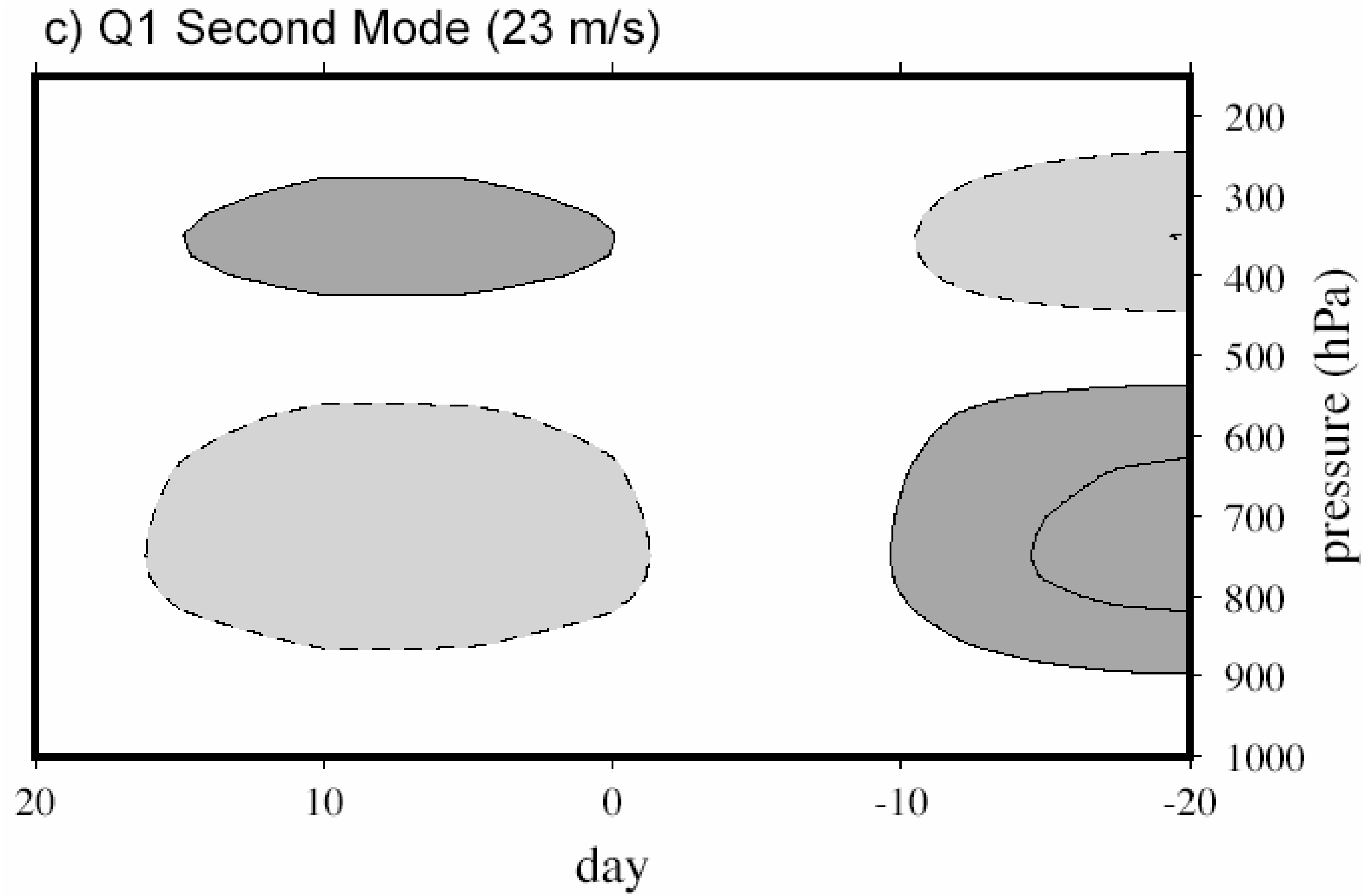

# Dynamical Structures

*All equatorial waves studied have tilted vertical structures, with:*

*Easterlies ahead of and westerlies following the convective region*

*Warm lower tropospheric temperatures ahead of the wave, with cooling behind. The mid-troposphere is warm within the convective region, indicating that latent heating more than compensates for vertical motion.*

*Waves are moist ahead (high CAPE) and dry following the deep convection*

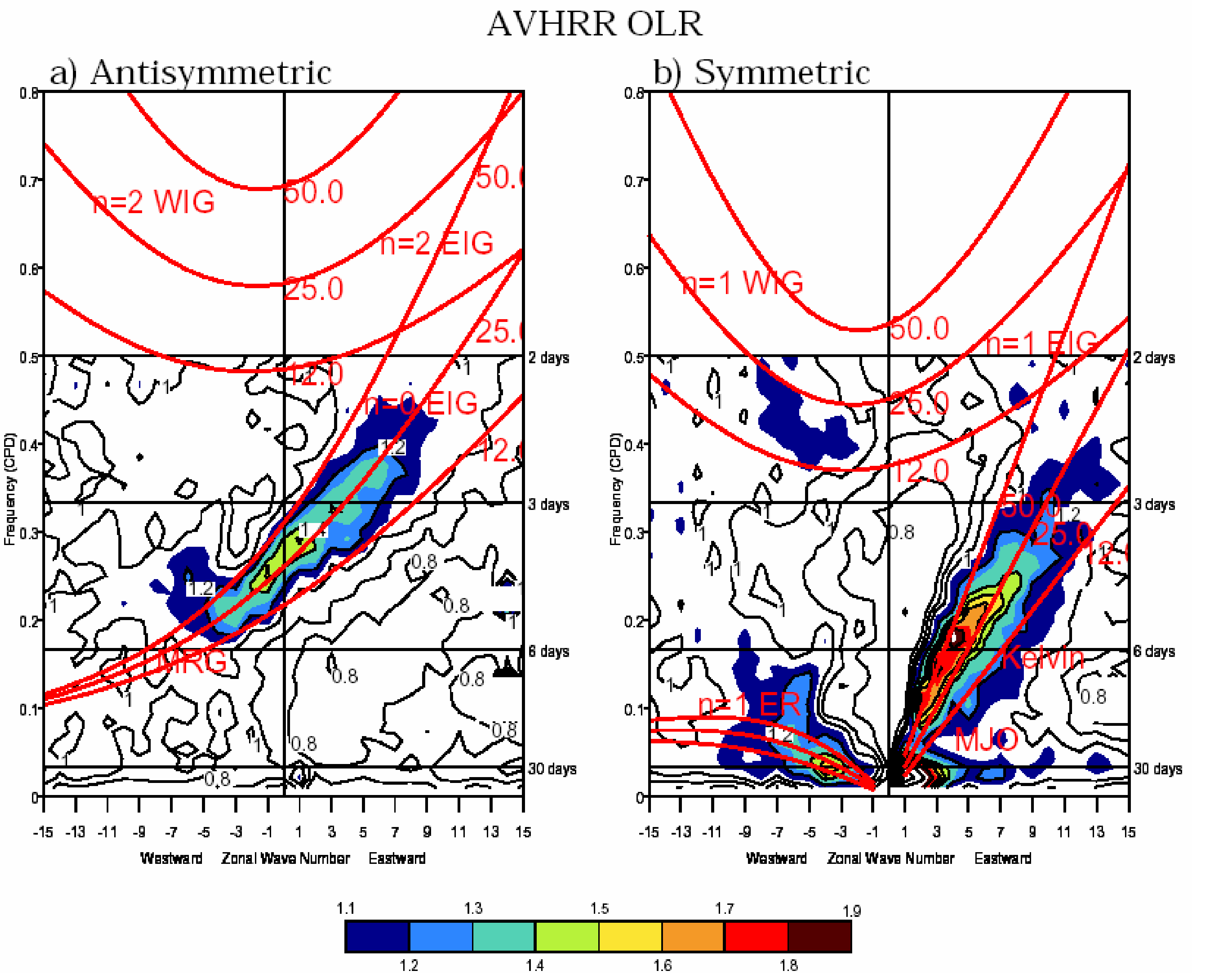

AVHRR OLR
a) Antisymmetric
b) Symmetric
n=2 WIG
n=2 EIG
n=0 EIG
MRG
n=1 WIG
n=1 EIG
n=1 ER
Kelvin
MJO
50.0
25.0
12.0
2 days
3 days
6 days
30 days
Frequency (CPD)
Westward Zonal Wave Number Eastward

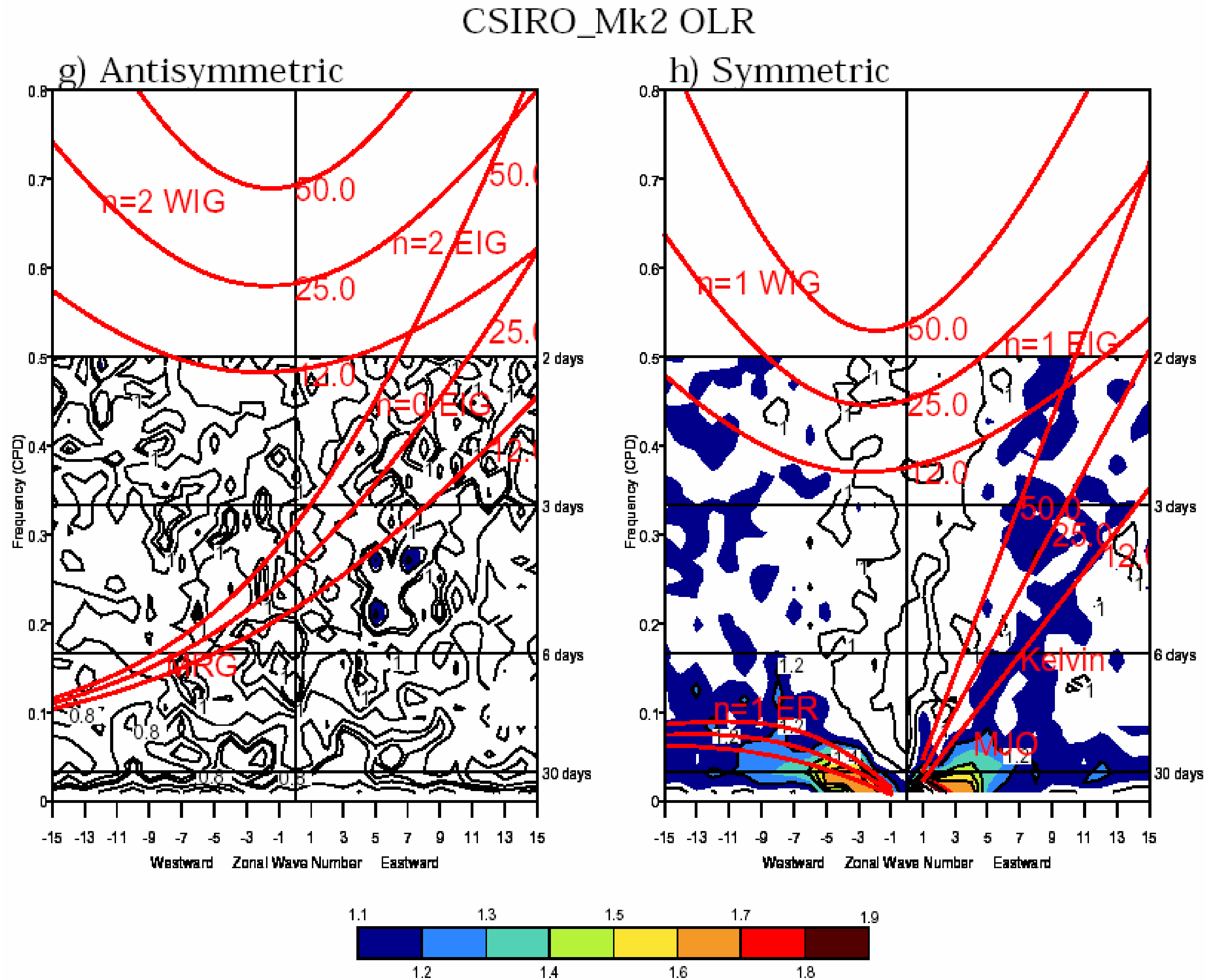
CSIRO_Mk2 OLR
g) Antisymmetric
h) Symmetric
n=2 WIG
n=2 EIG
n=0 EIG
MRG
n=1 WIG
n=1 EIG
n=1 ER
Kelvin
MJO
50.0
25.0
12.0
2 days
3 days
6 days
30 days
Frequency (CPD)
Westward Zonal Wave Number Eastward
1.1
1.2
1.3
1.4
1.5
1.6
1.7
1.8
1.9

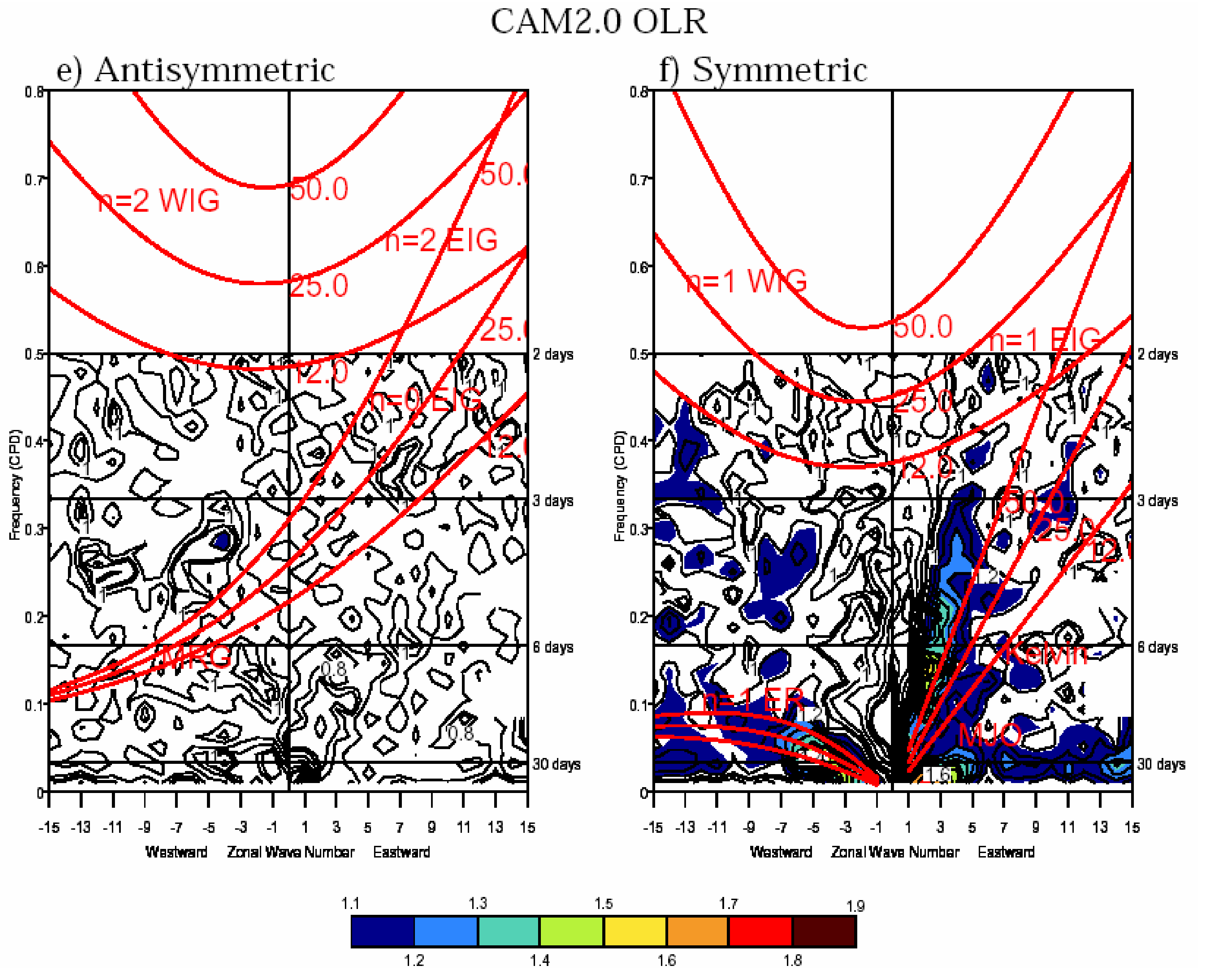

CAM2.0 OLR
e) Antisymmetric
f) Symmetric
n=2 WIG
n=2 EIG
n=0 EIG
MRG
n=1 WIG
n=1 EIG
n=1 ER
Kelvin
MJO
Frequency (CPD)
Westward Zonal Wave Number Eastward
2 days
3 days
6 days
30 days
1.1 1.2 1.3 1.4 1.5 1.6 1.7 1.8 1.9

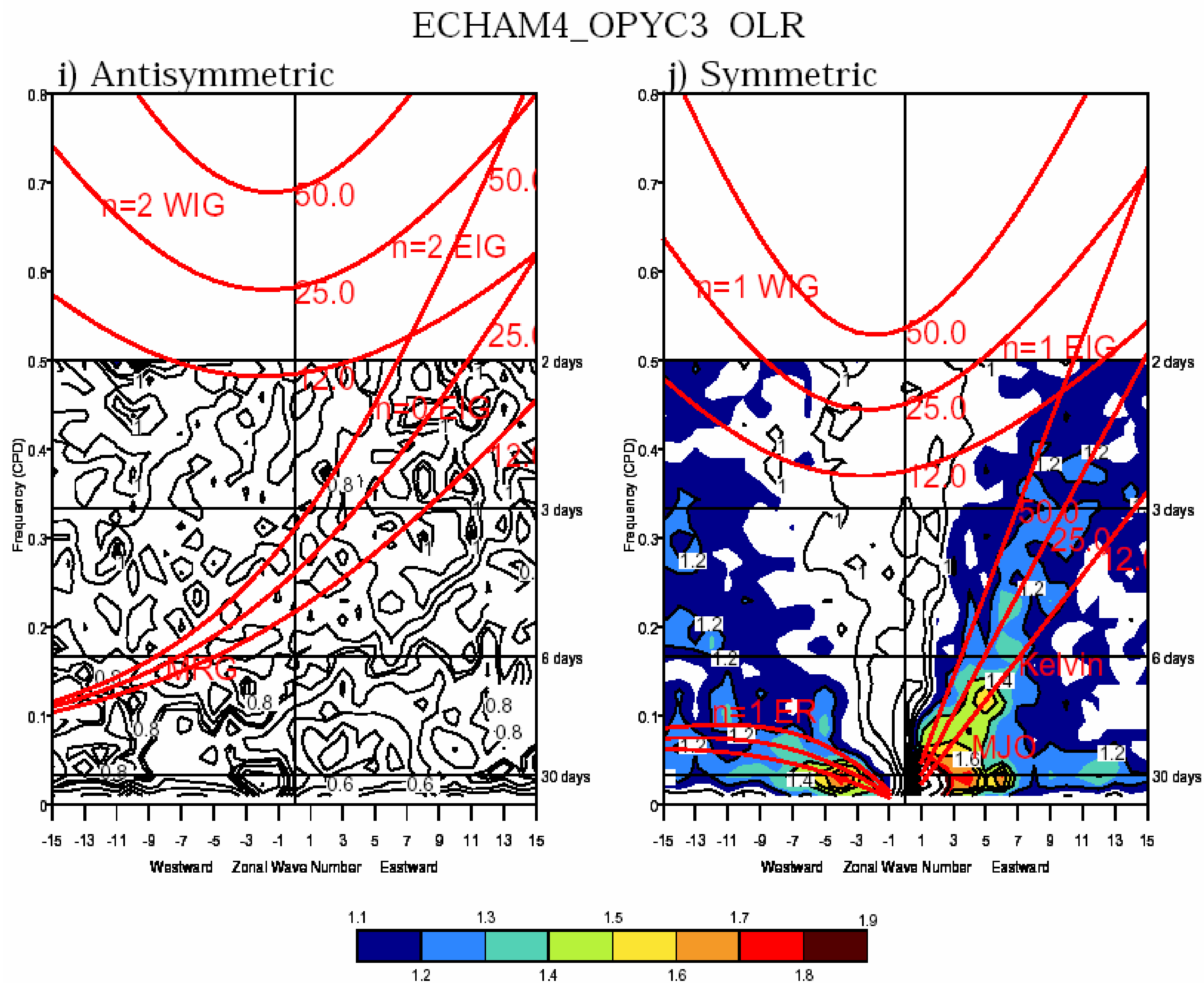

ECHAM4_OPYC3 OLR
i) Antisymmetric
j) Symmetric
n=2 WIG
n=2 EIG
n=0 EIG
MRG
n=1 WIG
n=1 EIG
n=1 ER
Kelvin
MJO
2 days
3 days
6 days
30 days
Frequency (CPD)
Westward Zonal Wave Number Eastward

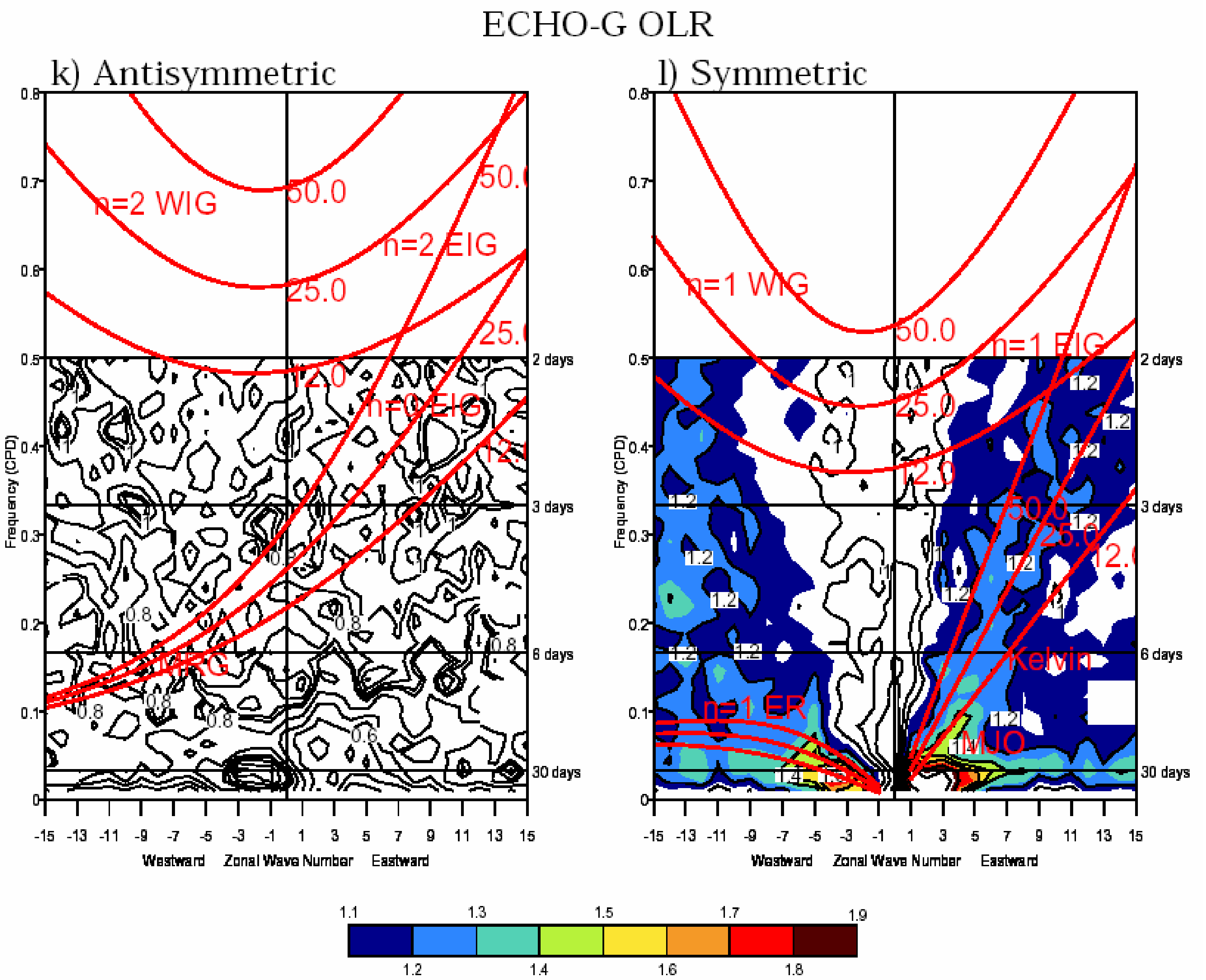

ECHO-G OLR
k) Antisymmetric
l) Symmetric
n=2 WIG
n=2 EIG
n=0 EIG
MRG
n=1 WIG
n=1 EIG
n=1 ER
Kelvin
MJO
50.0
25.0
12.0
2 days
3 days
6 days
30 days
Frequency (CPD)
Westward
Zonal Wave Number
Eastward
1.1
1.2
1.3
1.4
1.5
1.6
1.7
1.8
1.9

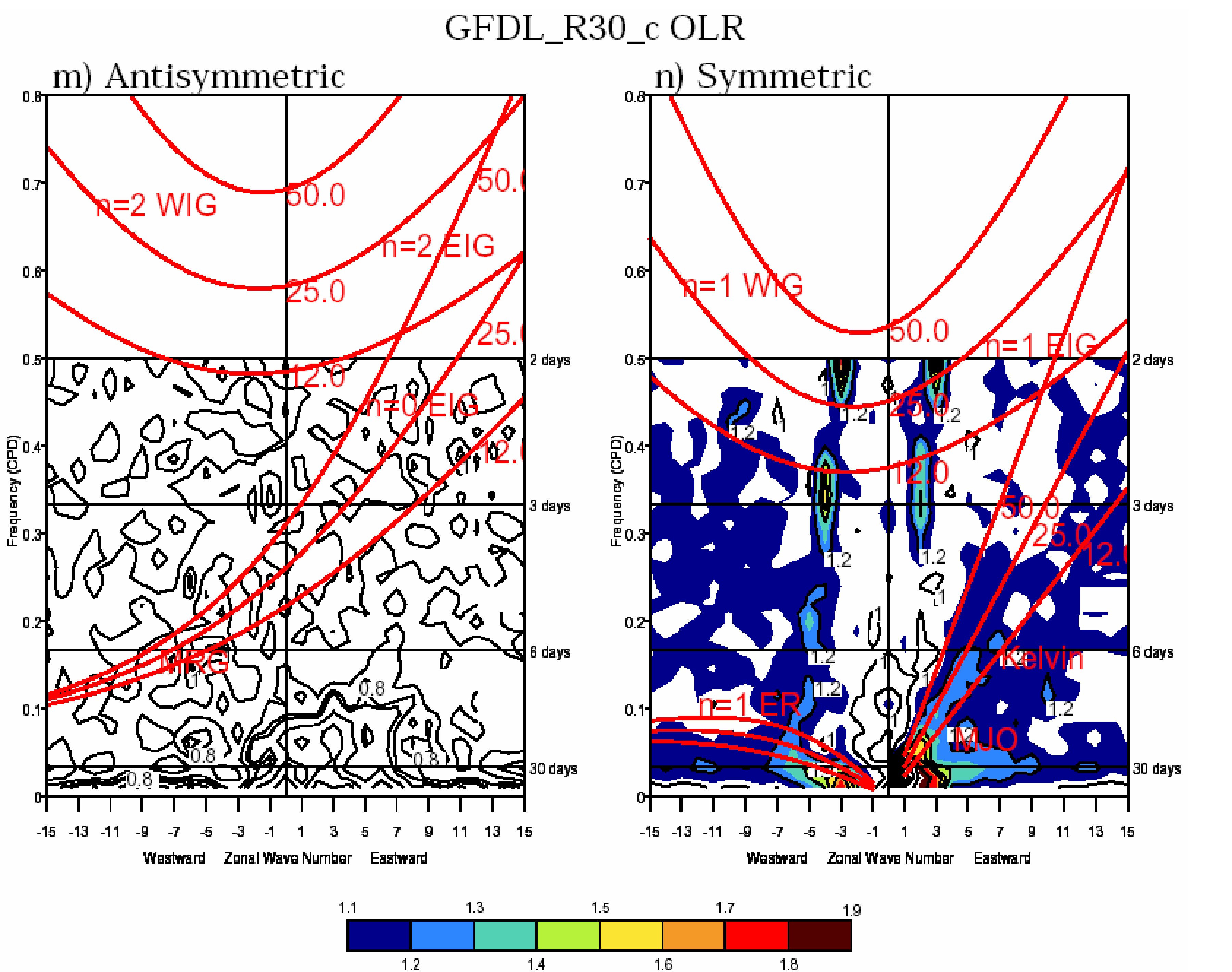
GFDL_R30_c OLR
m) Antisymmetric
n) Symmetric
n=2 WIG
n=2 EIG
n=0 EIG
MRG
n=1 WIG
n=1 EIG
n=1 ER
Kelvin
MJO
50.0
25.0
12.0
2 days
3 days
6 days
30 days
Frequency (CPD)
Westward
Zonal Wave Number
Eastward
1.1
1.2
1.3
1.4
1.5
1.6
1.7
1.8
1.9

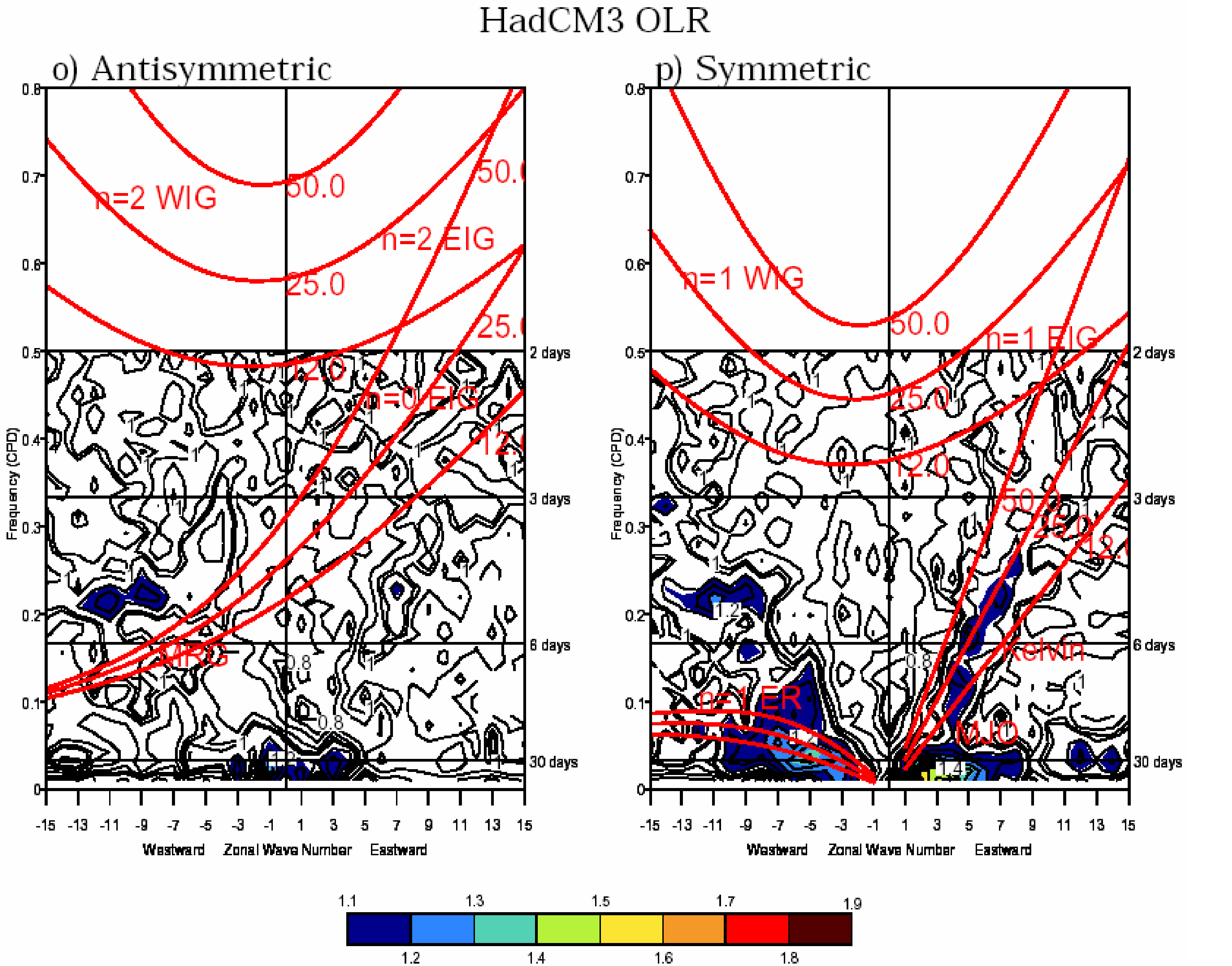
HadCM3 OLR
o) Antisymmetric
p) Symmetric
n=2 WIG
n=2 EIG
n=0 EIG
MRG
n=1 WIG
n=1 EIG
n=1 ER
Kelvin
MJO
50.0
25.0
12.0
2 days
3 days
6 days
30 days
Frequency (CPD)
Westward Zonal Wave Number Eastward
1.1 1.2 1.3 1.4 1.5 1.6 1.7 1.8 1.9

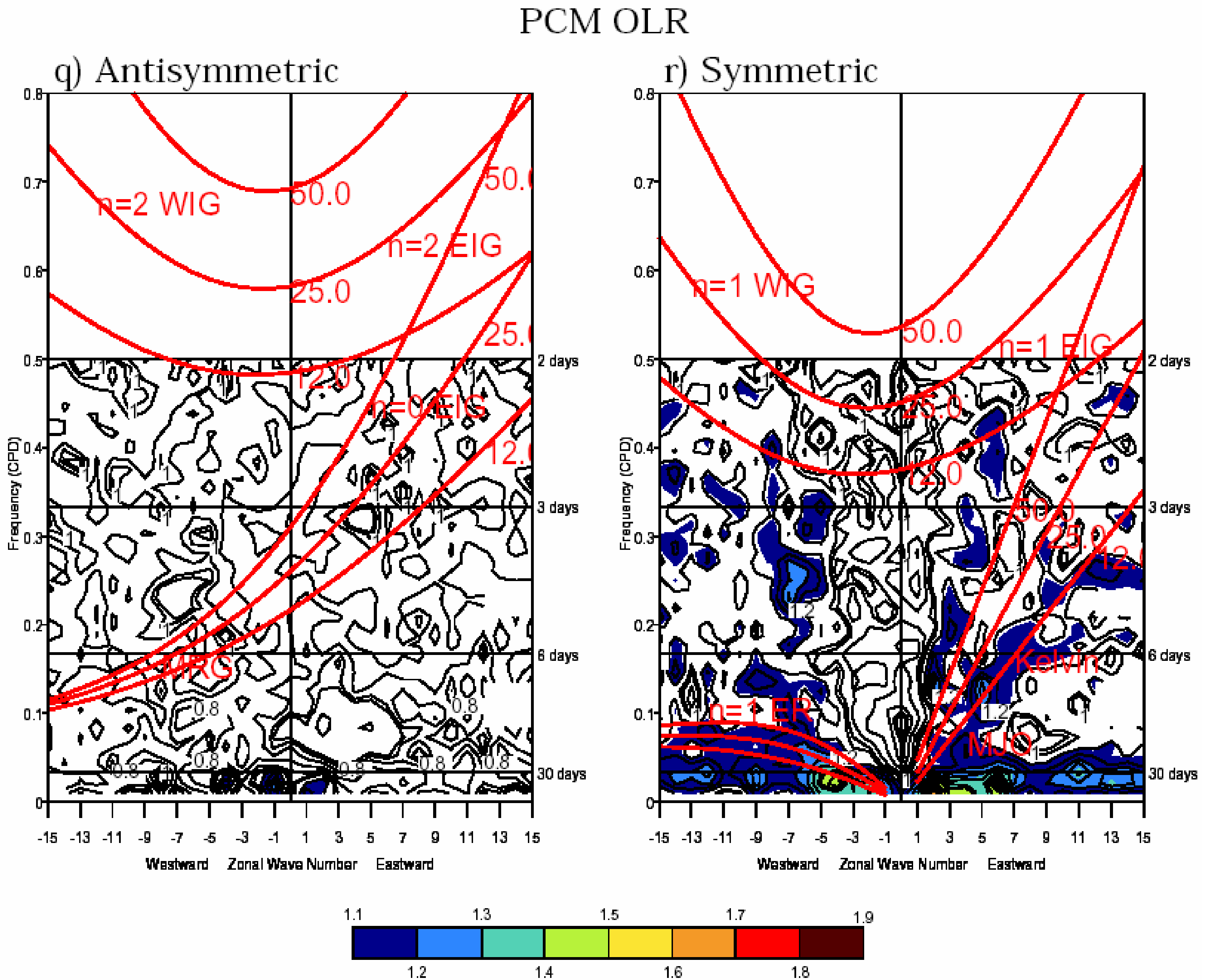
PCM OLR
q) Antisymmetric
r) Symmetric
n=2 WIG
n=2 EIG
n=0 EIG
MRG
n=1 WIG
n=1 EIG
Kelvin
n=1 ER
MJO
50.0
25.0
12.0
2 days
3 days
6 days
30 days
Frequency (CPD)
Westward Zonal Wave Number Eastward
1.1
1.2
1.3
1.4
1.5
1.6
1.7
1.8
1.9

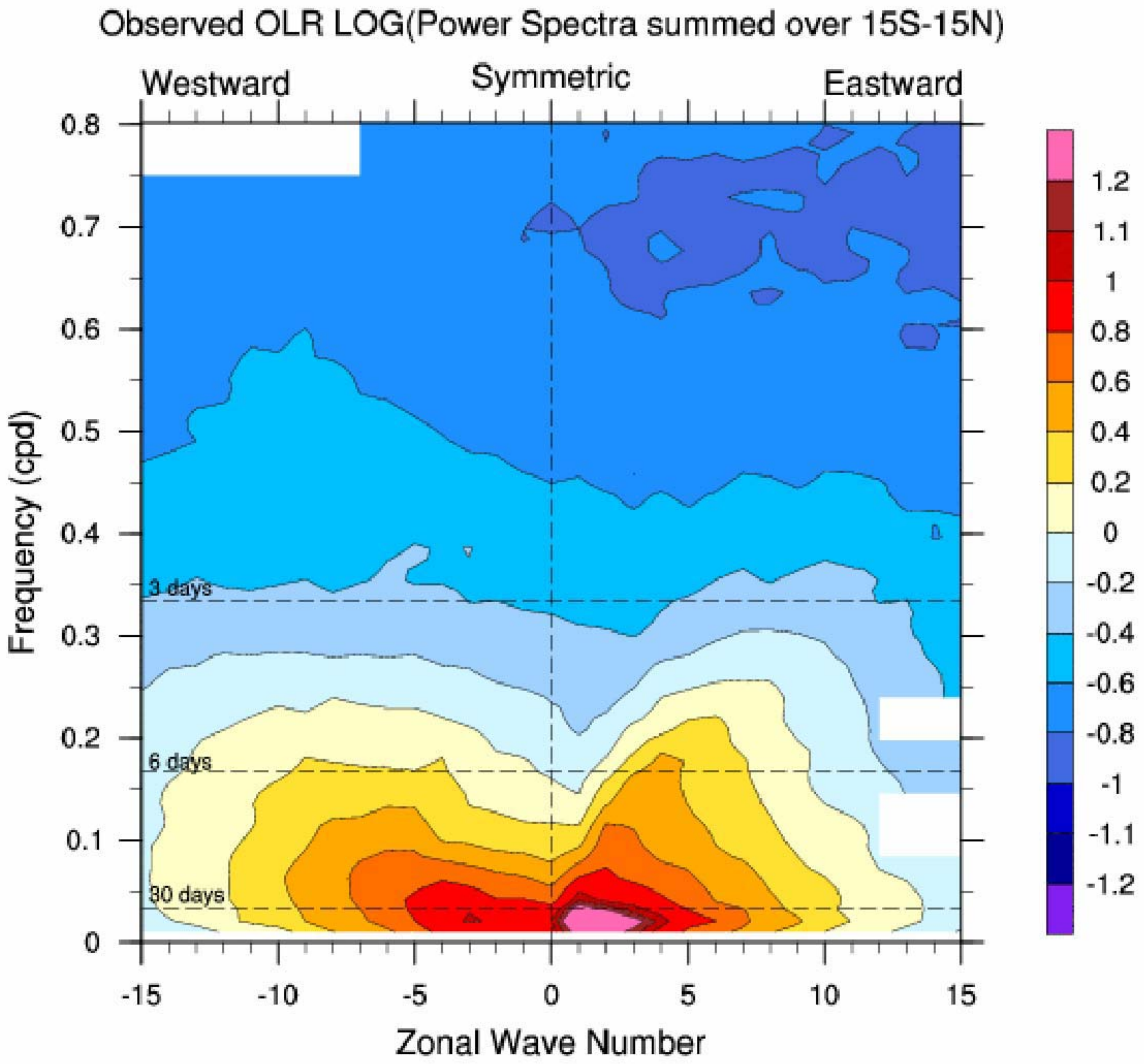
Observed OLR LOG(Power Spectra summed over 15S-15N)
Westward
Symmetric
Eastward
Frequency (cpd)
Zonal Wave Number
3 days
6 days
30 days
0.8
0.7
0.6
0.5
0.4
0.3
0.2
0.1
0
-15
-10
-5
0
5
10
15
1.2
1.1
1
0.8
0.6
0.4
0.2
0
-0.2
-0.4
-0.6
-0.8
-1
-1.1
-1.2

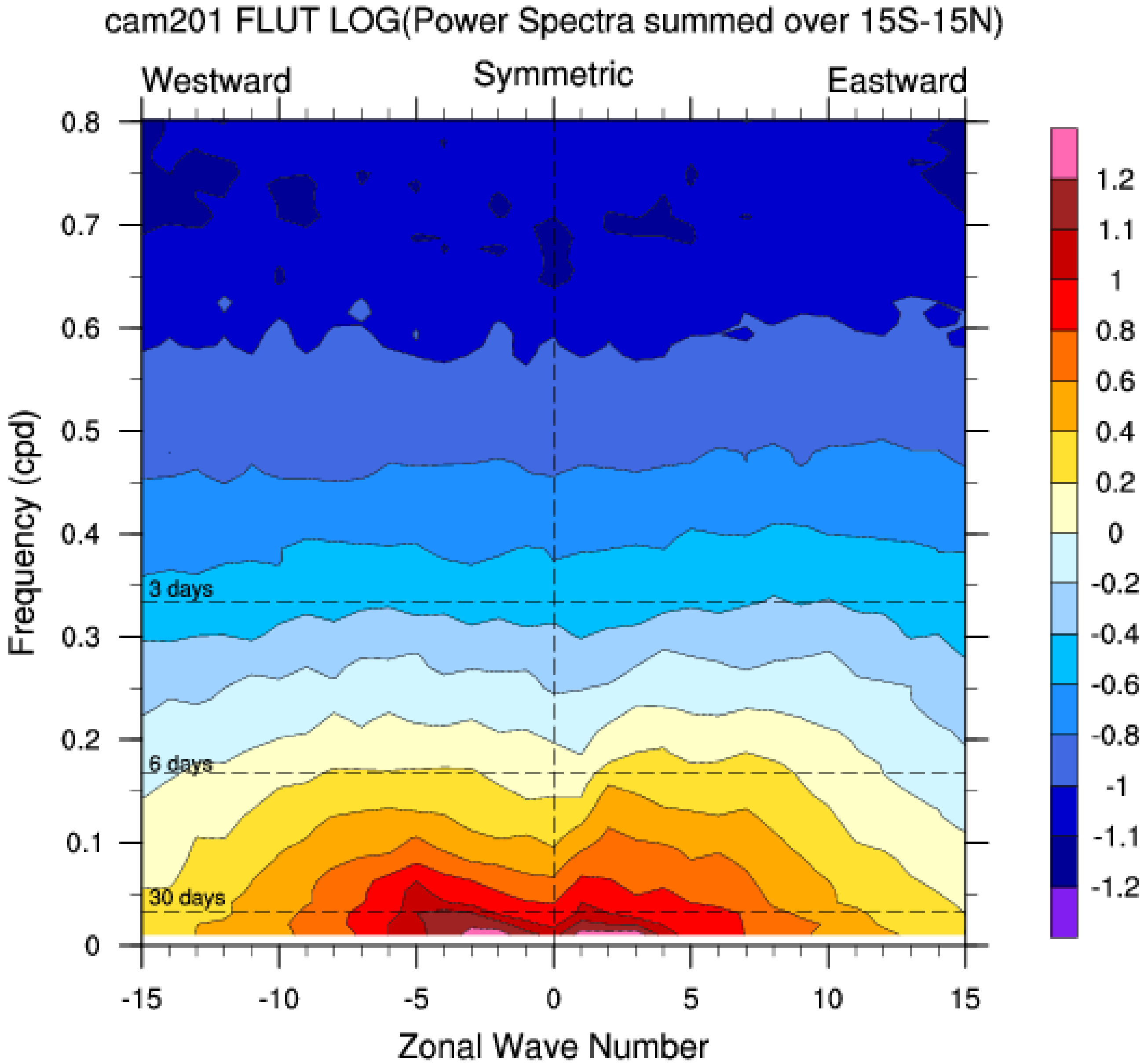

cam201 FLUT LOG(Power Spectra summed over 15S-15N)
Westward
Symmetric
Eastward
Frequency (cpd)
0.8
0.7
0.6
0.5
0.4
0.3
0.2
0.1
0
3 days
6 days
30 days
-15
-10
-5
0
5
10
15
Zonal Wave Number
1.2
1.1
1
0.8
0.6
0.4
0.2
0
-0.2
-0.4
-0.6
-0.8
-1
-1.1
-1.2

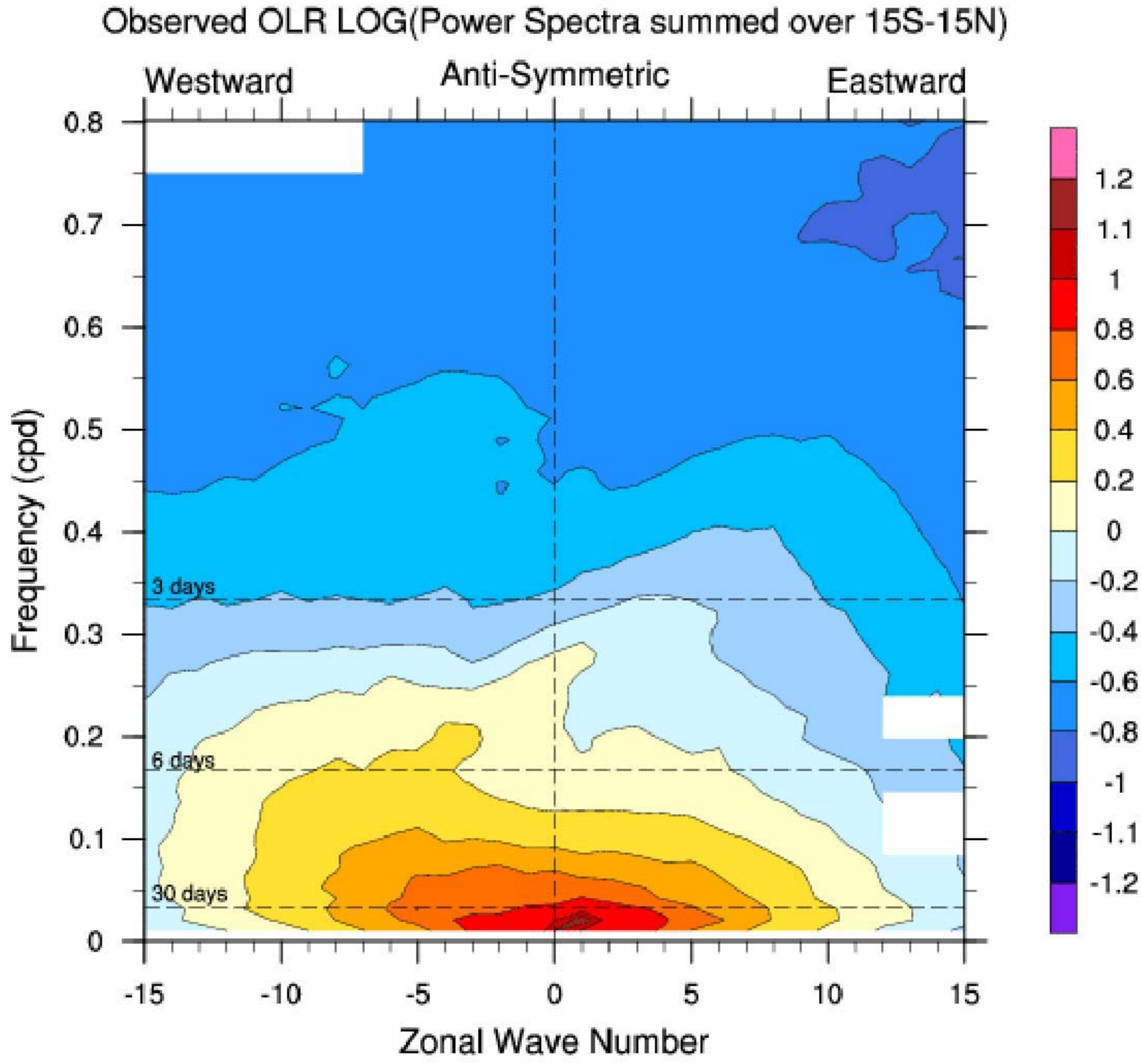

Observed OLR LOG(Power Spectra summed over 15S-15N)
Westward
Anti-Symmetric
Eastward
Frequency (cpd)
0.8
0.7
0.6
0.5
0.4
0.3
0.2
0.1
0
3 days
6 days
30 days
-15
-10
-5
0
5
10
15
Zonal Wave Number
1.2
1.1
1
0.8
0.6
0.4
0.2
0
-0.2
-0.4
-0.6
-0.8
-1
-1.1
-1.2

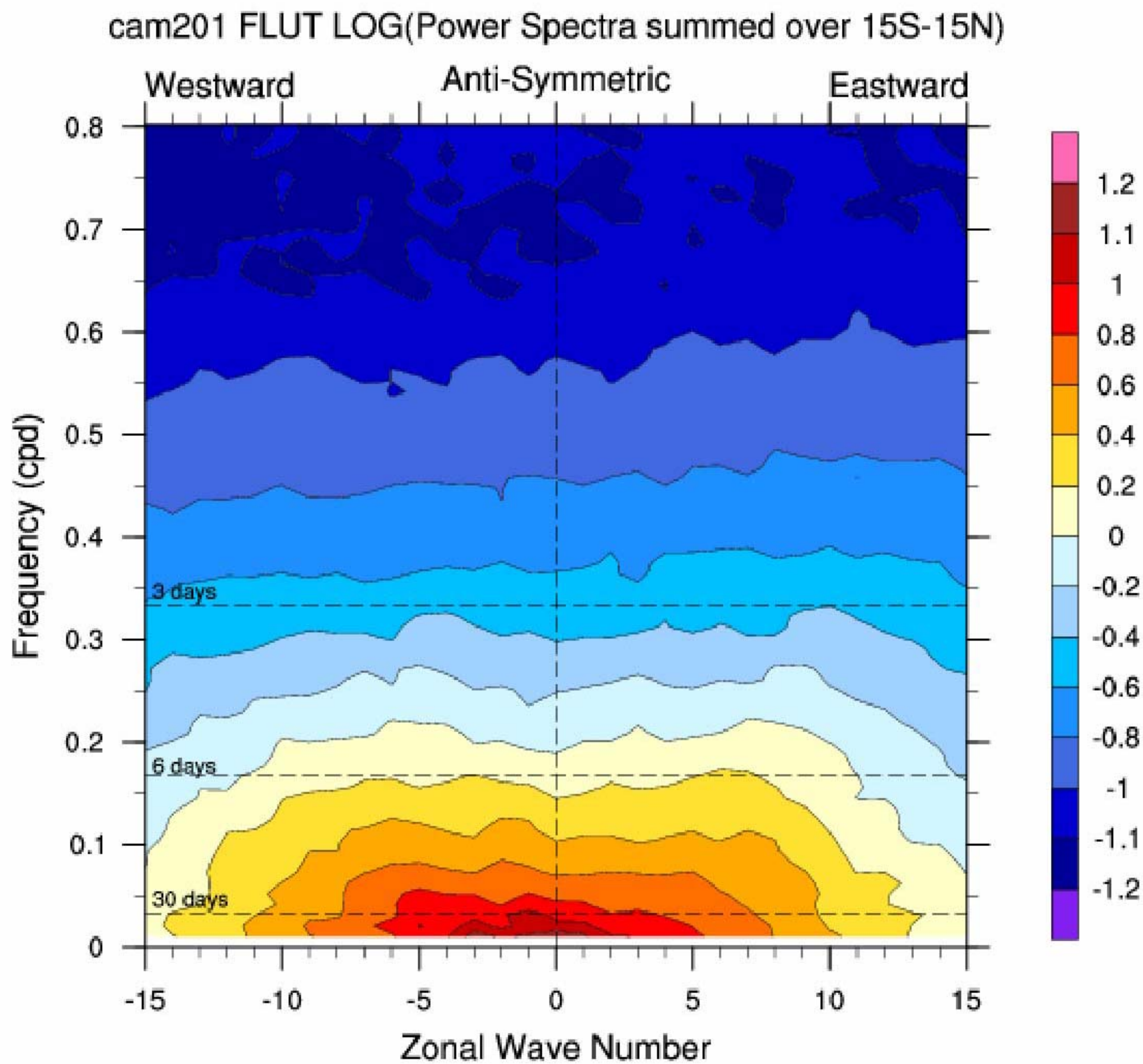

cam201 FLUT LOG(Power Spectra summed over 15S-15N)
Westward
Anti-Symmetric
Eastward
Frequency (cpd)
0.8
0.7
0.6
0.5
0.4
0.3
0.2
0.1
0
3 days
6 days
30 days
-15
-10
-5
0
5
10
15
Zonal Wave Number
1.2
1.1
1
0.8
0.6
0.4
0.2
0
-0.2
-0.4
-0.6
-0.8
-1
-1.1
-1.2

# Conclusions

*Although the MJO is comprised of a variety of higher frequency, smaller scale disturbances, the dynamical structures of all of these waves resemble each other in many important aspects, all consistent with shallow cumulus leading to deep convection followed by stratiform precipitation*

***There is a high degree of self-similar behavior seen in equatorial waves across a wide variety of scales***

*General Circulation Models do not represent such scale interactions, and most do not adequately represent the MJO or other equatorial modes sufficiently well.*

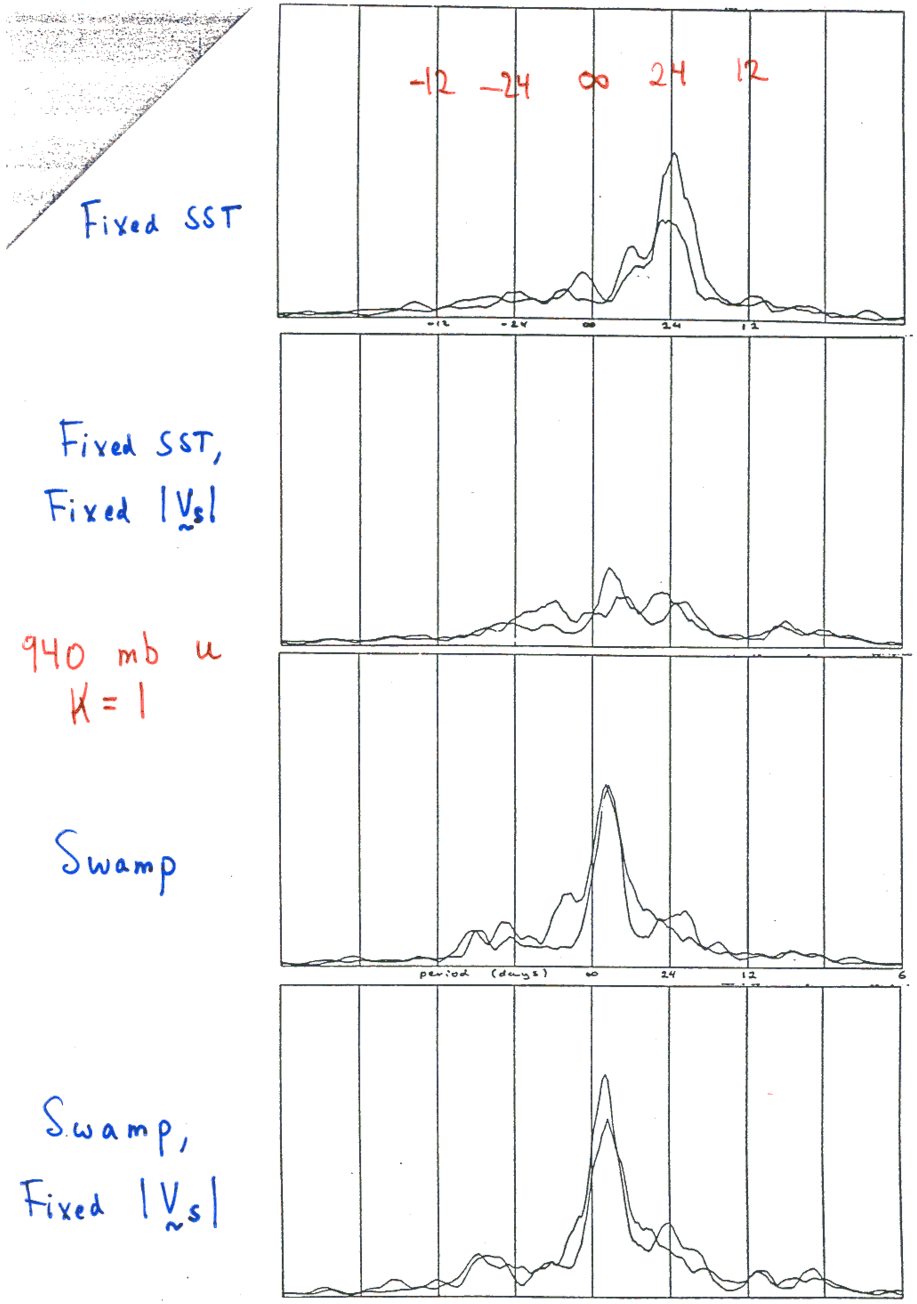


Figure 3. As for Figure 1, but for u at 940 mb, wavenumber 1. The vertical scale is one quarter that of Figure 1.

Neelin et al., JAS, 1987

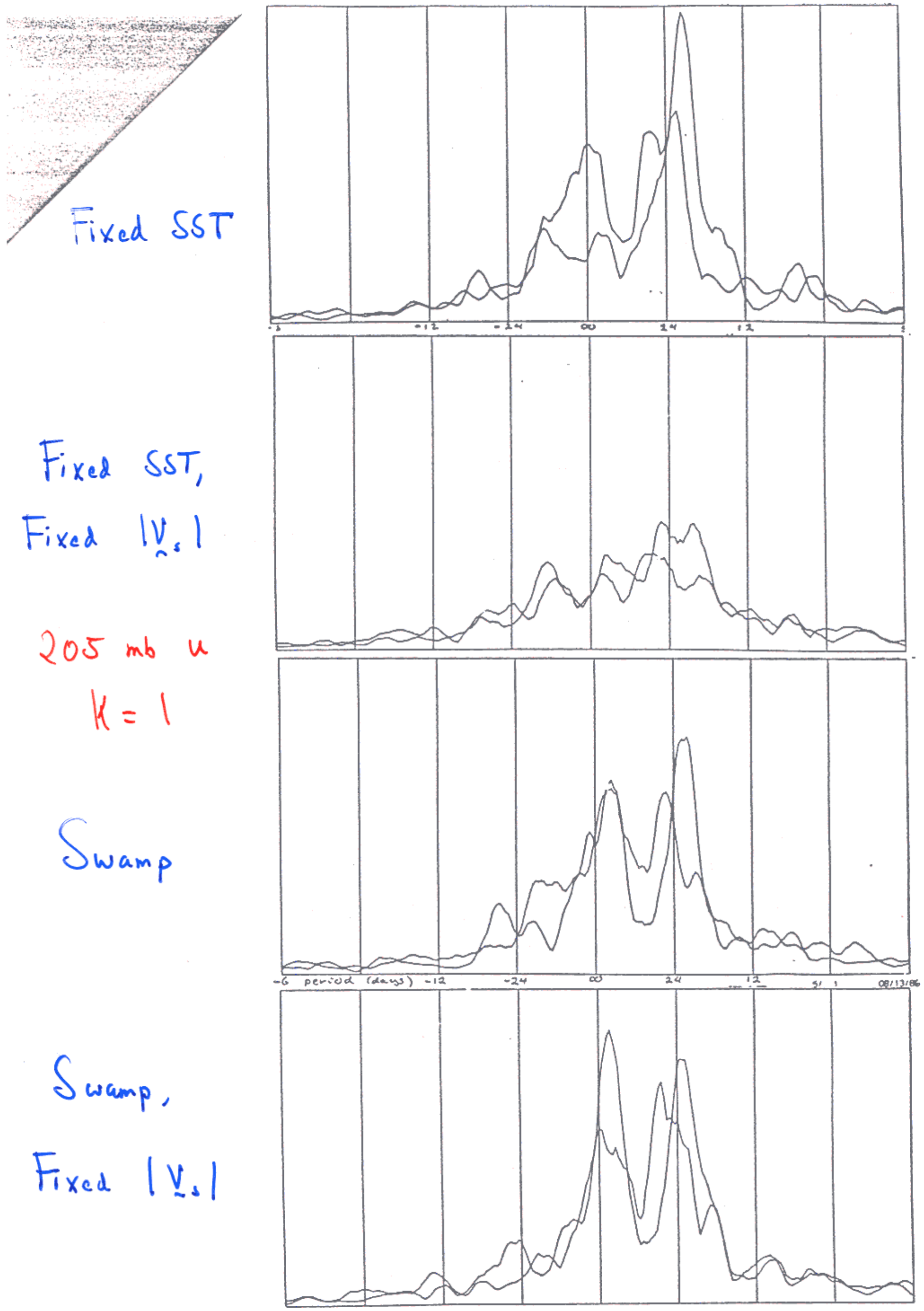
Fixed SST
-12
-24
∞
24
12
Fixed SST,
Fixed $|V_s|$
205 mb u
K = 1
Swamp
-6 period (days) -12
-24
∞
24
12
08/13/86
Swamp,
Fixed $|V_s|$

# Tropical cyclone activity and the MJO